EES Solar

REVIEW

View Article Online
View Journal

Cite this: DOI: 10.1039/d5el00210a

Progress in perovskite indoor photovoltaics

Jie Xu,[ab] Abhisek Chakraborty,[a] Zeynab Skafi,[a] Vaibhav Singh,[a] Diksha Thakur,[a] Ebin Joseph,[a] Shanyue Hou,[c] Zhoucheng Xu,[b] Xiang Liu,[c] Xueqing Xu,[d] Minggao Ouyang[b] and Thomas M. Brown *[a]

The rapid growth of the internet of things (IoT) and artificial intelligence (AI) has created strong demand for efficient indoor photovoltaics (IPVs). Photovoltaic materials with bandgaps of 1.8–2.0 eV can theoretically achieve power conversion efficiencies (PCEs) of 53–56% under artificial light sources. Among competing technologies, perovskite solar cells (PSCs) stand out due to their low-cost fabrication, adjustable bandgap, mechanical flexibility, and outstanding performance under low-light conditions. State-of-the-art PSCs have achieved experimentally-measured indoor power conversion efficiencies exceeding 45% (42%) on rigid substrates and 42% (35%) on flexible substrates under 1000 lx (200 lx) indoor light. Even though meaningful comparison across studies remains challenging due to the lack of standardized indoor photovoltaic characterization protocols, these advances have attracted substantial industrial interest, with emerging companies actively developing PSC-based self-powered IoT devices. To accelerate industrialization, a comprehensive understanding of PSC development, challenges, and opportunities is essential. This review systematically examines six key areas: rigid devices, flexible devices, lead-free PSCs, perovskite modules, applications in self-powered indoor devices, and related patents. We summarize recent progress, highlight current limitations, and discuss potential strategies, while also creating visual maps of the scientific landscape in this arena, aiming to provide an integrated perspective on the future of perovskite IPV.

Received 16th December 2025
Accepted 5th March 2026

DOI: 10.1039/d5el00210a

rsc.li/EESSolar

Broader context

The rapid expansion of the Internet-of-Things (IoT), wireless sensor networks, and smart home technologies has connected about 18.6 billion devices worldwide in 2024, a number expected to more than double in the next decade. The surge in connected electronics has created an urgent demand for sustainable, maintenance-free power sources capable of efficiently harvesting indoor illumination that is already present in building environments. Conventional batteries face limitations in lifetime, maintenance, and waste management, highlighting the need for alternative energy solutions. Indoor photovoltaics (IPV) provide a promising route toward self-powered electronic systems that harvest ambient light. Among available technologies, perovskite solar cells stand out due to their tunable bandgaps, flexibility, and low-cost fabrication. The demonstration of exceptional low-light efficiencies exceeding 45%, outperforming both silicon and organic photovoltaics, positions perovskite PVs as a leading candidate for powering electronic devices indoors. This review highlights recent advances in perovskite IPV, spanning rigid and flexible devices, lead-free materials, scalable module designs, and applications in self-powered electronics. It also analyzes emerging commercial products, industrial activity, and global patent trends, using visual maps to connect research areas. The review concludes by identifying key challenges and outlining clear strategies to accelerate the next phase of perovskite IPV development.

1 Introduction

The rapid expansion of the Internet of Things (IoT), wireless sensor networks (WSNs), and smart home technologies has connected approximately 18.6 billion devices worldwide in 2024, and this number is expected to more than double in the next decade (Fig. 1a).[1–3] Improving the sustainability of the energy supply for IoT sensors to make them more resilient, affordable, dependable, and energy-efficient faces significant challenges.[1,4] Many IoT devices need to operate autonomously without a grid connection, and current mainstream approaches rely on primary batteries (non-rechargeable) or secondary batteries (rechargeable) to power these devices. However, numerous IoT applications impose strict restrictions on battery size, often requiring them to be in the centimeter range or smaller, complicating battery use.[5] Furthermore, the use and replacement of batteries can significantly impact the lifespan of IoT products. The typical power consumption of household and personal electronics and wireless devices ranges from micro-watts (μW) to watts (W) (Fig. 1b).[6–8] Environmentally friendly indoor photovoltaic (IPV) cells offer one of the best solutions to

[a]CHOSE (Centre for Hybrid and Organic Solar Energy), Department of Electronic Engineering, Tor Vergata University of Rome, Via del Politecnico 1, 00133 Rome, Italy. E-mail: thomas.brown@uniroma2.it

[b]School of Vehicle and Mobility, Tsinghua University, Beijing 100084, P. R. China

[c]School of Materials Science and Engineering, Beihang University, Beijing 100191, P. R. China

[d]Guangzhou Institute of Energy Conversion, Chinese Academy of Sciences, CAS Key Laboratory of Renewable Energy, Guangdong Provincial Key Laboratory of Renewable Energy, Guangzhou, 510640, P. R. China

power these electronic products without batteries, as they can convert ambient low light into electricity.[5,9–13]

The fundamental difference between indoor and outdoor photovoltaics lies in the type of light absorbed. Outdoor photovoltaics mainly absorb sunlight, which spans a wide spectral range from 300 to 4000 nm, comprising about 2% ultraviolet (UV), 47% visible, and 51% infrared (IR) light.[14] In contrast, indoor photovoltaics primarily absorb light from indoor sources, such as commonly used light-emitting diode (LED) lights, which have a spectrum mainly in the visible light range (400–750 nm) (Fig. 2a).[15] This difference leads to varying requirements for the optimal bandgap of the absorber material under different conditions. For outdoor photovoltaics, the optimal bandgap is 1.1–1.5 eV, while for indoor PV, it is 1.8–2 eV (Fig. 2d). Furthermore, the irradiance of light found indoors ($\sim$0.1–10 W m^{-2}) is typically 100 to 10 000 times lower than that of the outdoor light (1000 W m^{-2} at peak),[16] leading to much lower photogenerated currents. As a result of different optimal bandgaps and the larger effect of recombination on performance, photovoltaic devices that perform efficiently in sunlight do not always work well under indoor lighting and *vice versa*, as illustrated in Fig. 2b.[17,18] Moreover, the maximum Shockley–Queisser (S–Q) limit for power conversion efficiency (PCE) is significantly higher for indoor photovoltaics ($\sim$55–56%) compared to outdoor photovoltaics ($\sim$33%).[19] This is because no single-junction cell can fully capture the broad AM 1.5 G solar spectrum and retain a significant voltage, leading to significant losses due to non-absorption and thermalization. In contrast, a single-junction cell allows better utilization of the

Left to right (Vaibhav Singh, Abhisek Chakraborty, Ebin Joseph, Jie Xu, Thomas M. Brown, Diksha Thakur, Zeynab Skafi)

The Centre for Hybrid and Organic Solar Energy (CHOSE) team at the Tor Vergata University of Rome has pioneered indoor photovoltaics (iPV), publishing its first study in 2015 and its first perovskite iPV work in 2016. Since then, the group has produced numerous publications on solar cells and modules customized for indoor light harvesting and their measurement on both rigid and flexible substrates.

Jie Xu received his PhD from CHOSE and is currently a postdoctoral researcher ("Shuimu Tsinghua Scholar" member) at Tsinghua University.

Abhisek Chakraborty is a Marie Curie postdoctoral researcher at CHOSE, working on novel semiconductor materials for indoor light harvesting.

Zeynab Skafi is a research fellow at the Tor Vergata University of Rome, focusing on flexible and indoor perovskite solar cells.

Vaibhav Singh is a PhD researcher at CHOSE working on design optimization, system integration, and applications of indoor photovoltaic technologies.

Diksha Thakur received her PhD from Taiwan and is now working at CHOSE as Postdoctoral Associate developing sustainable perovskite solar cells.

Ebin Joseph received his PhD from CHOSE and is currently continuing his research there as a Postdoctoral Researcher.

Thomas M. Brown, founder and initiator of indoor photovoltaics research at CHOSE, is professor of Organic and Biological Electronics.

Shanyue Hou

Shanyue Hou (H-index of 8) is a PhD student at the School of Materials Science and Engineering, Beihang University, China, whose materials science discipline ranks among the top 10 nationally and top 100 globally. She has been engaged in perovskite research since her undergraduate studies, focusing on the design, crystallization kinetics, and interface engineering of wide-bandgap and 2D perovskite materials for stable and efficient solar cells. She has authored or co-authored over 20 peer-reviewed papers in leading journals including Advanced Energy Materials *and* Advanced Functional Materials.

Zhoucheng Xu

Zhoucheng Xu is currently pursuing a PhD degree at Tsinghua University, Beijing, China, where he is with the State Key Laboratory of Automotive Safety and Energy. He received his Bachelor's degree from the School of Vehicle and Mobility, Tsinghua University. His research interests focus on perovskite materials, photovoltaic devices and systems, and new energy system technologies. He is particularly interested in the design, optimization, and application of perovskite-based solar energy conversion systems for sustainable energy development.

narrow emission spectrum of indoor lamps (typically LED or fluorescent).[20]

Over the past decade, indoor photovoltaics have garnered significant interest from the research community. This interest is driven by their potential as a renewable energy source for IoT-based devices and the variety of materials that can utilize the visible spectrum of artificial light sources.[21–23] Consequently, the number of publications on different PV materials for indoor light harvesting has increased substantially during this period (Fig. 2c). Perovskite solar cells (PSCs) have received the most attention in the indoor PV field due to their advantages, including simple manufacturing technology, low cost, adjustable bandgap, mechanical flexibility, and high defect tolerance.[24–28] Given these benefits, it is not surprising that perovskites are leading the race for the highest efficiency and output power among all indoor PV technologies. Perovskites, with a bandgap of 1.67 eV, have already achieved an indoor efficiency of around 45% (Fig. 2d).[29,30] Large-area devices have also shown impressive performance, achieving PCEs of 43% and 31% on rigid and flexible substrates, respectively, both with an active area of 12 cm^2.[31,32] These promising results have drawn significant attention from industry, prompting emerging companies to pursue the development of PSC-based self-powered IoT devices. To further drive industrial adoption, a thorough understanding of the progress, challenges, and prospects in PSC technology is crucial.

In this review, we focus on the field of perovskite indoor photovoltaics and subdivide it into six main aspects, including rigid devices (Section 2), flexible devices (Section 3), lead-free perovskite devices (Section 4), perovskite solar modules (Section 5), PV-powered indoor device applications (Section 6), patent landscape (Section 7). Finally, we discuss the state of the art of perovskite photovoltaics under various aspects and the challenges faced by this field (Section 8), before coming to the conclusions (Section 9).

Xiang Liu

Xiang Liu (H-index of 48) is a Professor at the School of Materials Science and Engineering, Beihang University, and a recipient of China's National High-Level Overseas Young Talent Program. He obtained his PhD in Physics from The University of Hong Kong and conducted postdoctoral research at Tsinghua University and Argonne National Laboratory, USA. His research focuses on ion/electron transport and failure mechanisms in solid-state energy materials, aiming to develop high-safety all-solid-state lithium batteries and perovskite solar cells. He has published over 70 papers in Nature Energy, Joule, Advanced Materials, and other leading journals, with over 9000 citations.

2 Rigid lead-halide perovskite solar cells for indoor photovoltaics

The earliest reports on the indoor PV performance of lead-halide perovskites date back to 2015–2016.[17,33] Both regular (n-i-p) and inverted (p-i-n) architecture devices achieved high

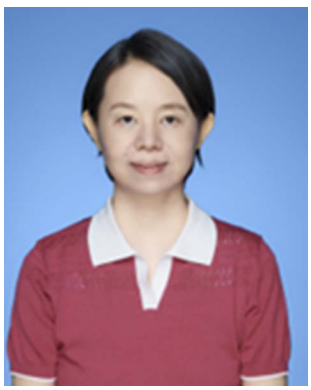

Xueqing Xu

Xueqing Xu is Deputy Director of Solar Energy Laboratory, Guangzhou Institute of Energy Conversion (GIEC), Chinese Academy of Sciences (CAS), a member of the CSTM Electronic Material Standards Committee, Director of the Guangdong Materials Research Society, Executive Director of the Shenzhen Solar Energy Society, and Project Evaluation Expert of the Ministry of Science and Technology, National Natural Science Foundation of China, and Guangdong Science and Technology Department. She has been engaged in the research of optoelectronic materials and devices, including luminescent colloidal quantum dots, optoelectronic functional films, perovskite solar cells, and quantum dot light-emitting diodes. As the PI or co-PI, she has undertaken over 40 scientific research projects such as the National "863" Programme, National Natural Science Foundation of China, and provincial and municipal science and technology research projects. She has published more than 130 academic papers in high quality journals.

Minggao Ouyang

Minggao Ouyang (H-index of 115) is a Professor and Academician at the Chinese Academy of Sciences at Tsinghua University, serving as Vice Chair of the Academic Council. He is a world-leading expert in new energy power systems, hydrogen energy, and vehicle electrification and the founding Editor-in-Chief of eTransportation. In 2024, he received the Global Energy Prize in the category of New Ways of Energy Application for his technical leadership in strategic planning, research, demonstration, and commercialization of new energy vehicles, particularly for addressing challenges in hydrogen fuel cell durability, lithium-ion battery safety, and vehicle-to-grid interaction. Professor Ouyang has published over 600 papers, holds nearly 200 patents, and has received multiple National Invention Awards for his pioneering contributions to China's clean energy transition.

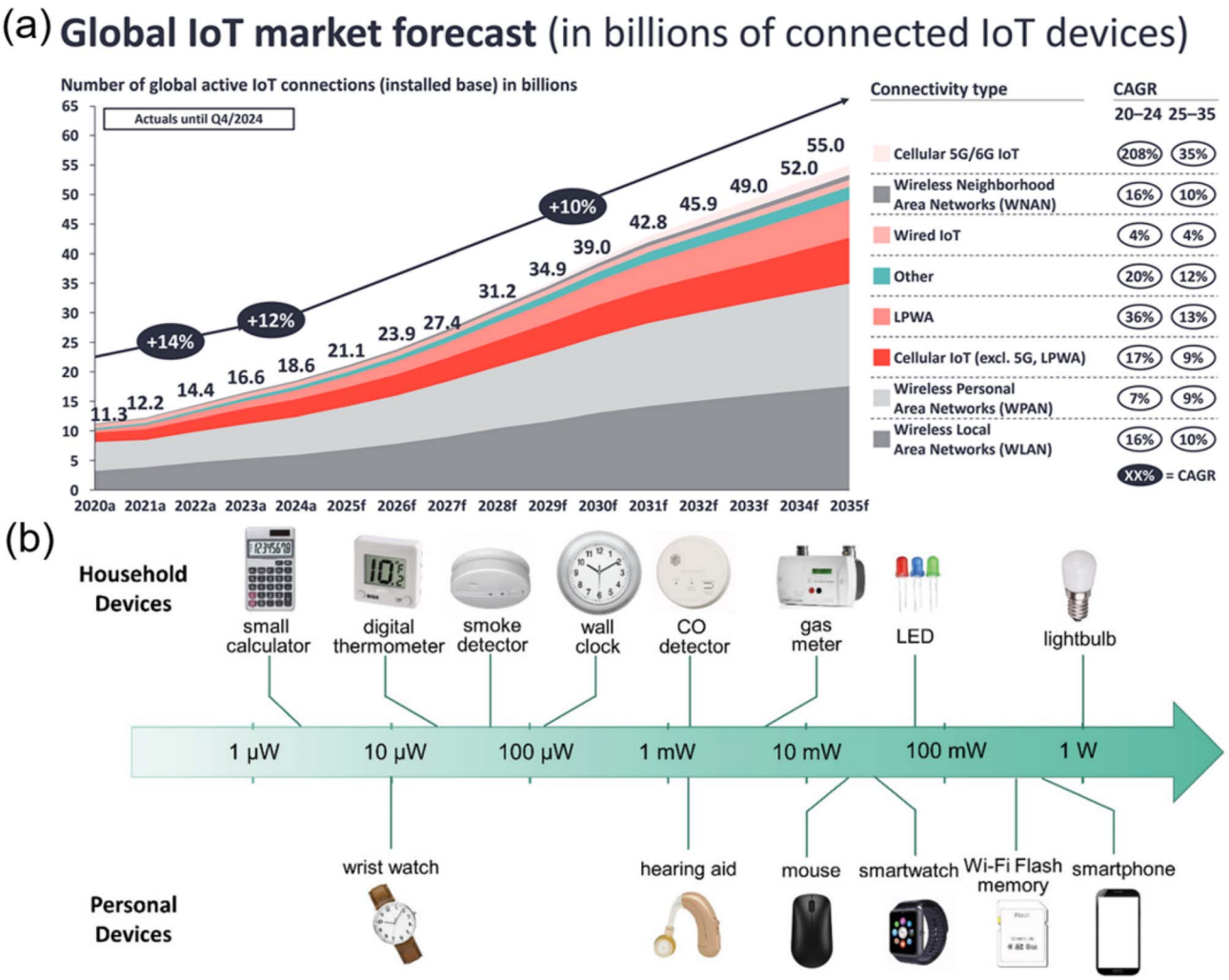

Fig. 1 (a) Current and future trends of the global internet of things (IoT) market;[3] (b) common indoor electronic devices and their power consumption. Reproduced from ref. 6 with permission from Wiley-VCH GmbH, copyright 2021.

indoor efficiency, exceeding 25%,[17,33] highlighting the significant potential of PSCs in indoor PV applications. However, this efficiency was about half of the theoretically optimal efficiency (~56% for commonly used LED light). Since then, increasing attention and research efforts have been directed towards enhancing efficiency.[34,35] Within a decade, efficiency has surged by over 60%, reaching an impressive PCE of ~45% under 1000 lx indoor light (Fig. 3a).[29] Recently, Wang *et al.* achieved a PCE of 45.5% with a V_{OC} of 1.15 V under extreme conditions of low temperature (198 K) at 1000 lx (Fig. 3a and b) and a PCE of 42.0% with a V_{OC} of 1.09 V at 200 lx.[30]

In the pursuit of improving efficiency, substantial research has been undertaken in the field of composition and bandgap engineering to match the bandgap of perovskites with the spectra of light sources.[34,35,37,47] Xu *et al.* studied the indoor performance of PSCs with bandgaps ranging from 1.5 to 2.3 eV and found that the bandgap is not the main parameter, but there are others that influence performance more, such as film quality.[35] Wide bandgap perovskites, *e.g.* 1.7–2.0 eV, theoretically better suited for indoor light harvesting, often exhibit suboptimal film quality, high defect density, and phase segregation, among other challenges (Fig. 3c).[35,48] Zhang *et al.* reported suppressed V_{OC} in high-bromine-content PSCs based on the $Cs_{0.17}FA_{0.83}PbI_{3-x}Br_x$, $0.6 \leq x \leq 1.6$, perovskite. In particular, for compositions with $x > 1.2$, they attributed the reduced V_{OC} not only to the commonly recognized halide segregation but also to the high density of bromine vacancy defects (Fig. 3d).[31] The combination of bandgap engineering and defect passivation is one of the effective strategies to improve the poor indoor efficiency of wide bandgap perovskites. For example, Cheng *et al.* demonstrated this approach by introducing a triple-anion $CH_3NH_3PbI_{2-x}BrCl_x$ perovskite, raising the bandgap from 1.61 eV ($MAPbI_3$) to 1.8 eV (Fig. 3e). Simultaneously, the incorporation of chloride ions successfully restrained halide segregation of iodide and bromide, leading to suppressed trap states and nonradiative recombination loss. This innovative strategy resulted in a remarkable indoor efficiency of 36% under a fluorescent lamp at 1000 lx, setting a record at the time (Fig. 3f).[37]

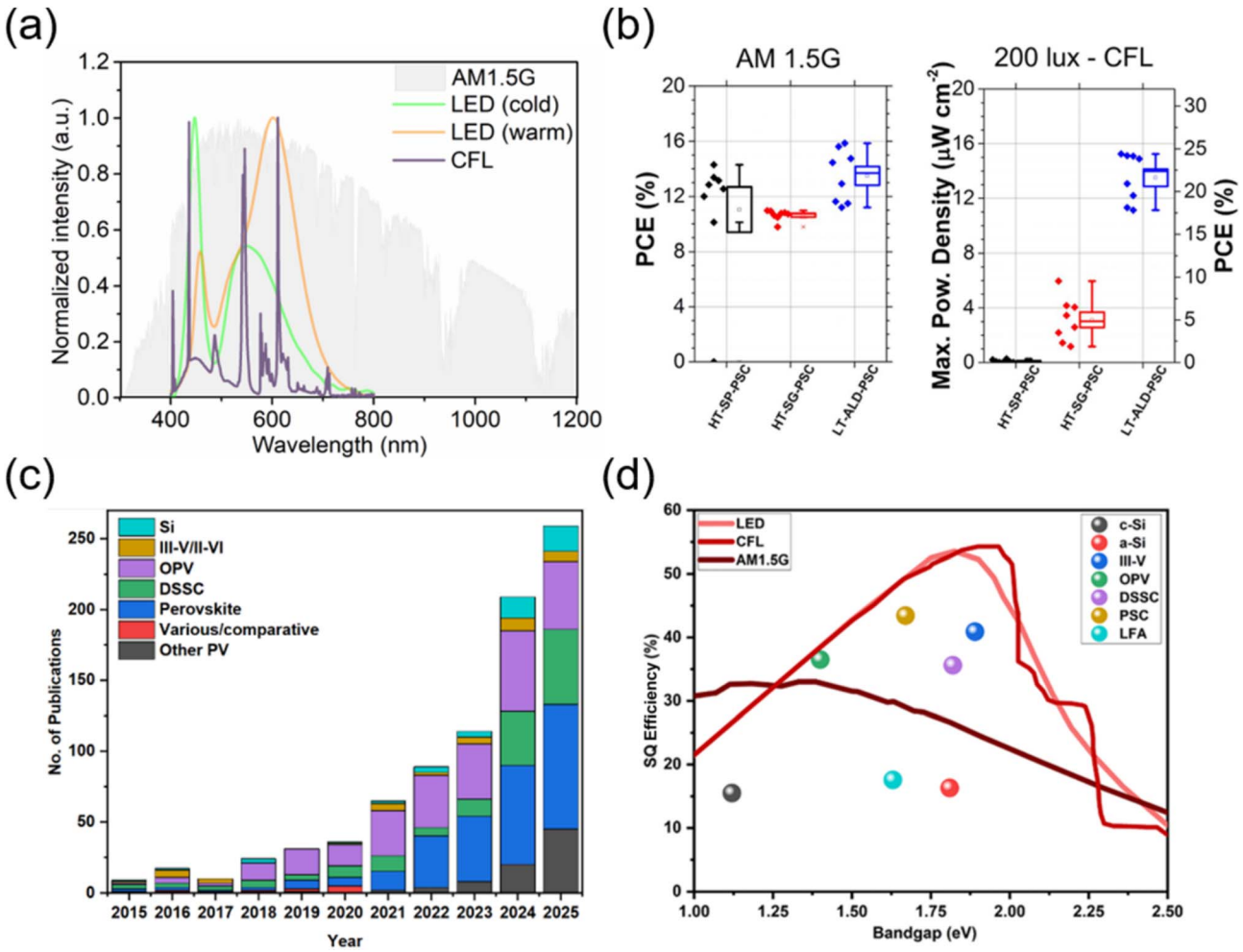

Fig. 2 (a) Emission spectra of sunlight, a white light-emitting diode (LED) and compact fluorescent light (CFL). (b) Comparison of power conversion efficiency (PCE) of the same batch devices measured under AM 1.5 G (1000 W m^{-2}) and a CFL lamp at 200 lx. Reproduced from ref. 17 with permission from Elsevier, copyright 2016. (c) Number of publications on indoor light harvesting from 2015 to 2025 according to photovoltaic technology. (d) Theoretical efficiency limit under 1 sun, LED, and CFL and the respective highest reported efficiencies of various PV technologies under 1000 lx with respect to bandgap.

Structural engineering of the electron transport layer (ETL) has been shown to effectively enhance device performance.[25,49] Dagar *et al.* demonstrated that a solution-processed tin oxide (SnO_2)/magnesium oxide (MgO) composite ETL improved efficiency by ~20% compared with devices using only SnO_2. The thin MgO capping layer promoted film uniformity, suppressed interfacial carrier recombination, and enhanced device stability (Fig. 4a).[25] Trap passivation, including additive engineering and interface engineering, has emerged as a crucial strategy for enhancing the indoor PV efficiency, for both narrow bandgap and wide bandgap PSCs.[50–54] He *et al.* incorporated guanidinium ions into the $(FAPbI_3)_{0.97}(MAPbBr_3)_{0.03}$ perovskite (with a bandgap of 1.59 eV) and employed the CH_3O-PEABr interface for perovskite surface passivation. These approaches effectively mitigated defects at the grain boundaries of the perovskite film, resulting in a tenfold and fivefold increase in the charge carrier lifetime at the crystal surface and in the bulk, respectively. As a result, indoor PV efficiency was enhanced to 40.1% (Fig. 4b). This marks the first instance of indoor efficiency surpassing the 40% threshold.[39] Remarkably, this efficiency corresponds to ~80% of the theoretical maximum (~50%) for 1.59 eV narrow bandgap cells.[35] Wang *et al.* fabricated devices with $FA_{0.92}$-$MA_{0.08}PbI_3$ (E_g = 1.53 eV) perovskite using 6-methoxynicotinamide hydrochloride (APO) as an additive to passivate intrinsic defects within the perovskite. The devices achieved a record PCE of 45.5% with a high V_{OC} of 1.15 V and FF of 85.2% measured under 1000 lx LED illumination and low-temperature extreme conditions (198 K) (Fig. 4e), demonstrating the capability of this type of perovskite for energy conversion applications in harsh environments such as outer space and polar regions.[30] It should be noted that indoor PCE values are strongly dependent on spectral irradiance, illuminance, calibration methodology, device type, and testing environments, and therefore are not directly comparable across different studies.[55–58] Nevertheless, these results demonstrate the strong capability of PSCs to achieve high efficiency under specific artificial lighting conditions. In October 2025, Li *et al.* reported an asymmetric isothiourea–guanidine hybrid dihydrochloride

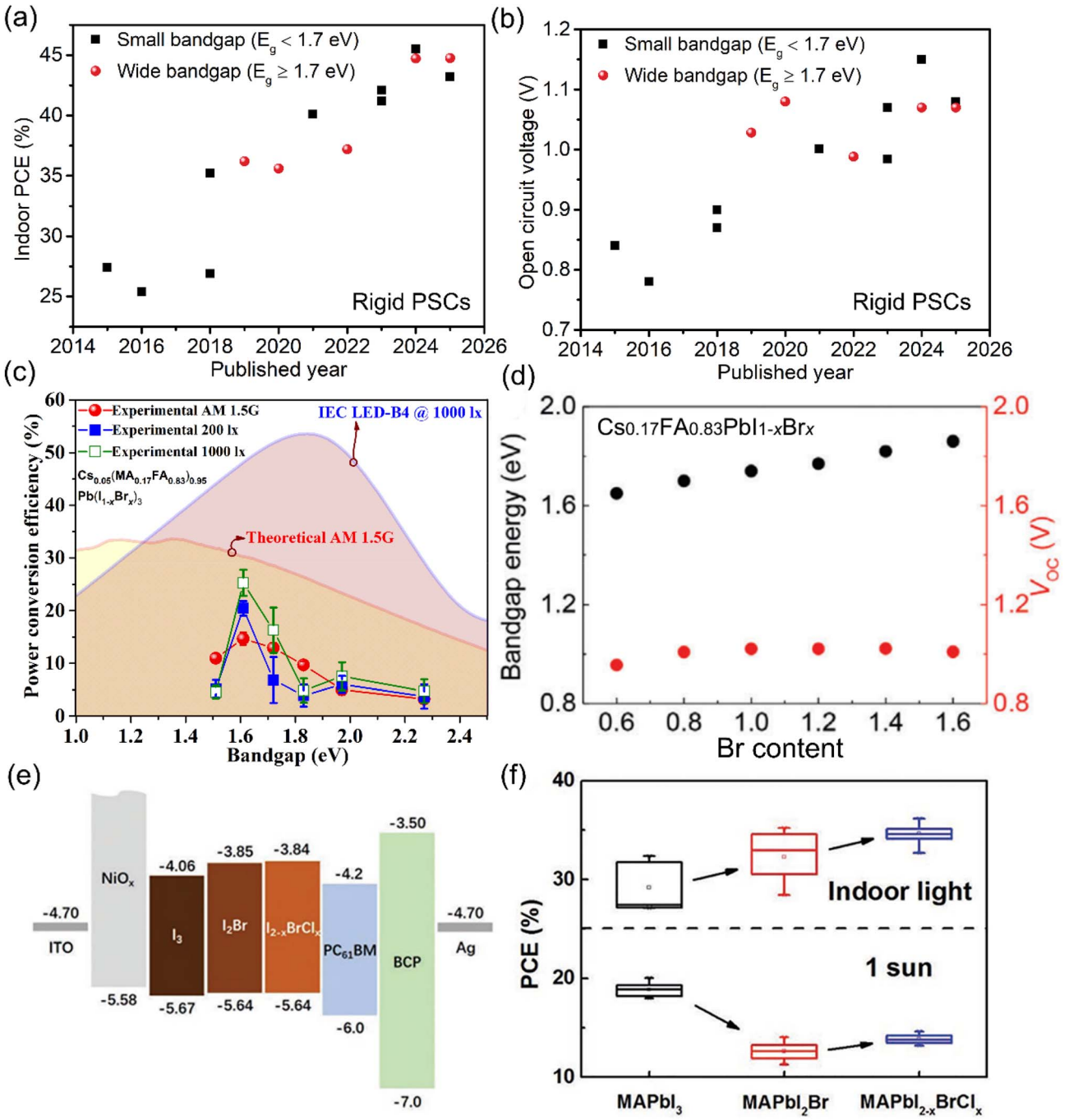

Fig. 3 (a) Summary of indoor power conversion efficiency (PCE) and (b) corresponding open circuit voltage (V_{OC}) of the representative devices from articles published in 2015,[33] 2016,[17] 2018,[25,36] 2019,[37] 2020,[38] 2021,[39] 2022,[40] 2023,[41,42] 2024,[29,30] and 2025,[43,44] using perovskites with bandgaps (E_g) ≥1.7 eV (red circles) and <1.7 eV (black squares). (c) The average PCE of experimental $Cs_{0.05}(MA_{0.17}FA_{0.83})_{0.95}Pb(I_{1-x}Br_x)_3$ devices as a function of bandgap, compared with the theoretical maximum PCE (Shockley–Queisser limit/SQ limit/detailed balance limit) under AM 1.5 G (1000 W m^{-2}) illumination and 1000 lx LED-B4 indoor lighting (IEC 62607-7-2).[45] The figure is adapted from ref. 35 with permission from American Chemical Society, copyright 2023; specifically, the SQ limit under LED-B4 illumination was extracted from ref. 46 and replaces the originally used SQ limit of the theoretical white LED. (d) Bandgap energy and V_{OC} of the $Cs_{0.17}FA_{0.83}PbI_{1-x}Br_x$ based solar cells as a function of Br content. Reproduced from ref. 31 with permission from Wiley-VCH GmbH, copyright 2022. (e) Band alignment of the $MAPbI_3$ (E_g = 1.61 eV), $MAPbI_2Br$ (E_g = 1.79 eV) and $MAPbI_{2-x}BrCl_x$ (E_g = 1.80 eV) devices including transport layers and electrodes. Reproduced from ref. 37 with permission from John Wiley and Sons, copyright 2019. (f) The statistics of PCE for these three types of devices under 1 sun and a fluorescent lamp at 1000 lx, respectively. Reproduced from ref. 37 with permission from John Wiley and Sons, copyright 2019.

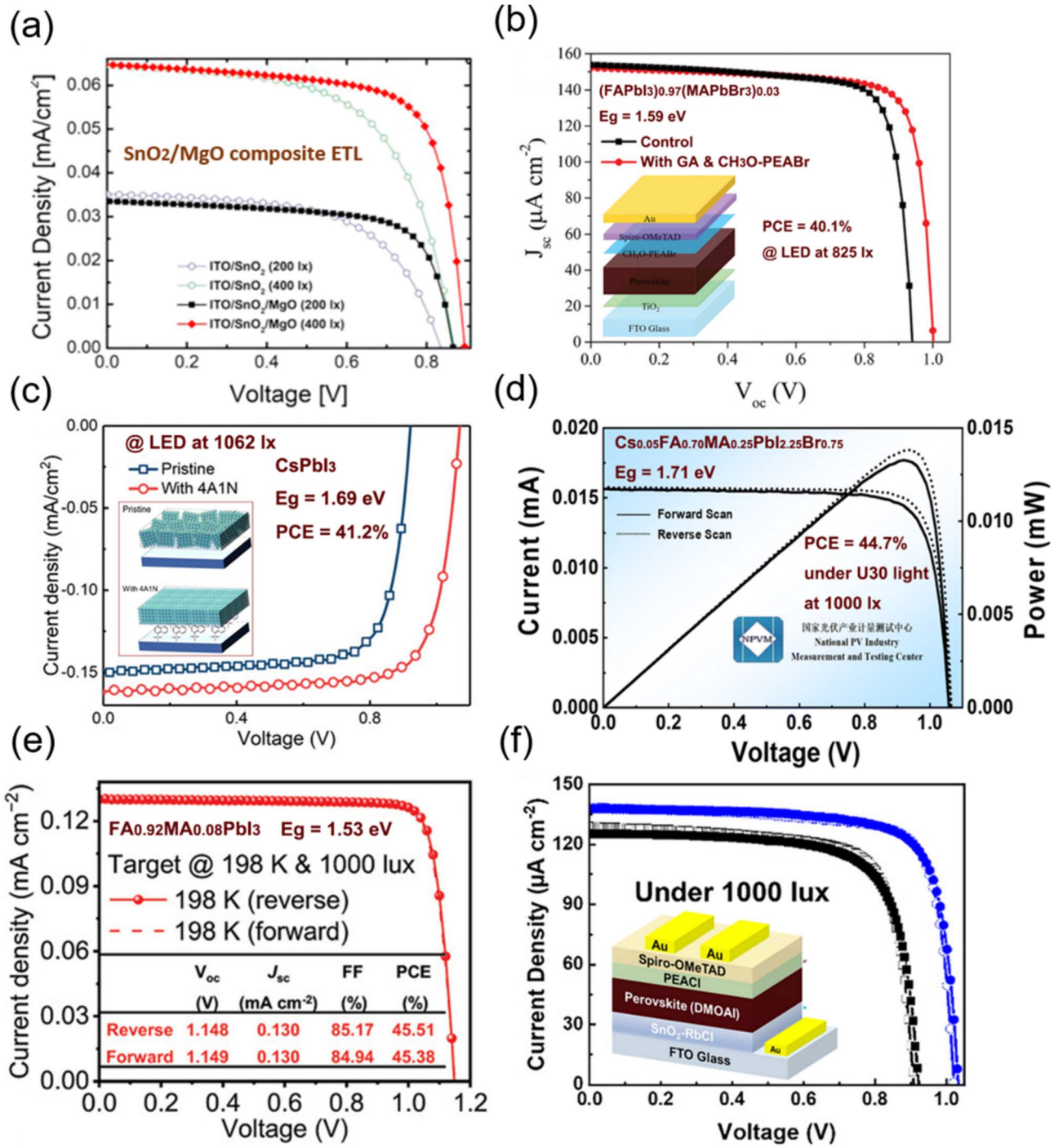

Fig. 4 (a) Current density–voltage (J–V) curves for the $CH_3NH_3PbI_3$ based perovskite solar cells (PSCs) with/without MgO as a composite SnO_2-based electron transport layer (ETL), measured under 200 and 400 lx LED illumination. Adapted from ref. 25 with permission from Elsevier, copyright 2018. (b) J–V curves for the $(FAPbI_3)_{0.97}(MAPbBr_3)_{0.03}$ (E_g = 1.59 eV) PSCs with/without GA incorporation in the perovskite bulk and CH_3O-PEABr as the interface, measured under 824.5 lx LED illumination (301.6 μW cm^{-2}). The inset shows the device architecture. Adapted from ref. 39 with permission from Wiley-VCH GmbH, copyright 2021. (c) J–V curves of the $CsPbI_3$ (E_g = 1.69 eV) PSCs with/without the 4A1N molecule as a buried interface. The inset shows a schematic diagram of perovskite grown on TiO_2. Adapted from ref. 42 with permission from Wiley-VCH GmbH, copyright 2023. (d) Indoor current–voltage (I–V) curves of the $Cs_{0.05}FA_{0.70}MA_{0.25}PbI_{2.25}Br_{0.75}$ (E_g = 1.71 eV) PSCs with oleylammonium iodide and trichloromethane as dual additives under 1000 lx U30 light, certified by the Chinese National PV Industry Measurement and Testing Center (NPVM). Adapted from ref. 29 with permission from RSC Publishing, copyright 2024. (e) J–V curves of the $FA_{0.92}MA_{0.08}PbI_3$ (E_g = 1.53 eV) PSCs with a 6-methoxynicotinamide hydrochloride (APO) additive, measured under 1000 lx LED illumination and low-temperature conditions (198 K). Adapted from ref. 30 with permission from Wiley-VCH GmbH, copyright 2024. (f) J–V curves for the $FA_{0.64}MA_{0.36}Pb(I_{0.64}Br_{0.36})_3$ (E_g = 1.75 eV) PSCs with/without a triple synergistic passivation strategy combining RbCl, DMOAI, and PEACl, measured under 1000 lx LED illumination. Reproduced from ref. 50 with permission from Wiley-VCH GmbH, copyright 2025.

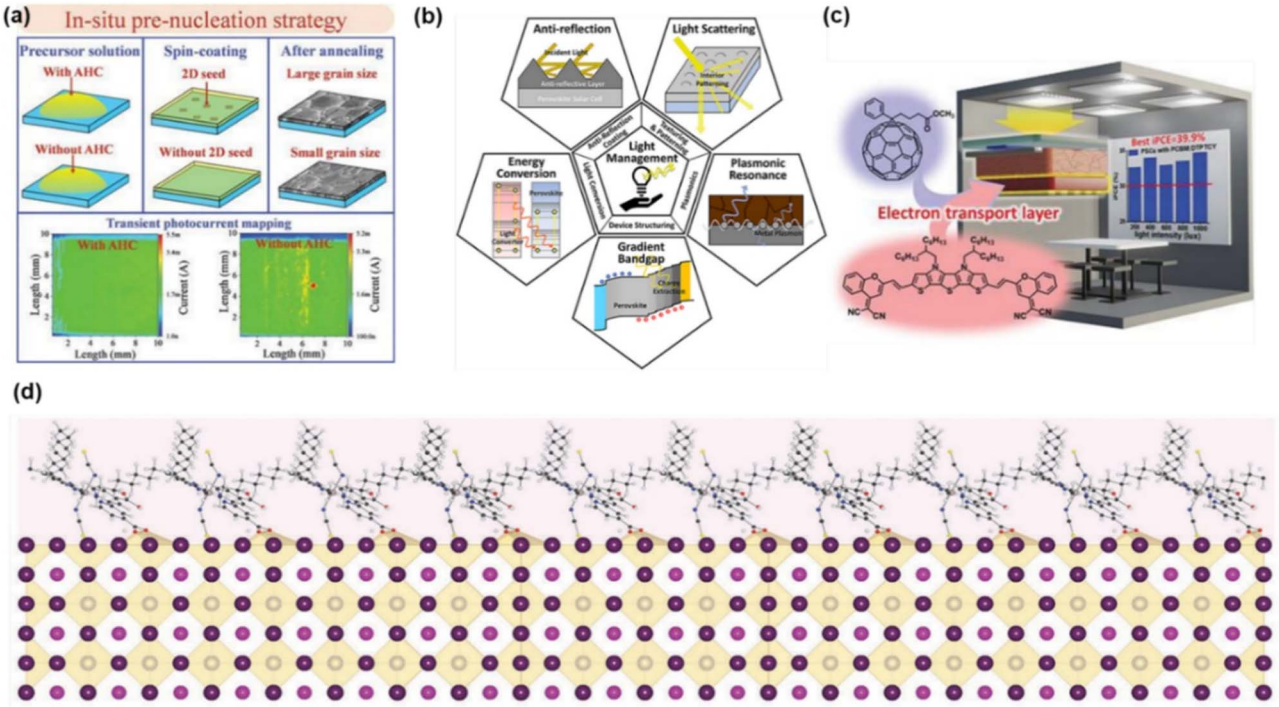

Fig. 5 (a) β-Alaninamide hydrochloride (AHC) is utilized to spontaneously form a layer of 2D perovskite nucleation seeds for improved film uniformity, crystallization quality, and solar cell performance. Reproduced from ref. 41 with permission from Wiley-VCH GmbH, copyright 2023. (b) Anti-reflection coatings, up and down conversions, plasmonic phenomena, and device structure adjustment have been used to ensure the effectiveness and potential of PSCs for optimum device operation. Reproduced from ref. 70 with permission from Elsevier, copyright 2023. (c) Employing PCBM:DTPTCY as the ETL results in passivation perovskite defects, facilitation of energy alignment at the ETL/perovskite interface, and enhancement of carrier transport efficiency. Reproduced from ref. 94 with permission from Wiley-VCH GmbH, copyright 2023. (d) Schematic diagram of the configuration of the SAM on the perovskite surface. Reproduced from ref. 92 with permission from Wiley-VCH GmbH, copyright 2022.

additive for $FA_{0.9}Cs_{0.1}PbI_3$ perovskite (with a bandgap of 1.53 eV). The isothiourea moieties selectively directed crystal growth along the (001) plane and suppressed the formation of dimethyl sulfoxide-PbI_2 and other undesirable intermediate phases. Meanwhile, the guanidine groups anchored iodide ions through N–H···I hydrogen bonding, thereby reducing the activation energy for ion migration. As a result, the perovskite films exhibited lower defect density and relieved residual stress, leading to a PCE of 44.60% under 1000 lx LED illumination (3000 K).[59] Moreover, optimization of the hole transport layer (HTL) is critical for improving device performance. In 2026, Chen *et al.* compared NiO_x films deposited by DC magnetron sputtering (DCMS) and high-power pulsed magnetron sputtering (HiPIMS) at different oxygen flow ratios (f_{O_2}). Optimal performance was achieved at 70% (DCMS) and 50% (HiPIMS), with HiPIMS showing slightly superior results due to reduced interfacial defects, enhanced charge transport and suppressed recombination, delivering a PCE of 40.5% under 1000 lx LED illumination (3000 K).[60] In 2026, it was reported that incorporating a phthalocyanine interlayer between the self-assembled monolayer (SAM) and the perovskite in a p-i-n device increased efficiency by ~10%, reaching a PCE of 30% under 1250 lx white LED illumination.[61]

Advancement of wide bandgap PSC-based technology is crucial for attaining elevated indoor photovoltaic efficiencies (*e.g.*, close or beyond the threshold of 50%).[46,62,63] Wang *et al.* employed wide bandgap (1.69 eV) all-inorganic $CsPbI_3$ as an absorber and functionalized the titanium oxide (TiO_2) layer using amino naphthalene sulfonates. High-quality perovskite films with large-sized grains were obtained by anchoring the $CsPbI_3$ perovskite crystal grains with a strong ion-dipole interaction, and the device achieved a high indoor PCE of up to 41.2% under 1062 lx LED illumination (Fig. 4c).[42] Minimizing bulk trap defects in bromine-enriched wide-bandgap perovskites is essential for elevating both V_{OC} and fill factor (FF) towards high-performance indoor photovoltaics.[64] Ma *et al.* reported an effective defect passivation strategy by introducing oleylammonium iodide solution in trichloromethane as a dual additive to the wide-bandgap $Cs_{0.05}FA_{0.70}MA_{0.25}PbI_{2.25}Br_{0.75}$ perovskite (1.71 eV) precursors.[29] This approach facilitates the formation of a high quality and less-defective perovskite film with mitigated halide segregation, leading to suppression of non-radiative recombination losses. As a result, the cell achieved a certified record PCE of 44.7% with a high V_{OC} of 1.07 V and FF of 82.3% under 1000 lx U30 light (338.2 μW cm^{-2}) (Fig. 4d) and a record PCE of 42.9% under 1000 lx LED (3000 K) illumination (301.9 μW cm^{-2}). Subsequently, the same group introduced chloroform ($CHCl_3$) surface treatment for the NiO_x layer, which optimized its surface morphology and electrical conductivity while reducing trap-assisted recombination at the

Table 1 Summary of device stability under continuous indoor illumination

Device architecture	Perovskite composition	Stability test conditions	Main results	Ref.
FTO/TiO_2/4A1N/perovskite/Spiro-OMeTAD/Ag	$CsPbI_3$	Under continuous LED (2956 K, 1062 lx) illumination at their MPP in an N_2 glovebox (≈ 20–25 °C)	Reserved ≈ 91% of its initial PCE after 540 h	42
ITO/NiO_x/perovskite/PCBM/BCP)/Ag	$MAPbI_{2-x}BrCl_x$	Devices were encapsulated and kept under continuous light soaking (1000 lx fluorescent light)	Devices sustained over 95% of original i-PCE after aging for 85 days	37
Glass/FTO/SnO_2–PbO/SnO_2/perovskite/Spiro-OMeTAD/Au	$MAPbI_3$	Unencapsulated 1 cm^2 devices were kept under continuous light soaking (300 ± 30 lx white-light LED) in a N_2 atmosphere	Devices retained ~93% of original PCE after 250 h	100
Glass/ITO/PTAA/perovskite/PEACl/C_{60}/BCP/Ag	$(FA_{0.6}MA_{0.4})_{0.9}Cs_{0.1}Pb(I_{0.6}Br_{0.4})_3$	Unencapsulated devices were kept under continuous light soaking (1000 lx white LED light) in a N_2 atmosphere	Devices retained >96% of their initial efficiencies in over 1000 h	38
Glass/ITO/SnO_2/perovskite/Spiro-OMeTAD/Au	$Cs_{0.17}FA_{0.83}Pb(I_{0.6}Br_{0.4})_3$	Unencapsulated devices were kept under continuous light soaking (1000 lx white LED light) in a N_2 atmosphere	Devices retained >83% of their initial efficiencies in over 1200 h	96
Glass/ITO/SnO_2/perovskite/Spiro-OMeTAD/Au	$(FAPbI_3)_{0.85}(MAPbBr_3)_{0.15}$	Unencapsulated devices were kept under continuous light soaking (1000 lx white LED light) under ambient air conditions with controlled humidity (relative humidity at 25–35%)	Devices retained >80% of their initial efficiencies in over 800 h	101
FTO/c-TiO_2/mTiO_2/Li_2CO_3/perovskite/DTAQTPPO/spiro-OMeTAD/Au	$FAPbI_3$	Unencapsulated devices were kept under continuous light soaking (1000 lx white LED light) in a N_2 atmosphere	Devices retained >80% of their initial efficiencies in over 2000 h	54
ITO/MeO-2PACz/2D perovskite/$PC_{61}BM$/BCP/Ag	$EDA(FA)_4Pb_5I_{16}$ ($n = 5$)	Unencapsulated devices were kept under continuous light soaking (1000 lx white LED light) under ambient air conditions with controlled humidity (relative humidity at 85%)	Devices retained ~95% of original PCE after 53 h	52

NiO_x/perovskite interface. This interfacial engineering further enabled an outstanding indoor PCE of 44.74% under LED illumination (1000 lx, 301.9 μW cm^{-2}, 3000 K).[43] Notably, this efficiency of ~45% corresponds to nearly 80% of the theoretical maximum efficiency (56.4%) for 1.71 eV wide bandgap PSCs.[29] Huang *et al.* developed a triple synergistic passivation strategy combining rubidium chloride (RbCl), *N*,*N*-dimethyloctylammonium iodide (DMOAI), and phenethylammonium chloride (PEACl) to enhance wide-bandgap $FA_{0.64}MA_{0.36}Pb(I_{0.64}Br_{0.36})_3$ solar cells (E_g = 1.75 eV). RbCl facilitated uniform crystal growth, relieved lattice strain, and reduced interfacial energy barriers, while DMOAI and PEACl suppressed bulk and surface defects and photoinduced halide segregation. Collectively, these improvements yielded a 110 mV increase in V_{OC} under 1000 lx and a PCE of 37.6% (Fig. 4f).[50]

Among the many strategies for improving indoor PV performance, low-dimensional perovskites (*e.g.*, quasi-two dimensional (2D) Ruddlesden–Popper phases) have shown promise in both widening the bandgap and improving intrinsic material stability under ambient conditions (Fig. 5a).[41,52] Another important design consideration is minimizing voltage losses associated with increased bandgap, which tend to amplify non-radiative recombination. Strategies such as optimizing energy-level alignment at the interfaces and using surface passivation layers have proven effective in suppressing trap-assisted recombination, thereby preserving V_{OC} and fill factor.[64–69] Furthermore, light management techniques such as photon recycling, photonic crystals, or reflective back electrodes (*e.g.*, ITO/Ag multilayers) can be integrated to enhance light absorption, compensating for the lower irradiance in indoor settings (Fig. 5b).[70–72] Under indoor light, the impact of defects is significantly amplified because the rate of photogenerated carrier generation is much lower than that under outdoor conditions. This makes defect-induced non-radiative recombination a primary limiting factor for device performance.[73–77] Therefore, managing both bulk and interfacial defects is crucial for high-performance indoor perovskite devices.[43,78–81] Improving the crystallinity and morphology of the perovskite films is a key approach to reducing bulk defects.[74,82–87] Advanced film formation techniques—such as antisolvent dripping with thermal control, gas-assisted crystallization, or vacuum-flash-assisted solution processing—enable the formation of large-grain, high-purity films with fewer grain boundaries and lower trap density.[88,89] In addition, mild annealing processes under controlled ambient conditions can reduce halide vacancies and Pb-related defects that otherwise serve as recombination centers. Interfacial defect passivation is equally critical, especially since carrier extraction is more sensitive to energy-level mismatches and traps under low-light operation.[90,91] Incorporation of self-assembled monolayers (SAMs)[92,93] or Lewis base molecules has been shown to effectively passivate under-coordinated Pb^{2+} sites and improve charge transfer across interfaces (Fig. 5d).[92] Recent studies have also demonstrated the use of multifunctional small molecules containing both ammonium and carboxylic groups (Fig. 5c), which can simultaneously passivate surface and grain boundary defects.[94] Although the theoretical gains in developing tandem

architectures under the narrower spectra of artificial light are smaller compared to standard test conditions (1 sun), they could enable to reach the 60% efficiency threshold.[71,95] The first experimental tandem cell for indoors was demonstrated in 2026 delivering a PCE of 30.1% under cold white LED light at 1000 lx.[95]

Research on stability of indoor PSCs should be conducted using specific tests compared to those used for outdoors. Unlike some of the harsher tests of the ISOS protocols, indoor PV cells are usually operated in a milder environment, such as using indoor lighting with lower light intensity and without ultraviolet or infrared radiation.[14] However, there is limited research on the stability of indoor PSCs. Some studies have shown that PSCs demonstrate good operational stability under continuous light soaking under indoor light sources. For instance, Cheng *et al.*[37] (Table 1) used a tailored triple-anion perovskite material in a device with the structure ITO/NiO_x/perovskite/PCBM/BCP/Ag. The encapsulated device retained 95% of its initial efficiency after over 2000 hours of continuous illumination under 1000 lx fluorescent light. Similarly, Li *et al.*[38] reported that triple-cation PSCs with the structure Glass/ITO/PTAA/perovskite/PEACl/C_{60}/BCP/Ag showed good stability during light exposure, with an unencapsulated device retaining 96% of its initial efficiency after 1000 hours of 1000 lx continuous LED light in a nitrogen atmosphere. Lee *et al.* constructed a 2D/3D bilayer by self-assembling a BA_2PbBr_4 layer beneath a wide-bandgap $Cs_{0.17}FA_{0.83}Pb(I_{0.6}Br_{0.4})_3$ perovskite on SnO_2, boosting efficiency from 38.2% to 43.7% and markedly improving stability. The unencapsulated device retained 83% of its initial efficiency after 1200 hours of continuous irradiation under 1000 lx LED light.[96] On the other hand, studies have indicated that indoor PV devices are more sensitive to defects, with the creation of defects in the PV devices leading to faster performance degradation compared to the very same device but tested under standard test conditions (STC).[19,35,97] In addition, since there is no widely accepted testing method for indoor PV stability assessment, it is difficult to compare test results from different laboratories. Even under continuous illumination test conditions, different test environments, such as temperature and humidity during device testing, can have a significant impact on the test results.[98] Therefore, it is crucial to standardize indoor PV stability testing methods and systematically study the performance of PSCs in the future and to consider conducting tests under real indoor environmental conditions.[99]

3 Flexible lead-halide perovskite solar cells for indoor photovoltaics

Using plastic films in PV products offers several advantages, such as making them light weight, increasing their specific power per unit of mass, and allowing easy integration with various surfaces.[102–104] PSCs are especially well-suited for new-generation PV applications due to their ability to be printed and integrated on a variety of thin flexible substrates in different forms and material types. This enables applications in both outdoor and indoor settings that are not achievable with traditional PV devices,[105] including smart buildings,[106] wearable and portable electronic devices,[107] wireless sensor networks[108] and self-powered IoT.[109,110] Additionally, the manufacturing process of flexible PSCs is relatively simple and cost-effective compared to flexible silicon PVs, which is currently the main PV technology commercially considered for indoor applications.[111] However, most literature on flexible perovskite PVs has primarily focused on a few indoor lighting cases, mostly under AM 1.5 G, 1000 W m^{-2}, conditions.

Highlights of reports on indoor flexible PSCs from 2017 to 2024 are shown in Fig. 6. A 2017 study by Lucarelli *et al.* developed the first-ever flexible PSCs for indoor light-harvesting.[24] They used a low-temperature atomic-layer (AL)-deposited compact TiO_2 layer combined with a UV-sintered mesoporous TiO_2, fabricated on a flexible plastic polyethylene terephthalate (PET) substrate highlighting the importance of low-temperature processes. Under white LED (WLED) light, the fabricated mesoscopic flexible indoor PSCs delivered efficiencies of 10.8% at 200 lx and 12.1% at 400 lx, with Maximum Power Densities (MPDs) of 7.2 and 16.0 μW cm^{-2}, respectively (Fig. 6a). They also observed that both mesoscopic and planar devices based on a sol–gel deposited compact layer exhibited poor indoor performance, even under AM 1.5 G illumination. The same group in 2018 reported[112] a fully solution-processed SnO_2/meso-TiO_2 ETL in flexible PSCs using a PET/ITO substrate. These flexible PSCs achieved an indoor PCE of 12.8% (MPD = 9.77 μW cm^{-2}) and 13.3% (MPD = 19.2 μW cm^{-2}) under 200 and 400 lx WLED illumination. The UV lamp-heated TiO_2 scaffold provided a low-temperature, efficient method to enhance the wettability of flexible substrates, improve rectification ratios, increase shunt resistance, and reduce series resistance. Through this bilayer ETL strategy, they fabricated the first laser-patterned flexible perovskite module with a PCE of 8.8% under 1 sun illumination. Consistent with this concept, Castro-Hermosa *et al.*[27] used ultra-thin (100 μm) flexible glass (FG) substrates coated with sputtered ITO through roll-to-roll processing and rotatable magnetron sputtering, as a novel flexible substrate for indoor PSCs. These FG/ITO substrates showed sheet resistances as low as 13 Ohm per sq and an impressive transparency level of around 81%, comparable to standard ITO coatings on glass and PET substrates. Additionally, they demonstrated flexibility, enduring over 1600 bending cycles at a curvature of 20.5 mm. Consequently, efficiencies of 20.6% (MPD = 16.7 μW cm^{-2}) and 22.6% (MPD = 35.0 μW cm^{-2}) were achieved under 200 and 400 lx WLED illumination (Fig. 6b), setting a record for indoor flexible solar cell technology efficiency in May 2020.

Solvent engineering is essential for achieving the ideal perovskite morphology with high crystallinity, which is crucial for efficient devices. Following that, Kim *et al.*[116] substituted toxic chlorobenzene (CB) with a novel green anti-solvent, butyl acetate (BA), to fabricate high-quality perovskite layers with enhanced grain size, improved charge carrier mobility, and reduced trap densities. As a result, their flexible indoor devices on polyethylene naphthalate (PEN)/ITO substrates exhibited efficiencies of 23.3% (with a MPD of 63 μW cm^{-2}) under 400 lx and 25.7% (MPD of 175 μW cm^{-2}) under 1000 lx WLED

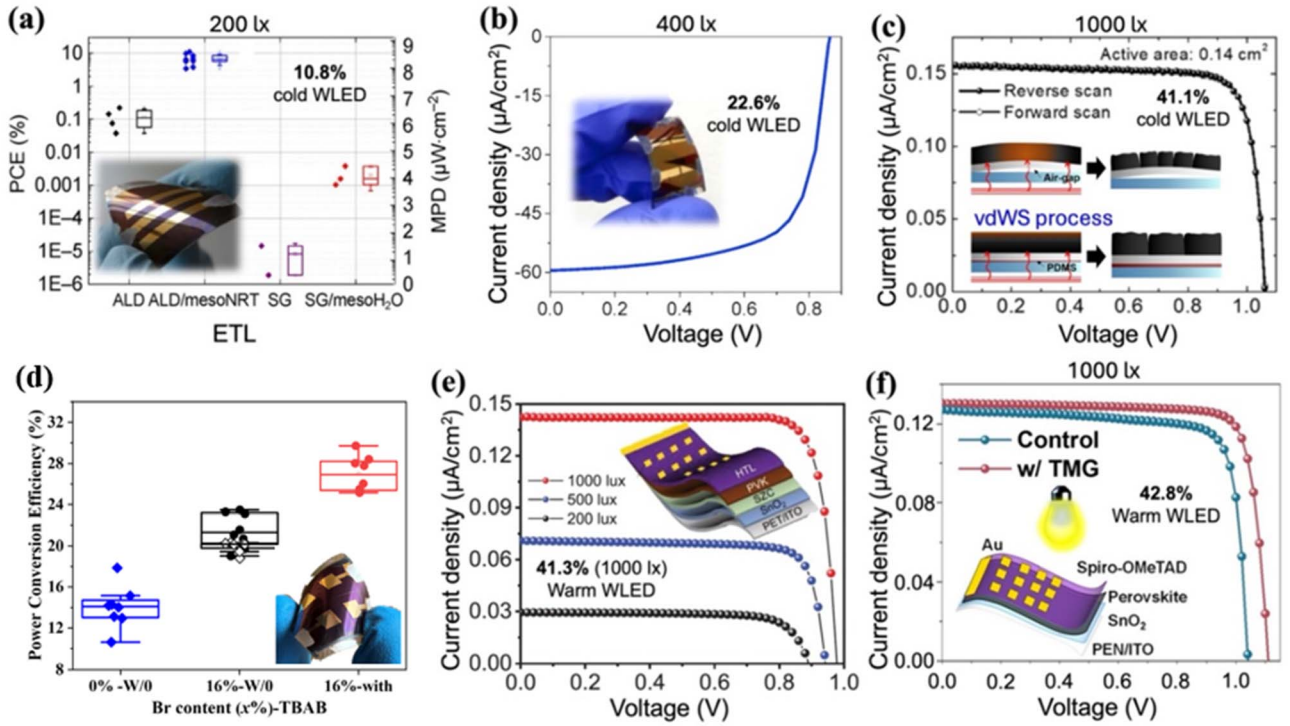

Fig. 6 (a) Power conversion efficiencies and maximum power densities of the first indoor flexible PSCs for planar and mesoscopic flexible solar cells based on two different compact layers that consist of compact TiO_2 deposited by atomic layer deposition (ALD) or by spin coating a TiO_2 sol, measured under 200 lx cold LED illumination. The inset shows an image of the fabricated flexible PSC. Adapted from ref. 24 with permission from Springer Nature, copyright 2017. (b) Current density–voltage (J–V) curve of the first flexible PSCs on an ultra-thin flexible glass (FG) substrate with device architecture FG/ITO/SnO_2/m-TiO_2/$CH_3NH_3PbI_3$/Spiro-MeOTAD/Au, measured under 400 lx cold LED illumination. The inset shows an image of the fabricated flexible PSC. Adapted from ref. 27 with permission from Elsevier, copyright 2020. (c) J–V curves of the champion flexible PSC fabricated by the van der Waals (vdWS)-induced lift-off process/oleylamine (OLA) perovskite treatment/vacuum process, measured under 1000 lx cold LED illumination. The inset shows a schematic of the annealing behavior in the conventional tape-holding process (control) and the vdWS-induced lift-off process, highlighting their effects on perovskite crystallization. Adapted from ref. 113 with permission from American Chemical Society, copyright 2022. (d) Box charts of the PCE obtained using $Cs_{0.08}(FA_{0.78}MA_{0.16})Pb(I_{0.84}Br_x)_3$ ($x = 0$ and 0.16) perovskites without (W/0) and with TBAB treatment with device architecture PET/ITO/SnO_2/triple-cation perovskite/Spiro-MeOTAD/Au, measured under a 230 ± 30 lx cold LED lamp. The inset shows an image of the fabricated flexible PSC. Adapted from ref. 26 with permission from Wiley-VCH GmbH, copyright 2023. (e) J–V curves of the champion flexible PSC with a 2-cyanoacetate (SZC) additive at the perovskite-buried interface, measured under a warm LED lamp at 200, 500, and 1000 lx. The inset shows a schematic of the fabricated device architecture. Adapted from ref. 114 with permission from Wiley-VCH GmbH, copyright 2024. (f) J–V curves of the champion flexible PSCs fabricated without (control) and with 1,1,3,3-tetramethylguanidine hydrochloride (TMG) slat incorporation, measured under a warm LED lamp at 1000 lx. The inset shows a schematic of the fabricated device architecture. Reproduced from ref. 115 with permission from AIP Publishing, copyright 2025.

illumination. In another report from November 2021,[117] a 3,4-ethylenedioxythiophene (EDOT)-assisted green anti-solvent strategy was used to create annealing-free rigid and flexible PSCs for both indoor and outdoor applications, aiming to accelerate the commercialization of PSCs. The flexible devices demonstrated excellent indoor performance with an efficiency of 22.8% at 1000 lx, thanks to enlarged crystal grain size and fewer defects in the synthesized triple-cation perovskite film.

Given the importance of mechanical stability in flexible devices for various indoor applications, research is increasingly focusing on enhancing mechanical flexibility. In the study conducted by Chen *et al.* in 2022,[118] they improved the mechanical and phase stabilities of perovskite films using a 3D crosslinking borax-grain boundary penetration treatment strategy, inspired by balloon glue, to achieve full-dimensional stress release in the perovskite film. This treatment resulted in lower trap states under weaker illumination from a warm WLED lamp, leading to a new record indoor efficiency of 30.7% (MPD = 20.5 μW cm^{-2}) at 212 lx and 31.9% (MPD = 106 μW cm^{-2}) at 1062 lx for flexible PSCs on a PEN/ITO substrate.

The annealing process critically affects the crystallization of perovskite films on flexible substrates, but air gaps caused by substrate warping can hinder heat transfer and lead to irregular phase change and crystallinity of perovskite films.[113] To overcome this drawback and enhance the performance of flexible PSCs under indoor and outdoor illumination, Gong *et al.*[113] developed a van der Waals stacking (vdWS)-induced lift-off process through a polydimethylsiloxane (PDMS) layer. This strategy created an air-gap-free interface in the glass/PDMS/ITO/PEN substrate, ensuring uniform heat transfer. The best-performing flexible devices achieved a PCE of 41.3% under 1000 lx WLED illumination (Fig. 6c), achieving a record

Table 2 Summary of indoor flexible PSCs with reported PCE. Given the diversity of indoor lighting conditions and measurement protocols, the reported efficiencies are intended to illustrate overall progress rather than enable direct comparison

Layer structure	Relevant literature	Reported PCE [%]	Maximum power density [μW cm^{-2}]	Active area [cm^2]	Light source	Illuminance [lx]
PET/ITO/c-TiO_2/m-TiO_2/PVSK/Spiro-OMeTAD/Au	24	10.8	7.2	0.2	Cold WLED	200
		12.1	16.0			400
PET/ITO/SnO_2/m-TiO_2/PVSK/Spiro-OMeTAD/Au	112	12.8	9.8	0.1	Cold WLED	200
		13.3	19.2			400
FG/ITO/SnO_2/m-TiO_2/PVSK/Spiro-OMeTAD/Au	27	20.6	16.7	0.1	Cold WLED	200
		22.6	35.0			400
PEN/ITO/SnO_2/PVSK/Spiro-OMeTAD/Au	116	23.3	63.0	0.12	Cold WLED	400
		25.7	175.0			1000
Plastic/ITO/SnO_2/PVSK/MoO_3/Ag	117	22.8		0.1		1000
PEN/ITO/SnO_2/PVSK/MoO_3/Ag	118	30.7	20.5		Warm WLED	212
		31.9	106			1062
PEN/ITO/vdWS/KCl-doped SnO_2/ PVSK/OLA/Spiro-OMeTAD/Au	113	41.2		0.14	Cold WLED	1000
PET/IZO/SnO_2/PVSK/Spiro-OMeTAD/Au	120	30.0	22.9	0.64	Warm WLED	200
		30.9	121.8			1000
PET/IZO/SnO_2/PVSK/P3HT/Carbon	120	24.7	18.9	0.64	Warm WLED	200
		25.4	100			1000
PET/IZO/SnO_2/PVSK/Carbon	120	22.3	17.1	0.64	Warm WLED	200
		23.1	90.9			1000
PET/ITO/SnO_2/3D PVSK/ 2D PVSK/OAI/Carbon	121	18.6	~70.0	0.64	Warm WLED	1000
PET/ITO/SnO_2/3D PVSK/	26	28.9	23.2	0.09	Cold WLED	200
1D PVSK/TBAB/Spiro-OMeTAD/Au		32.5	127.8			1000
PEN/ITO/NiO_x/PTAA/PVSK/C_{60}/SnO_2/Ag	122	36.1		0.09	Warm WLED	1000
PET/ITO/SnO_2/SZC/PVSK/Spiro-OMeTAD/Au	114	35.5	19.9	0.07	Warm WLED	200
		39.0	53.7			500
		41.3	115.3			1000
PET/ITO/SnO_2/KCl/PVSK/PTAA/ITO	106	18.8		0.3	Cold WLED	1200
Light-function sticker/PEN/ITO/ PTAA/Al_2O_3/PVSK/C_{60}/SnO_2/Ag	123	36.7	192.2	0.09	Warm WLED	1000
PET/ITO/NiO/SAM/PVSK/C_{60}/SnO_2/Cu	104	36.3		0.08	Warm WLED	1000
PEN/ITO/SnO_2/PVSK/Spiro-OMeTAD/Au	115	42.8	119	0.07	Warm WLED	1000

efficiency of indoor flexible PSCs based on the PEN substrate in June 2022.

Great efforts have been made recently into improving the indoor performance of flexible PSCs on PET substrates. PET is preferred over PEN for flexible PSCs because it is cheaper, more widely available, and benefits from mature recycling methods.[119] In July 2022, Teixeira *et al.*[120] reported devices fabricated on PET/indium zinc oxide (IZO) substrates with efficiencies of 30.0% (MPD = 22.9 μW cm^{-2}) and 30.9% (MPD = 121.8 μW cm^{-2}) under a warm WLED at 200 and 1000 lx, respectively. Additionally, a maximum efficiency of 25.4% (24.7%) and 23.1% (22.3%) was achieved for the first carbon-based indoor flexible devices with and without the hole transport layer (HTL) under 1000 lx (200 lx), respectively. This advancement opens opportunities for fabricating indoor PSCs using roll-to-roll manufacturing processes.

To ensure the stability and efficiency of indoor PSCs, it is important to suppress defects at the interface between the absorber layer and the charge transport layer. The same research group later published a study detailing the use of a one-step slot-die coating technique, emphasizing mass production, to fabricate a 2D/3D hybrid perovskite device with an *n*-octylammonium iodide (OAI) 2D capping layer.[121] By optimizing the manufacturing process, the flexible device produced by slot-die coating a SnO_2 and perovskite layer and blade-coating a carbon electrode layer achieved a significant PCE of 18.6% under 1000 lx WLED illumination. In August 2023, Skafi *et al.* achieved a new indoor performance record for flexible PSCs on PET/ITO substrates using a dual low-temperature approach.[26] They first optimized the perovskite layer bandgap through anion mixing (a 42% PCE improvement) and then passivated the trap states of the perovskite film by incorporating tetrabutylammonium bromide (TBAB) as a low-dimensional interfacial layer at the perovskite-HTL interface (a further 26% enhancement) (Fig. 6d). This resulted in efficiencies of 28.9% (MPD = 23.3 μW cm^{-2}) and a record 32.5% (MPD = 127.8 μW cm^{-2}) under 230 ± 30 lx and 1150 ± 150 lx WLED illumination, respectively. In December 2023, Zhang *et al.*[122] demonstrated an efficiency of 36.1% under 1000 lx warm WLED illumination by optimizing interfacial adhesion using a mechanically robust porous NiO_x nanoparticle layer on PEN/ITO substrates, which improved energy level alignment and reduced carrier recombination at the interface. Focusing on interfacial energy level alignment, Liu *et al.*[114] (March 2024)

employed a molecular bridge strategy using sodium 2-cyanoacetate (SZC) at the buried perovskite interface. This approach enabled simultaneous passivation of interfacial defects (bonding between the SnO_2 transport layer and perovskite, suppression of oxygen vacancies, and mitigation of under-coordinated Pb defects) while promoting bottom–up crystallization during flexible PSC fabrication. The resulting devices achieved efficiencies of 35.5% (MPD = 19.9 μW cm^{-2}) at 200 lx and 41.3% (MPD = 115.3 μW cm^{-2}) under 1000 lx warm LED illumination (Fig. 6e). In April 2024, Jafarzadeh *et al.*[106] reported bifacial and flexible PSCs for indoor applications using a fully bromide $FAPbBr_3$ absorber. The optimized devices, featuring a potassium-treated SnO_2/perovskite interface and PTAA as the HTL, achieved front- and back-illuminated efficiencies of 18.7% and 17.8%, respectively, under 1200 lx cold LED illumination.

To overcome the persistent optical losses in flexible PSCs caused by the plastic substrate, researchers have explored strategies that extend light absorption and reduce reflection, aiming to boost photocurrent and overall efficiency. In this context, He *et al.*[123] in January 2025 introduced a dual-function film sticker combining light-trapping and light-shifting capabilities. A fluorescence down-conversion material (V570) doped in PDMS converted UV photons (<380 nm) into visible photons capable of penetrating the PEN substrate, while the low-refractive-index PDMS with an inverted pyramid structure minimized reflectivity. This approach improved the J_{SC} by ≈6% (from 121.63 to 129.23 μA cm^{-2}), yielding a PCE of 36.65% (certified 34.03%) with an MPD of 192.2 μW cm^{-2} under 1000 lx artificial light.

Although several perovskite PV devices have achieved record indoor PCEs, many still suffer from relatively low V_{OC}, which limits their practical use, as higher V_{OC} reduces the number of cells needed to power indoor electronics. Previous efforts to address this have included triple-anion perovskites, wide-bandgap tuning, and interface passivation, yielding PCEs above 40% but often with compromised V_{OC}. Moreover, flexible PSCs remain less explored, with reported PCEs up to 41.3% but V_{OC} below 1 V. To address this challenge, in July 2025 Datt *et al.*[104] developed dual-cation, mixed-halide FACsPbIBr-based PSCs, targeting a balance between a high V_{OC} of 1.11 V (≈14% higher than that reported in the literature for flexible indoor PSCs) and high PCE of 36.3% under 1000 lx illumination.

In 2025, Ma *et al.*[115] demonstrated the critical role of film growth modulation in flexible fabrication. By employing 1,1,3,3-tetramethylguanidine hydrochloride (TMG) as a crystallization mediator, they achieved ordered perovskite growth with enlarged grain sizes, reduced grain boundary density, and improved interfacial contact. The resulting devices delivered the highest reported PCE to date for flexible PSCs on PEN/ITO substrates, 42.8% (MPD = 119 μW cm^{-2}) under 1000 lx (Fig. 6f), and retained over 80% of their initial efficiency after 16 000 bending cycles, highlighting crystallization control as a key strategy to simultaneously enhance mechanical durability and carrier dynamics in flexible PSCs. More details of the published studies are provided in Table 2. It is worth noting that due to the lack of standardized indoor photovoltaic testing protocols, the reported PCEs in Table 2 offer an indicative overview of performance progress rather than precisely comparable benchmarks.[56]

These advancements result from efforts to enhance the crystal structure of perovskite films, implement interface engineering to passivate defects at the perovskite/carrier transport material interface, and improve the mechanical properties of the perovskite films. Despite these achievements, there is still room to further improve the stability and efficiency of indoor flexible PSCs through appropriate material stack combinations and effective encapsulation (such as ultra-high permeation barriers and passivation) strategies.[124] Such improvements are crucial for practical use in indoor environments, powering devices like wearable electronics, IoT devices, and indoor sensors. Furthermore, developing a manufacturing process using scalable roll-to-roll printing techniques will be vital in accelerating market entry.

4 Lead-free perovskites and perovskite-inspired derivatives for indoor photovoltaics

The development of lead-halide perovskites (LHPs) with excellent optoelectronic properties, such as outstanding charge mobility, long carrier diffusion length and lifetime, high absorption coefficient and low exciton binding energies, has shown great promise for indoor and outdoor photovoltaic applications.[125–131] A major hurdle to their commercialization has been the potential toxicity of lead and the poor stability of LHP devices under ambient conditions.[132,133] However, recent life-cycle assessment studies suggest that the environmental sustainability of perovskite photovoltaics depends on multiple factors beyond elemental considerations alone, with some lead-free alternatives exhibiting comparable or even higher environmental impacts than lead-based materials.[134–139] For instance, CH_3NH_3I alone accounts for 62.31% of human toxicity potential in perovskite devices, whereas PbI_2 contributes only 3.68%.[138] From cost and Global Warming Potential (GWP) perspectives, lead is significantly cheaper with the lowest GWP of just 1.3 kg CO_2-eq. per kg, compared to some of the proposed lead-free alternatives such as Sn, Sb, Bi, and Ag.[139] Nevertheless, the search for lead-free materials that could replicate or exceed the optoelectronic properties of LHPs continues, driven by both regulatory considerations and the goal of developing diverse material platforms for indoor photovoltaic applications.[133,134,140] Homovalent substitution of Pb by tin (Sn) led to the introduction of lead-free perovskites (LFPs) which exhibit similar structural and electronic symmetry to LHPs. These materials offer excellent optoelectronic properties such as a tunable bandgap (~1.3–1.7 eV), low exciton binding energy and long carrier diffusion lengths. However, the poor stability of Sn under ambient conditions was not as promising for long-term commercial use. The heterovalent substitution of Pb^{2+} by electronically similar trivalent metals such as bismuth (Bi^{3+}) and antimony (Sb^{3+}) led to perovskite-inspired materials (PIMs), which exhibit lower structural or electronic dimensionality than

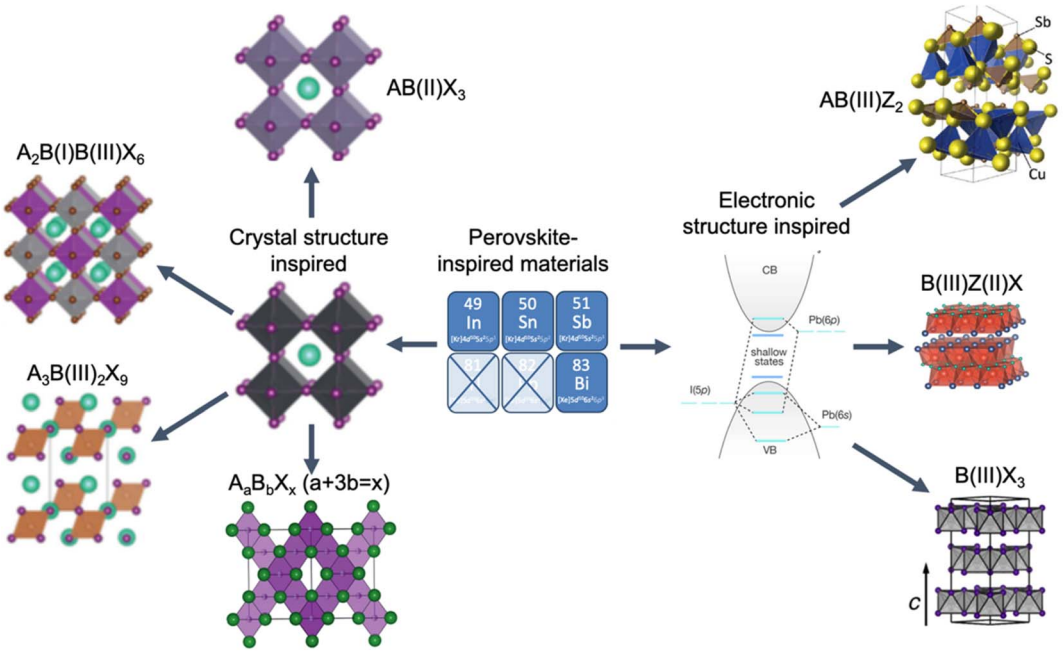

Fig. 7 Schematic showing the two strategies for finding lead-free alternatives (LFAs), based on the crystal structure and arrangement of metal-halide octahedra (LFP), or based on identifying materials that could mimic the perovskite electronic structure like in a perovskite inspired material (PIM).

LHPs but are environment-friendly and stable under ambient conditions.[130,141] These materials usually offer direct optical bandgaps tunable in the range of 1.6–2.8 eV and can be solution processed, making them potentially suitable for indoor photovoltaics.[142] Unlike Sn-based perovskites that possess the same structural and electronic symmetry as LHPs, PIMs lack the perovskite crystal structure but the trivalent metals (Bi^{3+} and Sb^{3+}) offer similar electronic symmetry to Pb^{2+}.[143] It has been proposed that such an electronic structure is conducive to defect tolerance that is highly desirable for various optoelectronic applications.[127,144] In fact, such defect tolerance has been observed in LHPs (Fig. 7), which is composed of Pb-s lone pair electrons hybridized with the I-p electrons that form the antibonding state at the valence band maximum and the Pb-p orbital hybridized with the I-p orbital forming an antibonding state in the conduction band minimum.

For simplicity, we will refer to both LFPs and PIMs as lead-free alternatives (LFAs) in the remainder of this section. The unique tunable optoelectronic properties of LFAs, combined with their compatibility with flexible substrates, have led several research groups to investigate these lead-free alternatives for indoor photovoltaics,[145] as they are expected to play an important role in emerging application areas such as smart sensors and the IoT. In this section, we discuss the performance of these LFAs under indoor lighting conditions and evaluate their ability to compete with existing emerging technologies.

4.1 Tin-based lead-free perovskites

Yang *et al.* reported the first performance of tin-based perovskites under indoor light. They used mixed halides to increase the band gap to ~1.63 eV to make them more suitable for indoor light utilization. Under 1000 lx indoor LED light, the mixed-halide tin perovskite ($FA_{0.75}MA_{0.25}SnBrI_2$) delivered a PCE of 10.45%, which was further improved to 12.81% by using an antioxidant (catechin) to suppress the oxidation of Sn^{2+} to Sn^{4+}.[146] The devices with catechin showed improved hole mobility and better stability in air when compared to the pristine devices. However, it must be mentioned that the best device was able to generate a V_{OC} and FF of only 0.28 V and 67%, respectively, and the stability of the device was generally poor, as the normalized PCE dropped by 20% in only 400 min of dark storage under ambient conditions. Later, Cao *et al.* improved the performance of the tin-based perovskite with the same composition ($FA_{0.75}MA_{0.25}SnBrI_2$) through interfacial engineering. In their work, they used potassium thiocyanate (KSCN) as an interfacial layer at the HTL/perovskite interface.[147] The interfacial engineering strategy upshifted the energy level of the perovskite, while the work function of the HTL (PEDOT: PSS) shifted downward, allowing for better energy alignment. In addition, the modified perovskite film showed efficient charge transfer, a 10-fold lower trap density of states (tDOS), and improved electron–hole mobility. The resulting perovskite device with KSCN modification delivered the highest PCE of 17.57% under 1062 lx LED illumination corresponding to a V_{OC}, J_{SC}, FF, and MPD of 0.57 V, 162 μA cm^{-2}, 64%, and 59 μW cm^{-2}, respectively (Fig. 8a). The modified device also showed improved stability, retaining 80% of its maximum PCE after 1200 h under dark storage. Wang *et al.* in 2026 found that formamidine acetate, as a vapor-deposited additive, enabled better film quality of evaporated $FASnI_2Br$ perovskite films.[148] Abdel-Shakour *et al.*[149] presented a new method for precisely

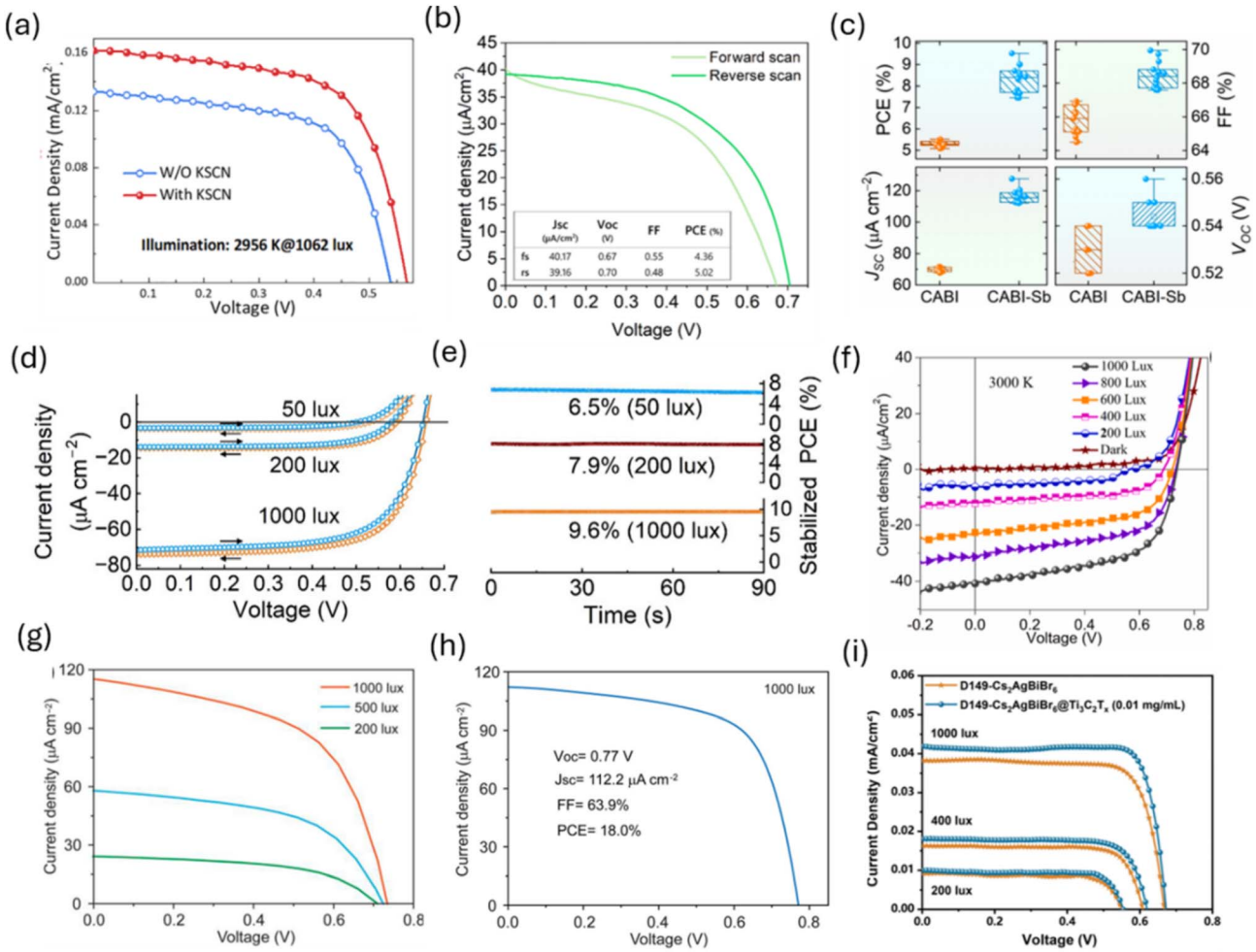

Fig. 8 *J*–*V* characteristic of (a) $FA_{0.75}MA_{0.25}SnBrI_2$ device under 1062 lx LED light. Reproduced from ref. 147 with permission from Elsevier, copyright 2021; (b) Ag_2BiI_5 device under 1000 lx LED light. Reproduced from ref. 152 with permission from American Chemical Society, copyright 2023; (c) CABI and CABI-SB devices under 1000 lx LED light. Reproduced from ref. 153 with permission from Wiley-VCH GmbH, copyright 2023; (d) CsMAFA-Sb:Bi devices and (e) their stabilized PCE under LED light at varying indoor light intensity (50, 200, and 1000 lx). Reproduced from ref. 130 with permission from American Chemical Society, copyright 2025; (f) $Cs_3Sb_2I_9$/ITIC device under LED light at varying indoor light intensity (200–1000 lx). Reproduced from ref. 154 with permission from Elsevier, copyright 2021; (g) selenium iPV devices at varying indoor light intensity (200, 500, and 1000 lx). Reproduced from ref. 155 with permission from American Association for the Advancement of Science, copyright 2022; (h) Se-based devices under 1000 lx LED light. Reproduced from ref. 156 with permission from Elsevier, copyright 2024; (i) D149 dye coated double perovskite $Cs_2AgBiBr_6$ devices with and without MXene $Ti_3C_2T_x$ at varying indoor light intensity. Reproduced from ref. 157 with permission from Elsevier, copyright 2022.

controlling $FASnI_2Br$ perovskite crystallization through strategic 6H-intermediate phase formation, achieved by leveraging the mesomeric (+M) interaction effect of 4-aminopyridine hydrochloride (4APCl) in the precursor solution. This controlled crystallization pathway resulted in superior perovskite films with substantially fewer defects. The optimized devices (IPVs) demonstrated a PCE of 21.55% under 1000 lx indoor lighting conditions, surpassing the performance of all previously reported lead-free perovskite IPVs. Panda *et al.*[150] recently improved the stability of tin-based perovskites by replacing the commonly used DMSO solvent with an *N*,*N*-diethylformamide (DEF) and *N*,*N*′-dimethylpropyleneurea (DMPU) (DEF:DMPU) solvent system. Under 200 and 1000 lx indoor illumination, the DMSO-free $FASnI_2Br$ based PV devices achieved an efficiency of 10% and 11.1%. After six months of storage under a nitrogen atmosphere, it achieved 11.9% efficiency under 1000 lx, demonstrating that DMSO-free processing enhances tin perovskite intrinsic stability. In 2026, Xiao *et al.* engineered the perovskite/C_{60} interface using a piperazine-functionalized fullerene derivative (TPPC), where the molecule's dipole moment of 1.97 debye served as the critical factor in optimizing interfacial energy level alignment through a cascade gradient. This dipole-driven modification effectively modulated hot carrier dynamics at the interface, yielding a champion PCE of 22.49% (active area of 0.1225 cm^2) and an output power density of 64.1 μW cm^{-2} under 1000 lx white LED illumination, with large-area devices (1.21 cm^2) achieving a certified PCE of 15.93%.[151]

4.2 Bi/Sb-based perovskite-inspired materials

Rudorffites with the chemical formula of $A_xB_yX_{x+3y}$ (where A^+ is Ag^+/Cu^+, B^{3+} is Bi^{3+}/Sb^{3+}, and X^- is I^-, Br^- or Cl^-) were one of the first LFAs to be tested under indoor light.[158–160] Turkevych *et al.* fabricated an indoor PV device using FTO/c-TiO_2/$AgBiI_4$/spiro-OMeTAD/Au which delivered efficiencies of 5.2% and 4.8% under 1000 lx and 500 lx LED light and a corresponding output power of 1.8 μW cm^{-2} and 0.8 μW cm^{-2}, respectively.[158] Among all PIMs, these materials offer a 3D network while the other PIMs offer lower structural dimensionality. Moreover, these materials have the highest reported efficiency to date (~6%) under 1 sun.[161] Guerrero *et al.*[152] fabricated another member of the rudorffite family – Ag_2BiI_5 – with a bandgap of 1.89 eV for harnessing the indoor light spectrum. The semi-transparent silver pnictohalide solar cell delivered a PCE of ~3.3% for a 100 nm film and ~5% for a 300 nm film under 1000 lx LED light (Fig. 8b). Optoelectronic investigation of the films revealed that trap-assisted recombination dominated in thinner films, while biomolecular recombination predominated in thicker films. Park *et al.* optimized $AgBiI_4$ thin films with a bandgap of 1.97 eV *via* hot air processing, which reduced metallic Bi^0 content and suppressed trap-assisted recombination, as evidenced by a reduced ideality factor from 1.96 to 1.04. The optimized device achieved a stabilized PCE of 3.4% (11.1 μW cm^{-2}) under 1000 lx and retained 88.9% of its initial efficiency after 35 days under ambient conditions without encapsulation.[162]

Mixed cation rudorffites such as Cu_2AgBiI_6 (CABI) have shown improved charge transfer and reduced trap sites but have performed poorly under 1 sun owing to their large bandgap (~2 eV).[160,163] However, for indoor photovoltaics, this material has an ideal bandgap and was first studied by Grandhi *et al.* under 1000 lx LED light.[164] Using hydroiodic acid (HI) as an additive, the CABI devices were able to achieve an efficiency of about 4.7%. The same group further improved the performance of the CABI devices under 1000 lx by using mesoporous TiO_2, which improved the performance of the CABI devices to 5.5%.[165] The mesoporous device structure showed improved shunt resistance from 6 kΩ cm^2 for planar devices to 12 kΩ cm^2 for mesoporous devices, improving the FF from 63% to 69% and J_{SC} and V_{OC} from 36 μA cm^{-2} to 73 μA cm^{-2} and 0.49 V to 0.54 V, respectively. Anesi *et al.* fabricated antimony-doped CABI (CABI-Sb) devices in which the bismuth was partially replaced by antimony. Under 1000 and 200 lx LED light, the CABI-Sb devices yielded an impressive PCE of 9.53% and 5.52%, respectively.[153] The antimony-doped films exhibited improved film morphology and reduced intrinsic defects in the CABI structure, which reduced self-trapping, leading to an improvement in J_{SC} from 72 to 128 μA cm^{-2} (Fig. 8c). Interestingly, even at a very low illumination of 50 lx, the device delivered an impressive PCE of ~4.3% (with a V_{OC} of 0.38 V). Lamminen *et al.* further improved the performance of CABI-Sb devices by replacing the A-site cations (Cu and Ag) with caesium (Cs), methylammonium (MA), and formamidium (FA), CsMAFA-Sb:Bi, and an interfacial layer (LFA/HTL) of dimethylphenethylsulfonium iodide (DMPESI). The champion device delivered efficiencies (stabilized PCE) of 7.94% (6.5%), 8.69% (7.9%), and 10.11% (9.6%) under 50, 200, and 1000 lx illumination (Fig. 8d and e).[130]

In addition to rudorffites, there are other LFAs that have been studied under indoor light. The most common of them has the chemical formula $A_3B_2X_9$ (where A is a monovalent cation, B is a trivalent cation Bi/Sb, and X is a halide).[166–168] Peng *et al.* reported the first indoor PV performance of this material ($Cs_3Sb_2Cl_xI_{9-x}$) together with bismuth oxoiodide (BiOI). Both materials had an ideal bandgap of 1.95 eV and 1.93 eV and delivered a PCE around 4–5% under 1000 lx FL and LED light.[169] They analyzed the performance of these materials and reported that $Cs_3Sb_2Cl_xI_{9-x}$ suffered from poor morphology leading to trap-assisted recombination, while improper energy alignment of the BiOI devices limited their performance. Singh *et al.*[154] improved the performance of $Cs_3Sb_2I_9$ based solar cells under indoor light by replacing the commonly used ETLs with an organic non-fullerene acceptor molecule indacenodithiophene (ITIC), which improved the energy alignment and absorption intensity and formed a heterojunction with the LFA that enabled efficient charge transfer. Compared to fullerene based ETLs ($PC_{61}BM$/$PC_{71}BM$), the ITIC-based devices delivered better performance in a p-i-n device architecture, achieving a PCE of 9.2 and 5.2% under 1000 and 200 lx LED light, respectively (Fig. 8f). Lamminen *et al.*[170] partially replaced the cesium in $Cs_3Sb_2Cl_xI_{9-x}$ with MA and formadinium (FA) cations to form $Cs_{2.4}MA_{0.5}FA_{0.1}Sb_2I_{8.5}Cl_{0.5}$. The triple cation PIM yielded a PCE of 6.37% with a J_{SC}, V_{OC}, and FF of 102 μA cm^{-2}, 0.55 V, and 52% under 1000 lx LED light due to the suppressed trap-induced recombination compared to double cation mixed halides ((CsMA)/(CsFA)SbICl). Nevertheless, the authors pointed out that these materials still suffer from intrinsic defects leading to a significant drop in V_{OC} from 0.8 V (under 1 sun) to 0.55 V. A. The more stable FF was attributed to improved shunt resistance from 390 Ω cm^2 (1-sun) to 32 000 (1000 lx) and 81 000 Ω cm^2 (200 lx) and lower dark current (1 μA cm^{-2}). They further compared devices based on different HTL materials such as P3HT, Spiro-OMeTAD, PTAA, and HTL-free and reported that P3HT offered the best energy alignment and superior performance among the HTL materials. The low stability of the P3HT based devices was improved by doping the P3HT layer with 2,3,5,6-tetrafluoro-7,7,8,8 tetracyanoquinodimethane (F4-TCNQ), which retained its original efficiency even after 149 days of storage under ambient dark conditions. It should be noted that the HTL-free devices performed better than Spiro-OMeTAD and PTAA. Furthermore, for $Cs_3Sb_2I_3Cl_6$ based solar cells, Jie *et al.*[166] introduced a mesoporous TiO_2 scaffold and optimized its thickness, enhancing the electron transport layer and yielding a tenfold PCE increase under LED illumination. Further incorporation of MA and cesium (Cs) ions in devices with structure FTO/c-TiO_2/m-TiO_2/$MA_xCs_{3-x}Sb_2I_3Cl_6$ ($x = 0$–3)/Spiro-OMeTAD/Au led to an additional 50% PCE improvement. The optimized $MA_{1.5}Cs_{1.5}Sb_2I_3Cl_6$ composition achieved 2% efficiency at 250 lx and 3% at 1250 lx.[166] LFAs with the configuration $A_3B_2X_9$ generally have a 0D structure and require chlorine incorporation to achieve a more favorable 2D structure.[169] Recently, Guo *et al.* elucidated the role of chlorine doping in such LFAs, which, while facilitating 2D structure formation, simultaneously

intensifies electron–phonon interactions, causing increased carrier localization and non-radiative loss.[171] By using the MA cation and high-temperature annealing at 240 °C, they were able to get phase-pure $Cs_3Sb_2I_9$ (2D). Under 1000 lx WLED light, the 2D-$Cs_3Sb_2I_9$ device exhibited a record indoor PCE of 8.2% with J_{SC} = 102.87 μA cm^{-2}, V_{OC} = 0.70 V, and FF = 0.52. Krishnaiah *et al.* partially replaced Cs with Ag to form $Cs_2AgBi_2I_9$ that showed smaller exciton binding energy and weaker exciton-phonon coupling, delivering a PCE of 4.61% and 7.6% under 200 and 1000 lx illumination.[128] In 2026, Kamppinen *et al.* determined, for the first time, the optical constants of bismuth-based LFAs *via* spectroscopic ellipsometry, enabling realistic indoor device simulations (1000 lx). The optoelectronic study combined with simulation revealed a significant gap between the theoretical limits and actual performance owing to nonradiative recombination and poor charge transport, providing clear directions for future optimization.[145]

Selenium (Se, a p-type semiconductor), which has a bandgap of 1.9 eV, was recently investigated as a potential material for indoor PVs. The selenium-based iPV device delivered a PCE of 15.1% and 14.3% under 1000 and 200 lx LED light by using a telluride interlayer, which enabled improved adhesion of the selenium film to the substrate and helped suppress defects (Fig. 8g).[155] In addition to impressive device performance, selenium also offers low-temperature processing, a high absorption coefficient (>10^5 cm^{-1}), low toxicity, and excellent stability.[155] Lu *et al.*[156] further improved the performance of Se-based devices to 18.0% efficiency under 1000 lx indoor illumination through a critical melting-annealing strategy (Fig. 8h). This approach provides sufficient energy to overcome the high activation barrier of disordered Se chains, enabling their incorporation into the lattice—a consequence of trigonal Se's unique one-dimensional crystal structure. The resulting films exhibited 2.3-fold lower trap density than conventional Se films.[156] One of the primary challenges in fabricating efficient Se indoor photovoltaics is the unavoidable presence of Te impurities originating from commercially available Se feedstocks. Leveraging selenium's intrinsic antioxidative properties arising from lanthanide-like contraction, a selective oxidation strategy was employed to eliminate these narrow-bandgap Te impurities during thermal evaporation, yielding high-purity Se films with a wide bandgap of 1.88 eV ideally suited for indoor photovoltaics. The resulting devices delivered a PCE of 20.1% under 1000 lx illumination, outperforming amorphous silicon and all lead-free perovskite indoor photovoltaics, while demonstrating exceptional stability with no efficiency degradation after 20 000 hours under ambient conditions without encapsulation.[172]

Yang *et al.*[157] fabricated an iPV device based on a double perovskite ($Cs_2AgBiBr_6$) and improved its performance by using an organic dye D149 at the ETL/PIM interface and doping the double perovskite with MXene ($Ti_3C_2T_x$). The engineering strategy resulted in suppression of non-radiative recombination and improved charge collection, which improved the efficiency from 6.48% to 7.23% under 200 lx LED light. Under 1000 lx LED light, the device delivered a lower PCE of 7.18%, as the FF dropped from 78% (under 200 lx) to 76.9% (1000 lx). The authors hypothesized that the poor energy alignment of the dye led to additional recombination pathways, reducing the shunt resistance. A similar effect of the dye was also observed under 1-sun illumination, where the V_{OC} improved slightly from 0.946 V to 0.955 V when $Cs_2AgBiBr_6$ was doped with MXene, but then dropped to 0.72 V when the dye was added (Fig. 8i).

5 Perovskite modules for indoor photovoltaics

At the low light intensities characteristic of indoor environments, the parallel resistance (R_p, in Ω cm^2) represents the dominant parasitic resistance governing the efficiency of indoor PV devices. The total parallel resistance can be expressed as a function of the specific bulk shunt resistance of the absorber material (R_{sh}, in Ω cm^2) and the specific shunt resistances associated with localized point defects (r_D, in Ω cm^2).[173,174] With the transition from small-area to large-area devices, the r_D typically increases with device area (Fig. 9a), resulting in a reduction of the parallel resistance and, consequently, a deterioration of photovoltaic performance.[173,175] As the cell area increases, the R_p decreases significantly (Fig. 9b). Enhancing R_p can be achieved by mitigating the effective density of point defects, for instance, through the segmentation of a monolithic device into smaller sub-cells within a module, thereby spatially redistributing the defects. Alternatively, the incorporation of chemical additives or the engineering of interfacial layers can further improve the parallel resistance and suppress defect-induced recombination pathways.[35,112,173] To integrate photovoltaics into electronic products and generate enough power, as well as reach the voltages at which many power management integrated circuits operate efficiently, it is imperative to manufacture large-area modules with series-interconnected cells. Currently, only a limited number of studies have effectively showcased the successful development of large-area indoor perovskite modules.[176,177] De Rossi *et al.*[178] fabricated a module through screen printing, using commercially available screen printable pastes, on an A4-sized conductive glass substrate. The module featured an effective active area of 198 cm^2, an aperture area of 435.6 cm^2, and a low geometric fill factor (GFF) of 45.5%. Notably, this module achieved a good PCE of 11% and 18% under 200 lx and 1000 lx fluorescent lighting (Fig. 9c), respectively,[178] demonstrating the potential of perovskite modules for indoor applications. Zhang *et al.* fabricated perovskite modules comprising six sub-cells with an active area of 12.18 cm^2, an aperture area of 12.96 cm^2 and a high geometric FF of 94% (Fig. 9d), leading to a small cell-to-module (CTM) efficiency loss.[31] The module achieved an active area efficiency of 31.0% (I_{SC} = 235.5 μA, V_{OC} = 6.0 V, and FF = 80.6%) under 1000 lx LED (3000 K) illumination and a certificated indoor PCE of 36.4% (by the Chinese National Photovoltaic Industry Measurement and Testing Center) under 1000 lx TL84 light (Fig. 9d). Notably, this is the first report on indoor PV certification for perovskite modules, holding significant importance in advancing the standardization and sustainable progress of this field.[31] From the same research group, Ma *et al.* developed efficient 2D–3D bulk

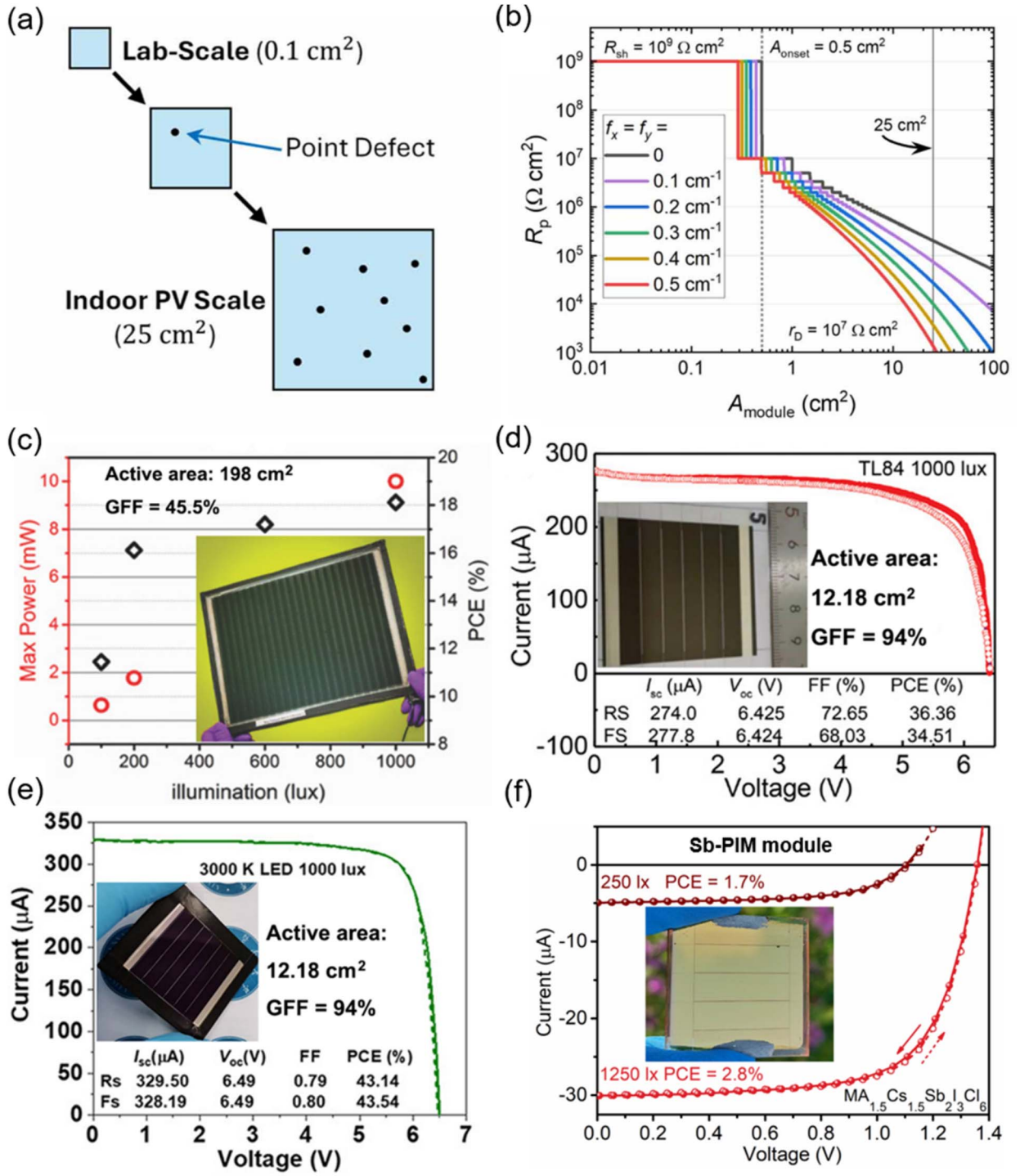

Fig. 9 (a) Scaling of point defects with device area. Reproduced from[173] with permission from IOP Publishing, copyright 2025. (b) The variation of parallel resistance with device area. Reproduced from[173] with permission from IOP Publishing, copyright 2025. (c) Maximum output power and PCE of the best module at different illumination levels under a fluorescent lamp. The inset shows a photograph of the perovskite module, featuring an aperture area of 435.6 cm^2 (an effective active area of 198 cm^2) and a geometric fill factor (FF) of 45.5%. Adapted from ref. 178 with permission from John Wiley and Sons, copyright 2018. (d) Certificated current–voltage (I–V) curves of perovskite modules measured under TL84 light (1000 lx) according to IEC60904 and SEMI PV89 test standards, measured at the Chinese National Photovoltaic Industry Measurement and Testing Center (NPVM). The inset shows a photograph of the perovskite module, comprising six sub-cells with an aperture area of 12.96 cm^2 (active area of 12.18 cm^2) and a geometric FF of 94%. Adapted from ref. 31 with permission from Wiley-VCH GmbH, copyright 2022. (e) I–V curves of oleylammonium iodide treated perovskite solar module measured under 1000 lx LED light. The inset shows a photograph of the perovskite module, comprising six sub-cells with an aperture area of 12.96 cm^2 (active area of 12.18 cm^2) and a geometric FF of 94%. Adapted from ref. 32 with permission from Elsevier, copyright 2023. (f) I–V curves for the $MA_{1.5}Cs_{1.5}Sb_2I_3Cl_6$ module measured under 250 lx and 1250 lx LED illumination. The inset shows a photo of the module, comprising three sub-cells with an aperture area of 2.6 cm^2 (active area of 2.52 cm^2) and a geometric FF of 97%. Adapted from ref. 166 with permission from Elsevier, copyright 2025.

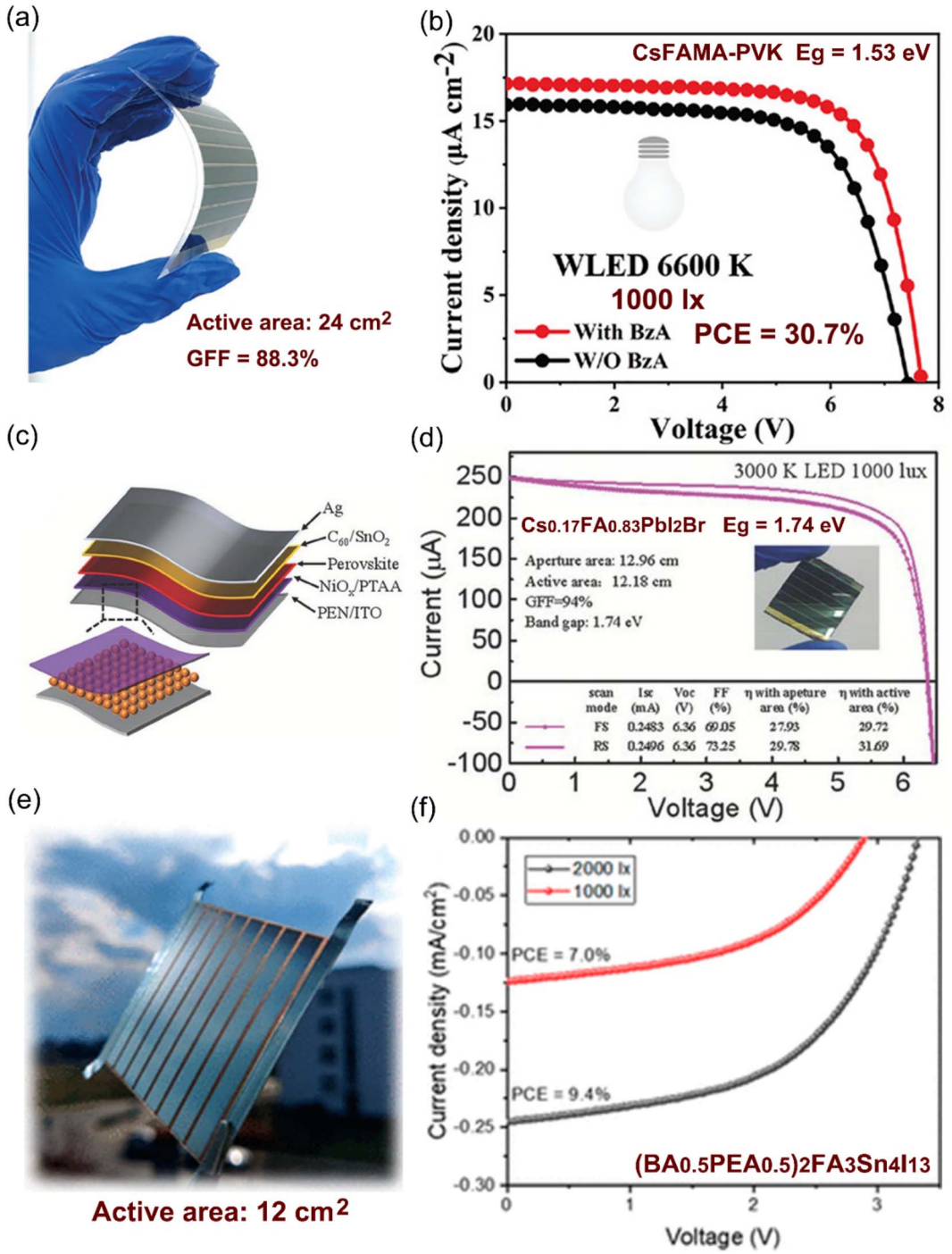

Fig. 10 (a) Photograph of CsFAMA lead halide flexible perovskite module comprising eight sub-cells with an active area of 24 cm^2 and a geometric fill factor (GFF) of 88.3%, and (b) current density–voltage (*J*–*V*) curves of the flexible modules with/without a benzyl acrylate (BzA) interface layer, measured under 1000 lx white LED (6600 K) illumination. Adapted from ref. 179 with permission from Wiley-VCH GmbH, copyright 2022. (c) Schematic illustration for a flexible ITO/NiO_x/PTAA/$Cs_{0.17}FA_{0.83}PbI_2Br$/$C_{60}$/$SnO_2$/Ag device, and (d) *J*–*V* curves of the flexible module, comprising six sub-cells with an active area of 12.18 cm^2 and GFF of 94%, measured under 1000 lx LED illumination (3000 K). Adapted from ref. 122 with permission from Wiley-VCH GmbH, copyright 2024. (e) Photograph of flexible $(BA_{0.5}PEA_{0.5})_2FA_3Sn_4I_{13}$ perovskite module containing eight sub-cells with an active area of 12 cm^2, and (f) *J*–*V* forward scans for the $(BA_{0.5}PEA_{0.5})_2FA_3Sn_4I_{13}$ module, measured under 1000 and 2000 lx LED (~3280 K) illumination, respectively. Adapted from ref. 180 with permission from American Chemical Society, copyright 2023.

heterostructures by introducing oleylammonium iodide into wide-bandgap perovskites, which effectively passivated defects and suppressed halide phase segregation.[32] By employing this approach, they fabricated perovskite modules with the same size as previously reported, containing six sub-cells with an active area of 12.18 cm^2 and a geometric FF of 94%. The module

achieved a record indoor PCE of 43.5% with a V_{OC} of 6.49 V (average V_{OC} of 1.08 V for each sub-cell), I_{SC} = 328.2 μA, and FF of 80% (Fig. 9e).[32] Notably, this value is close to the record indoor PCE of small-area cells maintained by this research group.[29]

Reports on flexible indoor perovskite modules are even fewer. The development of high-efficiency indoor flexible perovskite modules enables the self-powering of indoor IoT on many types of surfaces, even curved ones, as well as wearable devices. Zhu *et al.*[179] reported a flexible perovskite module comprising eight sub-cells with an active area of 24 cm^2 and a geometric FF of 88.3% (Fig. 10a). The module delivered an active area efficiency of 30.7% (I_{SC} = 411.4 μA, V_{OC} = 7.7 V, FF = 72.4%, and maximum power output = 2.29 mW) under 1000 lx white LED (6600 K) illumination (Fig. 10b).[179] This implies that it can be integrated with some wearable sensors and provide them with the necessary power.[110]

Zhang *et al.*[122] employed a wide bandgap perovskite $Cs_{0.17}FA_{0.83}PbI_2Br$ (E_g = 1.74 eV) as an absorber and optimized the interfacial adhesion properties through a porous NiO_x nanoparticle layer on PEN/ITO substrates (Fig. 10c). With this strategy, the laboratory flexible cell achieved a record indoor PCE of 36.1% (J_{SC} = 121.5 μA cm^{-2}, V_{OC} = 1.06 V, and FF = 84.6%) under 1000 lx warm WLED light and a record indoor PCE of 31.7% (I_{SC} = 249.6 μA, V_{OC} = 6.4 V, and FF = 73.3%) for a 12.18 cm^2 (active area) module (Fig. 10d).[122] The efficiency loss observed when scaling from small-area cells to large-area modules primarily arises from film non-uniformity, a higher density of defects, and increased resistance and interconnection losses.[122,179] Although such high efficiency has surpassed that of any other PV technology,[28] the development of high-

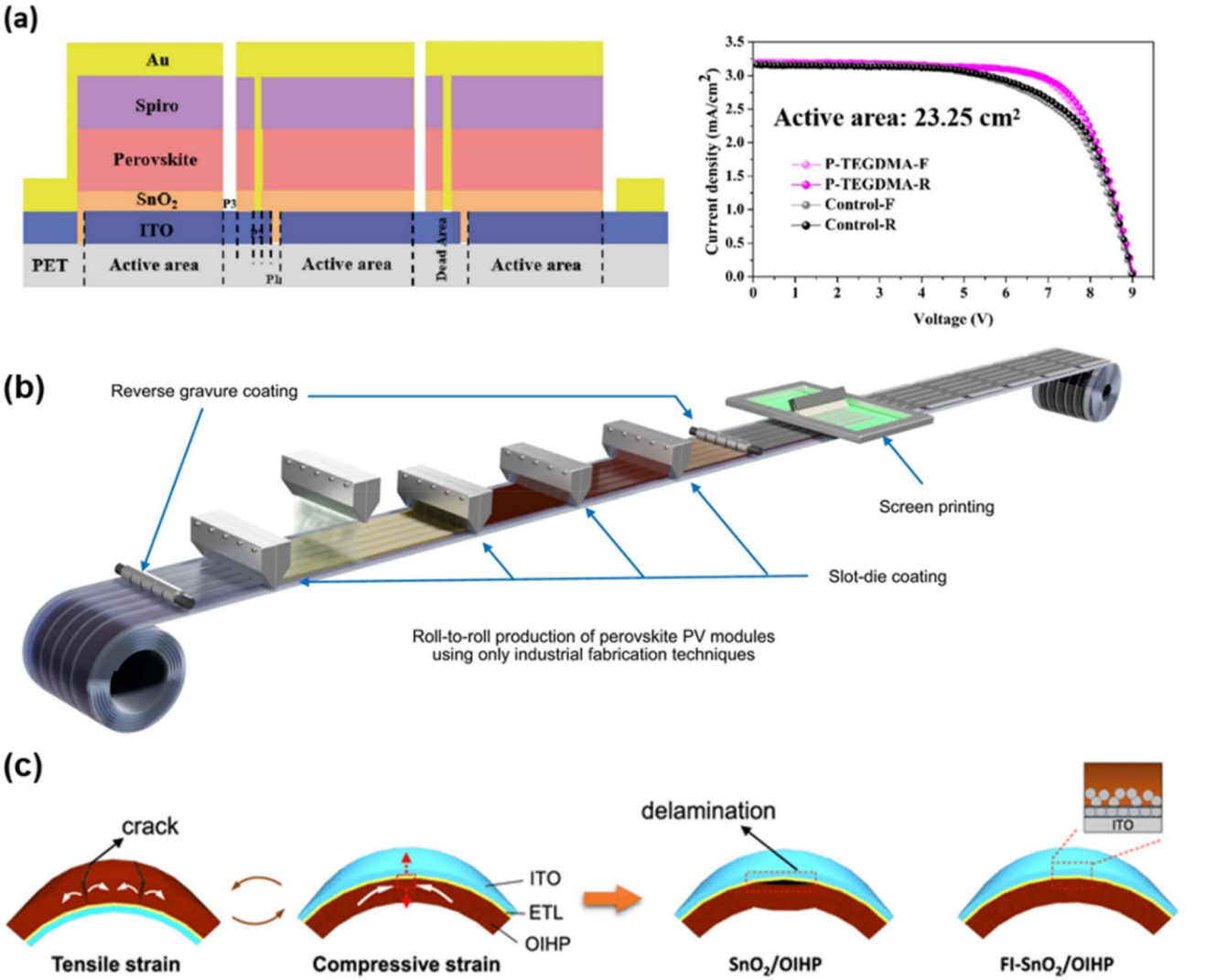

Fig. 11 (a) The configuration with a cross-section view of a flexible module with high efficiency under indoor 1000 lx LED light. Reproduced from ref. 183 with permission from Elsevier, copyright 2025; (b) schematic illustration of roll-to-roll production of a module meant for the outdoors. Reproduced from ref. 184 with permission from Springer Nature, copyright 2024; (c) schematic illustrations showing the strains in module layers in different bending states (left panel) and the film states after bending cycles (right panel). Reproduced from ref. 186 with permission from Springer Nature, copyright 2021.

efficiency indoor flexible modules requires intensified research efforts directed towards narrowing the efficiency disparity with rigid counterparts.

Lead-free perovskites have recently come to the fore because they aim to address a main issue with perovskite technology, the potential toxicity of lead (Pb).[181,182] Currently, only two research reports on lead-free perovskite modules have been found.[180,182] One is on the first lead-free antimony-based perovskite PV modules, comprising three sub-cells with an active area of 2.52 cm^2 and a geometric FF of 97%.[182] The module has an architecture of Glass/FTO/c-TiO_2/m-TiO_2/$MA_{1.5}Cs_{1.5}Sb_2I_3Cl_6$/Spiro-OMeTAD/Au and achieved an indoor PCE of 1.7% and 2.8% under 250 lx and 1250 lx LED illumination (Fig. 9f).[166] The other one was published by Żuraw *et al.* who reported the first flexible lead-free tin-based perovskite PV modules, containing eight sub-cells with an active area of 12 cm^2 (Fig. 10e).[180] Modules were fabricated in a p-i-n configuration with an architecture: PET/ITO/PEDOT/Al_2O_3 bilayer/$(BA_{0.5}PEA_{0.5})_2FA_3Sn_4I_{13}$/$C_{60}$/bathocuproine (BCP)/Ag and achieved a PCE of 7.0% (366 μW cm^{-2}) and 9.4% (738 μW cm^{-2}) measured under 1000 and 2000 lx LED (~3280 K) illumination, respectively (Fig. 10f).[180]

Scalable fabrication of high-performance indoor perovskite photovoltaics is essential to meet the demands of real-world applications, particularly in the context of powering distributed IoT devices. In recent years, a variety of solution-based deposition techniques, such as slot-die coating, blade coating, and spray coating, have been widely explored for the scalable formation of uniform perovskite films. These methods offer excellent control over film thickness, are compatible with ambient or low-temperature processing, and are particularly well-suited to flexible or large-area substrates. For instance, Xu *et al.* developed a flexible perovskite photovoltaic module incorporating a photopolymerized network, which demonstrated a record indoor PCE of 30.2% under 1000 lx WLED illumination on an 18 cm^2 device. They also demonstrated that slot-die-coated flexible perovskite modules with a triethylene glycol dimethacrylate polymer interlayer achieved outstanding humidity resistance and bending stability, delivering a PCE of 42.1% over 0.07 cm^2 area and 40.1% over 23.25 cm^2 area under 1000 lx WLED illumination,[183] as shown in Fig. 11a. Building upon these techniques, roll-to-roll (R2R) processing has emerged as a potential industrial solution for manufacturing flexible IPVs. R2R systems integrate scalable coating methods with continuous substrate handling, enabling layer-by-layer printing in a high-throughput, cost-effective fashion.[184,185] Weerasinghe *et al.*[184] reported the first fully roll-to-roll fabricated perovskite solar cell module, including all functional layers and carbon electrodes, achieving 11.0% PCE under 1-sun illumination in large-area serially interconnected modules, entirely printed under room conditions without vacuum processing of metal electrodes (Fig. 11b).[184] Nevertheless, high-throughput scalable fabrication of indoor perovskite photovoltaics is still in its early stages with no relevant data found for fully R2R process fabrication of PV devices for indoors, leaving ample room for innovation in module design, materials engineering, and process integration.

Despite the progress made in the field of indoor perovskite photovoltaics, there remains a critical lack of standardized protocols for mechanical testing of indoor devices. While outdoor PVs benefit from well-established stability tests (*e.g.*, IEC 61215),[187,188] there is no consensus regarding durability metrics for indoor-specific modules. This gap hampers reproducibility and hinders fair performance comparison. It is needed to develop dedicated protocols for flexible IPVs, particularly at indoor light intensities and under real-use mechanical cycles.[189] On the other hand, in addition to the intrinsic material design, encapsulation and post-treatment strategies are pivotal in enhancing the mechanical durability of IPVs, especially for flexible or wearable applications. Unlike rigid modules, IPV devices are more susceptible to delamination, cracking, and degradation under repeated bending or compression, as illustrated in Fig. 11c.[186] To address this, advanced encapsulation architectures—including multilayer polymer barriers, atomic layer deposition (ALD) of metal oxides, and UV-curable epoxy coatings—have shown significant effectiveness in providing both environmental and mechanical protection.[190] For example, Sutherland *et al.* reported that pre-conditioned flexible encapsulant materials can significantly reduce interfacial degradation and improve long-term stability of IPV devices.[191]

6 Device applications powered by indoor perovskite photovoltaics

Within indoor energy harvesting, photovoltaics represents the most mature technology, though the optimal type of energy scavenging depends on the environment.[19] Driven by the continuous knowledge exchange between chemistry, physics, materials science and engineering, perovskite solar cells are witnessing significant advancement with ever improving processibility, mechanical flexibility and weight reduction. These features allow them to be used in many different applications with little dependence on shape or design.[192]

Although aspects such as device architecture, production strategies, large-area modularization, application scope, and long-term stability are still under development, we present below several approaches for their potential use across different fields.[52,89,99,114,115,121,193–195]

6.1 Internet of Things

The integration of photovoltaic cells with IoT devices has revolutionized data management, enabling cognitive buildings that seamlessly interact with smart grids.[196] The role of buildings is evolving from mere consumers to prosumers.[197] Indoor perovskite photovoltaics can play a crucial role in this transformation.[111] As both IoT and indoor perovskite photovoltaics advance technologically, their applications is expected to expand significantly, thereby increasing their competitiveness. The future lies in integrated device segments with diverse applications.[111,198–201] To ensure longevity and efficiency, focus must be on material selection and optimizing under indoor environments. Prioritizing a higher voltage output from individual cells enhances junction quality and minimizes the need

Table 3 Summary of device applications powered by indoor perovskite photovoltaics

Type of perovskite device	Total active area	Illuminance/ input power	PCE/output power	Application	Main results	Ref.
Solar cell (E_g: 1.6–1.8 eV)	0.078 cm^2	LED (872 μW cm^{-2})	PCE ~34.9% (23.8 μW)	Driving of a sodium-ion battery and electronic devices for diverse applications (test case-an MX2202 environmental recorder)	Continuous power for 24 h with no battery loss, with less than 6% power loss after continuous operation at maximum load for over a week	208
Solar module (2 cells in series, E_g: ~1.84 eV)	0.7 cm^2	CFL (160 μW cm^{-2})	PCE ~13.2% (14.5 μW)	Battery assisted radio frequency identification temperature sensor	Backscatter communication range increased by 7.2 times reaching a maximum of 5.1 m while maintaining a high-frequency measurement period of 1.24 s	202
Solar module (2 cells in series, quasi-two-dimensional perovskite)	2 cm^2	LED (600 lx, 215 μW cm^{-2})	PCE ~29.6%	Autonomous wearable biosensor	In 12 h time span depending on the illumination the wearable device switched its on-body measurement sequence to adjust its power with data intervals from 8 s to 60 s, while it withstood mechanical stress. The device persistently extracts sweat and simultaneously monitors physiochemical markers using a spectrum of electrochemical techniques.	110
Solar module (3 cells in series)	3 cm^2	LED (3000 K, 1000 lx)	PCE ~14% (121 μW)	Radio-frequency backscatter device composed of an integrated circuit, an internal temperature sensor and a Cu antenna	Communication range restricted at 0.43–0.96 m was improved to 1.95–2.05 m with tin halide perovskite with an increased frequency of 930 MHz. Broad absorption from 300 to 760 nm	211
Solar module (6 cells in series)	—	LED (3800 K,1000 lx, 316.7 μW cm^{-2})	PCE ~41.6% (reported for 0.1 cm^2 cell)	IOT evaluation board with a Bluetooth low energy (BLE) protocol chip and humidity pressure and temperature sensor	The temperature, humidity and pressure data were recorded continuously for ≈ 24 h through the mobile application	212
Solar module (6 cells in series)	2.9 cm^2	0.01 sun (1 mW cm^{-2})	PCE ~14%	Indoor self-powered skin optoelectronics developed by integration of ultra-flexible perovskite solar cells and a PNC-LED (monochromatic light source)	Ultra-flexible LED successfully powered and generated narrowband electroluminescence under indoor and outdoor conditions	213
Solar module (3 cells in series)	15 cm^2	LED (4000 K,1000 lx)	PCE ~25.76%	Power management with a Zigbee communication module, temperature and humidity sensor	24 hours indoor environmental data monitoring and extensive 3D data collection	204
Mesoporous carbon solar module (6 cells in series)	1.95 cm^2	LED (average 800 lx)	1.094 coulombs (average charge generated during day)	IOT device using the module to charge a supercapacitor using an energy harvester. An ultra-low powered micro-controller connected to a temperature and humidity	The IOT device measures room temperature and atmospheric pressure every 20 min and transmits it every 6.5 hours	214

Table 3 (*Contd.*)

Type of perovskite device	Total active area	Illuminance/ input power	PCE/output power	Application	Main results	Ref.
				sensor. Transferring data using XBee communication		
Solar module	16.12 cm^2	—	—	A self-powered electronic price tag with a voltage requirement from 2.4 V to 3.6 V is powered by the module through the integrated circuit with a lithium ion battery	The integrated circuit provided continuous power supply to electronic price tags. A series connection of at least 3 solar cells could meet the requirement	195
Flexible perovskite mini-module	4.15 cm^2	LED (1000 lx, 500 lx, and 200 lx)	PCE ~13.8%, 9.69%, and 9.34% (221 μW cm^{-2}, 75 μW cm^{-2}, and 25 μW cm^{-2})	In a hybrid bifurcated design, series connected supercapacitors are layered on a paper substrate with the perovskite mini-module integrated on top through a diode	Delivering peak overall and storage efficiencies of 2.8% and 23% respectively. 3.8 V output making it viable for flexible real time applications	207
Perovskite solar cells	400 cm^2	200 lx	10 μW cm^{-2}	Solar cells in combination with energy harvester chip (E-peas AEM30110) and energy storage devices powers the system on chip (ESP32-S3), the transceiver and environmental sensors (illumination, temperature, humidity and CO_2)	The assessment of energy generation and consumption showed a surplus of 52 J day^{-1}, confirming that the platform can function continuously and reliably	215
Wide-bandgap perovskite solar module (6 cells connected in series)	12 cm^2	1000 lx (4000 K LED)	22.1%	Solar module integrated with a BQ25504 boost converter, 2 supercapacitors and a custom circuit to communicate *via* the ZigBee 3.0 protocol	Successful operation of the system to collect temperature and humidity data for 58–87 hours under 500–1000 lx indoor lightning	205
Flexible perovskite module (3 cells connected in series)	15 cm^2	1000 lx (4000 K LED)	PCE ~25.76% (~1 mW output)	Integration of a temperature and humidity sensor, BQ25570 energy management unit, and 70F capacitor with a ZigBee protocol	24 hours sustaining flexible node under varying illuminance (100 lx-1000 lx) and light conditions (2700 K, 4000 K, and 5000 K)	204
Single perovskite solar cell	1 cm^2	—	26 μW cm^{-2} (average)	Harvester is connected to an nrf52 MCU, a MAX17220 boost converter, 2 supercapacitors, and an IoT device (irradiance, temperature and humidity sensor)	Self-sustaining node with collection of environmental data with a harvesting mode to reduced/sleep mode ratio of 2 : 3 and performing 8–30 IV scans for self-assessment throughout the day	206
Perovskite solar cells (2 cells – series connected)	0.72 cm^2	2700 K desk lamp at 20 cm distance (0.1 sun)	1.1 mA cm^{-2} at 1.75V (approximately)	Integrated photorechargeable systems with 4 cm^2 zinc ion hybrid capacitors	Under a desk lamp, the device underwent 12 hours of photocharging followed by 12 hours in darkness. During illumination, it delivered 200 μW pulses for 1 s every 10 s, which later reduced to every 30 s in the dark. After charging, the IPRS reached over 1.8 V and remained above 1.1 V after 12 hours without light	216

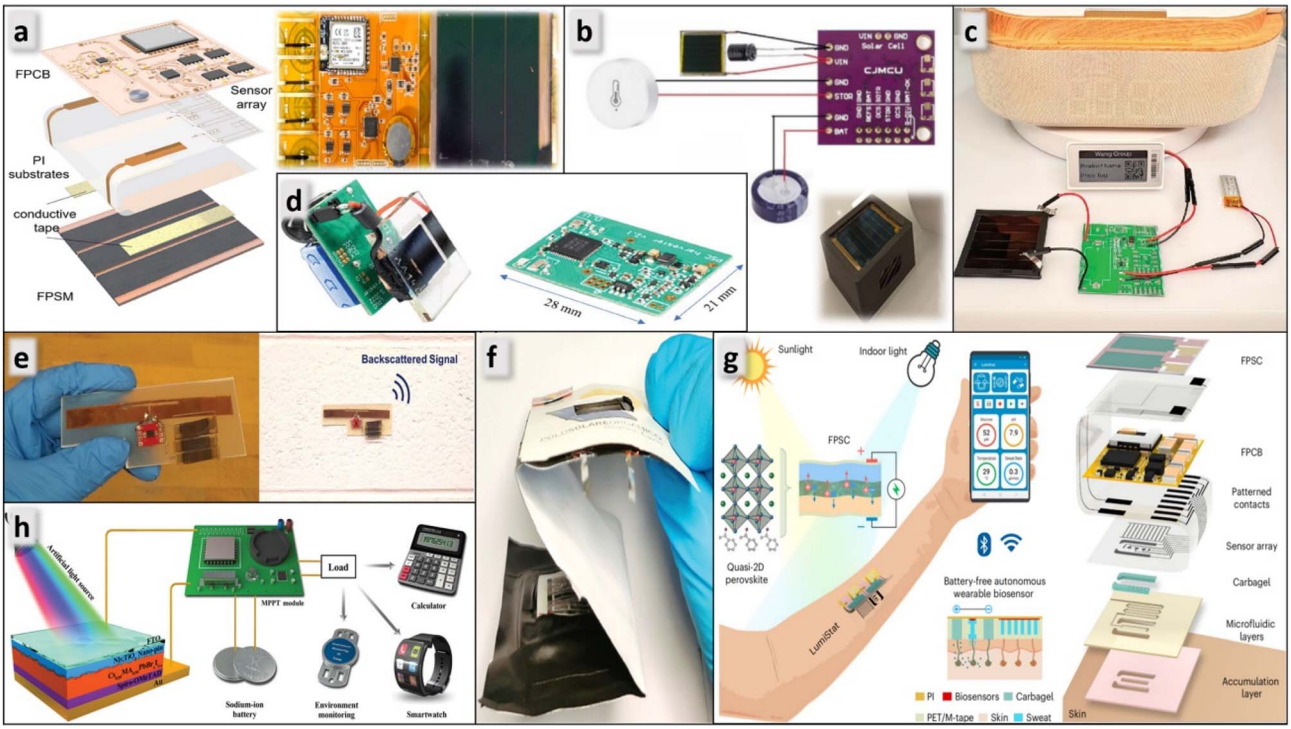

Fig. 12 (a) Flexible perovskite solar cell module powered 24 h self-sustaining flexible nodes. Reproduced from ref. 204 with permission from Wiley-VCH GmbH, copyright 2025. (b) Prototype of a commercial Tuya temperature-humidity sensor powered by a wide-bandgap perovskite solar cell. Reproduced from ref. 205 with permission from AIP Publishing, copyright 2025. (c) Electronic price tag powered by perovskite solar module. Reproduced from ref. 195 with permission from Oxford University Press, copyright 2025. (d) Self-sufficient IoT device with a remarkable 75% efficient light energy harvesting method. Reproduced from ref. 206 with permission from IEEE, copyright 2024. (e) Pictures of the indoor perovskite PV powered radio frequency identification (RFID) temperature sensor. Reproduced from ref. 202 with permission from John Wiley and Sons, copyright 2019. (f) Hybrid bifurcated structure of a flexible perovskite minimodule combined with a paper based ultra-flexible carbon printed supercapacitor. Reproduced from ref. 207 with permission from Wiley-VCH GmbH, copyright 2024. (g) Illustration of the energy autonomous wearable device that is powered under both outdoor and indoor illumination. Reproduced from ref. 110 with permission from Springer Nature, copyright 2023. (h) Systematic diagram of an artificial photon harvesting system. Reproduced from ref. 208 with permission from John Wiley and Sons, copyright 2020.

for multiple series connections, thereby reducing the overall risk of system failure.[202] Emerging technologies like RF backscatter, which operates on minimal energy (μW), are promising for integration for wireless communication.[203] Various sensors, including temperature, humidity, smoke, pressure and other sensing devices, are widely used in people's lives and workplaces. Using photovoltaic cells to power these sensors can avoid battery replacement and the use of cables. Table 3 provides an overview of demonstrations of IoT applications powered by PSCs.

Han *et al.*[204] introduced a hybrid (indoor/outdoor), flexible perovskite solar cell module (FPSM)-powered 24 h self-sustaining flexible node (SSN) integrated with sensors (temperature and humidity sensor), an energy management unit (BQ25570, Texas Instruments), energy storage (70 F capacitor), and wireless data transmission through a low-power Zigbee module (Fig. 12a). The FPSM-SSN exhibited uninterrupted operation under varying illuminance (100–1000 lx) across different light conditions (2700 K, 4000 K, and 6500 K). The foldable 24 cm^2 system comprised a 3-cell module with an effective area of 15 (5 × 3) cm^2, connected to the SSN using conductive adhesive in steps. Under warm light (2700 K, 1000 lx), the PCE reached 31.98% with ~1.4 mW output, while under standard indoor light (4000 K, 1000 lx), the PCE was 25.76% with ~1.2 mW output. The FPSM instantaneous power output at lower irradiances (0.1 mW cm^{-2} at 100 lx) was compensated for by the capacitor module. The SSN system was power-optimized by periodically waking up (for ≈0.15 s) from deep sleep at ≈200 μA to transmit signals at ≈300 μA (at a working voltage of 1.8 V), thus sustaining 24 h of operation with just 10 h of low-light exposure. The internal MPPT function monitored every 16 s and set the MPP at 80% of the open-circuit voltage. The PEDOT:PSS integrated with a carbon nanotube temperature sensor exhibited stable and sensitive temperature responses within 25–41 °C, and the PEDOT:PSS combined with a $Ti_3C_2T_x$ humidity sensor showed stable and sensitive humidity responses with a sensitivity of 0.616% RH^{-1} at 1000 lx-LED illumination.[204]

Sun *et al.*[208] developed PSCs using a $Cs_{0.05}MA_{0.95}PbBr_xI_{3-x}$ as an absorber, achieving a PCE of 36% (0.078 cm^2) under warm white LED light. They designed an integrated system for energy harvesting and storage. This system powered by indoor PSCs under practical conditions could run devices such as calculators, quartz clocks, and environmental monitoring equipment.

Under LED light illumination, it continuously powered an MX2202 environmental recorder (temperature and light logger) for over 24 h without any battery power loss (Fig. 12h), where power management was performed using a dynamic MPPT module based on a BQ25504 (Texas Instruments) and sodium-ion battery based storage element.[208]

Uršič *et al.*[206] presented the development of a self-sufficient IoT device with a remarkable 75% efficient light energy harvesting method at an input current in the microampere range (Fig. 12d). The IoT device acquired environmental data (irradiance, temperature, and humidity) and solar cell electrical parameters, including IV curves for long-term self-monitoring, which were transmitted over a Bluetooth Low Energy (BLE) connection to a nearby access point. A 1 cm^2 perovskite solar cell was deployed with a 1 F supercapacitor as charge storage to meet the low-power demand (6 μW). Energy harvesting under a combination of artificial and diffused light was performed in short bursts, complemented by periodic *JV* curve scanning at favourable illuminance levels (with MPPT tracking paused at low illuminance to save power). The high-capacitance input storage of the supercapacitor retained voltage in the vicinity of the MPP operational point, while a secondary supercapacitor was used for additional charge storage. The microcontroller unit was based on a system-on-chip (nRF52 series) by Nordic Semiconductor, which also supervised the generic MAX17220 boost converter to retain system voltage (upwards from 400 mV). Using illumination measurements from an RGB+IR sensor, the microcontroller unit (MCU) allocated energy between IoT functionality and energy harvesting, while also monitoring and tracking electrical parameters throughout its lifespan. Energy harvesting occured only 40% of the time, with the system in reduced operation or sleep mode for the remaining 60% (when the illumination or the PV cell output power fell below a minimum threshold, the cell was isolated). Quick charge transfer resulted in a ∼75% boost in efficiency, with an average of 70 s boost per day. On average, the device harvested approximately 26 μW from the solar cell when active. A significant portion of the collected energy was consumed as quiescent current, while only about 30% was utilized for IoT functionalities, including environmental data collection (irradiance, temperature, and humidity), wireless communication, and maximum power point tracking. Task scheduling enabled ∼2 tasks per min during sleep and ∼25 during operation, while intelligent illumination tracking yielded 8–30 IV scans per day. Overall, the device consumed 6 μW on average, dropping to 3.5 μW under dark conditions.[206]

Chen *et al.*[195] showcased the reliable operation of a yellow LED directly connected to a perovskite solar module, functioning only under illuminated conditions, followed by an electronic price tag (operating voltage is 2.4–3.6 V) powered through an integrated circuit combining lithium-ion batteries with a 6-cell series-connected perovskite solar module (a 3-cell connection was sufficient to meet the requirement). A superior efficiency of 42.01% was achieved at 1000 lx under a 3000 K LED on a 1 cm^2 device. Accelerated diurnal cycling indicated a promising T_{90} lifetime approaching 6000 h. Linear extrapolation of lifetime predictions for a 5-cell, 16.12 cm^2 ISOS-D-photocycle device suggested a T_{50} of approximately 3.5 years (Fig. 12c).[195]

Milyutin *et al.*[205] presented a prototype of a commercial Tuya temperature-humidity sensor powered by a wide-bandgap perovskite solar cell integrated with a BQ25504 boost converter and a supercapacitor (Fig. 12b). To mitigate power drops during peak load, a secondary capacitor was deployed, which also reduced power fluctuations through a custom-designed energy management circuit. A 1.75 eV bandgap PSC ($Cs_{0.17}FA_{0.83}Pb(I_{0.6}Br_{0.4})_3$) was used to operate the sensor under the ZigBee 3.0 protocol *via* a hub gateway. Autonomous functionality was demonstrated for 58–87 h under 500–1000 lx of 4000 K white LED illumination, with long-term stable operation at ≥3000 lx limited only by the PSC lifespan, expected to be around 2 years (longer than a typical single-use Li-ion battery). The integration consisted of six cells (2 cm^2 each) connected in series. After integration, the power density was 274 μW cm^{-2} at 1000 lx, while the PCE reached 22.1% at 800 lx. The sensor, operating between 2.5–3 V, was programmed with Arduino. Its power consumption was 9.6 μW in sleep mode and 150 mW in active mode, with a 300 s interval cycle. The weighted average energy consumption was calculated to be 1509.5 μW per cycle.[205] In 2026 Valastro *et al.* showed an IoT node, integrating high-precision temperature and humidity sensors, that was powered by a bifacial PSC architecture envisaged for vertical applications where light comes from both sides.[209]

6.2 Wearable biosensors

Wearable medical devices have advanced significantly, transitioning from simple step trackers to sophisticated tools capable of scientific health and environmental monitoring. These improvements have made sensors more portable and streamlined the interaction with medical services by enabling efficient data transfer.[210] Perovskite indoor photovoltaics can offer a superior alternative to some of the bulky and unsustainable power sources currently used in biosensors. For instance, Min *et al.*[110] studied a self-powered wearable biosensor that demonstrated the use of highly efficient quasi-2D flexible perovskite modules consisting of two cells joined in series with an active area of 2 cm^2 and a PCE of 30% under 600 lx LED light to generate electrical power from ambient light (Fig. 12g). This system included a similarly flexible and efficient circuit board for signal processing and wireless Bluetooth communication, dual carbagel-coated iontophoresis electrodes to stimulate sweat, a microfluidic module with interdigitated electrodes to sample and monitor sweat, and an electrochemical sweat biosensor array positioned closest to the skin. The compact device, measuring 20 mm × 27 mm × 4 mm, actively extracted sweat to monitor physicochemical markers using a range of electrochemical techniques. The data were then transmitted and displayed on a mobile application, showcasing the potential of integrated wearable technology for continuous and comprehensive health monitoring.[110]

6.3 Other integration prospects

Mathews *et al.*[202] demonstrated the use of low-cost indoor perovskite PV cells as an external power source for

backscattering sensors. They developed perovskite PV modules using a wide-bandgap perovskite with a composition of $(MA_{0.5}FA_{0.5})Pb(Br_{0.5}I_{0.5})_3$, which comprised three series-connected cells with a total combined active area of 0.7 cm^2. Under compact fluorescent lighting at an intensity of 0.16 mW cm^{-2}, the module achieved an output power of 14.5 μW and an efficiency of 13.2%. This module was employed to power a battery-assisted radio frequency identification (RFID) temperature sensor, which had a read range of 5.1 meters and retained a high measurement frequency of every 1.24 seconds (Fig. 12e). Their research illustrated the potential of integrating PSCs with sensors in a cost-effective manner for high-frequency data collection under indoor lighting conditions.[202]

Lomeri *et al.*,[207] through a hybrid bifurcated structure combined in series, fabricated a flexible perovskite minimodule with paper based ultra-flexible carbon printed supercapacitor (Fig. 12f). The series connected 5 cell solar minimodule with an active area of 4.15 cm^2 was strategically placed on top for seamless integration delivering a PSC module efficiency and power of 9.34% and 25 μW cm^{-2} respectively, under 200 lx – white LED light. The quasi solid state supercapacitors with a total area of 3.6 cm^2 were connected in both parallel and series on a sheet of paper and then attached in stacked configuration. The integrated system assembled on a single sheet of paper was connected through a diode (positive terminal connected to the solar module while the negative terminal is connected to the supercapacitor) to prevent any unwanted discharge. The system while testing functionality was able to power the calculator for over a minute and LEDs for more than 30 seconds. 2.8% of overall efficiency was achieved with a wide potential window of 3.8 V, 100% capacitance retention and coulombic efficiency over 10 000 repetitive GCD cycles. Under 200 lx white LED light, the power and voltage of the capacitor varied from 0.4 V, 1.6 μW to 0.18 V, 0.7 μW in resistances from 100 kΩ to 40 kΩ.[207]

6.4 Industrial applications

The commercialization of perovskite IPVs has accelerated in recent years, driven by advances from several emerging companies across the globe. Table 4 provides a summary of the companies developing perovskite PV specifically for indoors. In mid-2025, Solaires (Canada), in collaboration with Genesis Technology (China), delivered its first commercial batch of perovskite IPV modules to a global electronics manufacturer through their joint venture, SEI Energy, reporting efficiencies exceeding 35%. Founded in 2020, Solaires claims to develop IPV devices at approximately half the cost of conventional indoor photovoltaic modules, while achieving twice the power output and reducing greenhouse gas emissions by 50%. The demonstrated module consists of three cells connected in series, delivering a power density of 15–17 μW cm^{-2} and maximum power point voltage (V_{mpp}) of 1.7–1.9 V under 200 lx LED (4000 K) light, with overall dimensions of 75 × 35 mm^2 and an aperture area of 58.3 × 27.5 mm^2 (Fig. 13a).[217]

Saule Technologies, despite an uncertain commercialization future, has been a pioneer in inkjet-printed perovskite solar modules, characterized by their flexibility in shape and pattern customization.[226,227] The company's product portfolio included modules ranging from 25 × 66.2 mm^2 to 105 × 158 mm^2, delivering output powers between 170 μW and 2160 μW, with a V_{mpp} of 2.1 V in five of the eight available module configurations under 500 lx LED light (3200 K) (Fig. 13b).[218]

Perovskia has introduced digitally printed PSCs and modules, available as prototype samples. These devices delivered over 80 μW cm^{-2} at 1000 lx and can be adapted to various surface geometries without loss of performance (Fig. 13c).[219] In June 2025, Perovskia Solar AG received CHF 1.05 million (≈USD 1.3 million) from Innosuisse to automate its production line, targeting an output of up to 1 million custom solar cells per year. Over the past year, the company also raised USD 2.4 million in seed funding, partnered with more than ten IoT clients, and advanced its path toward industrial-scale commercialization.

In June 2023, Enecoat Technologies installed an integrated IoT CO_2 sensor terminal powered by perovskite solar cells at the Tokyo Metropolitan Government facilities for verification testing. The company was subsequently listed in the 2025 Forbes Asia "100 to Watch" ranking (Fig. 13d).[220]

Table 4 Summary of companies operating in the field of indoor perovskite photovoltaics and their technologies

Company	Country	Technological focus	Stage	Application stated
Enecoat	Japan	High efficiency, ultra thin film, lightweight, flexible, low temperature coating	Research and development (R&D)	Watches and wearables
Hallocell	Australia	Roll-to-roll manufacturing, performance, and tandem	Commercial production	Small electronics, IoT, and drones (Fig. 13g)
Perovskia	Switzerland	Digital printing, design, and sustainability	R&D	IoT, consumer electronics (Fig. 13i), wearables, retail, tracking and sensors
Saule Technologies	Poland	Versatility, simplicity, and low cost	Test-integration	ESLs (electronic shelf labels), IoT, and consumer electronics (Fig. 13f)
Solaires	Canada	Versatility, simplicity, affordable, and recyclable	Commercial production	Smart gadgets, IoT, and wireless energy transmission (Fig. 13h)
Singfilm	Singapore	Junction, efficiency, stability, design, and scalability	R&D	Sensors, ESLs, and trackers

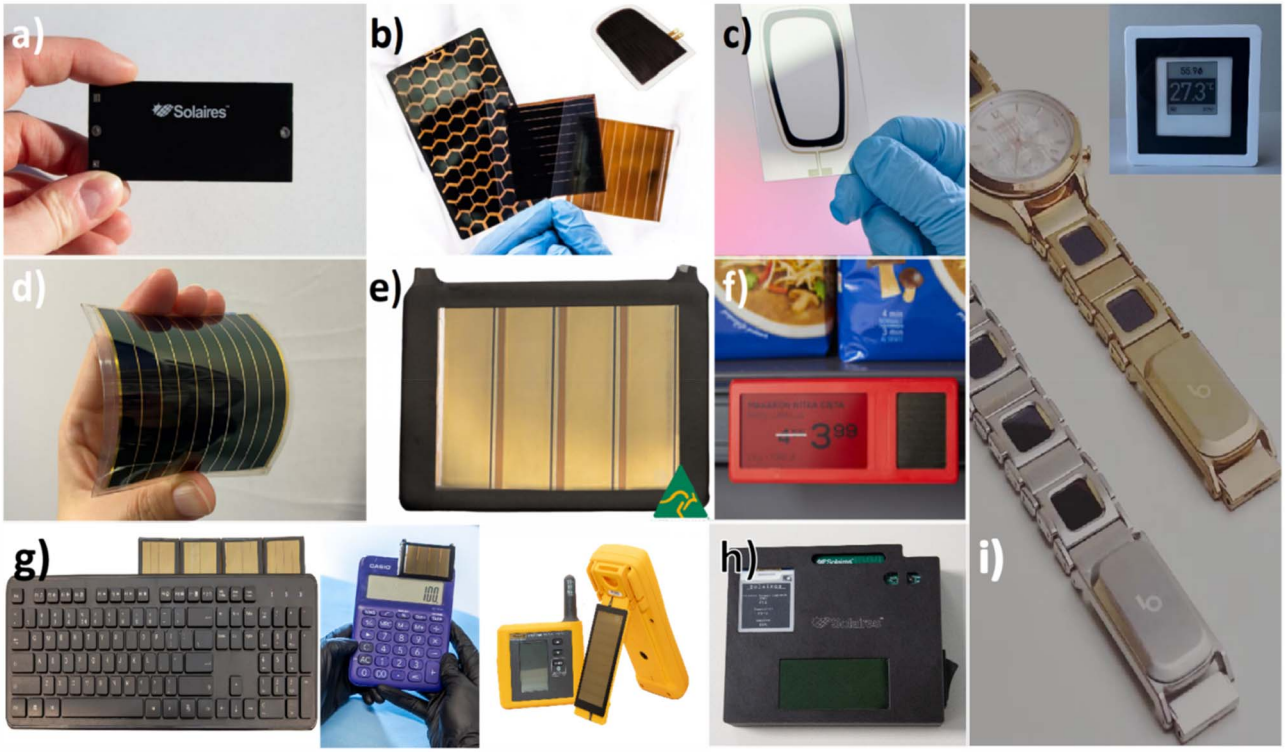

Fig. 13 Commercial players advancing indoor perovskite solar cells and modules. (a) 3-cell solar module by Solaires;[217] (b) different shapes and patterns by Saule Technologies;[218] (c) digitally printed solar cells by Perovskia;[219] (d) module by Enecoat;[220] (e) module by Hallocell;[221] (f) photovoltaic module integrated price tag by Saule Technologies;[222] (g) use cases by Hallocell;[223] (h) use case by Solaires;[224] (i) use cases by Perovskia.[225]

By June 2025, Hallocell, in partnership with Sofab Inks, launched its fully recyclable "Ambient Module" series based on perovskite photovoltaic cells manufactured in its Australian facility. Initially, the product line included a nine-cell module (116 × 57 × 0.6 mm^3, 6.8 g) delivering 1.22 mW at a V_{mpp} of 5.16 V under 1000 lx and a four-cell module (59.5 × 41 × 0.6 mm^3, 2.8 g) producing 0.55 mW at a V_{mpp} of 2.75 V (Fig. 13e).[221] This lineup was later supplemented by an additional four-cell module (60 × 22.5 × 0.6 mm^3, 1.7 g) generating 0.25 mW at a V_{mpp} of 2.8 V under the same illumination. The modules were priced at approximately AUD 36.23, AUD 29.59, and AUD 25.67, respectively (product pricing information was last accessed and verified in April 2026).

Finally, Singfilm introduced the Orchid Series, comprising perovskite modules and cells exhibiting operational durability beyond 10 years and storage stability exceeding 20 years, with performance levels of ≈20 μW cm^{-2} under 200 lx indoor illumination.[228]

7. Patents of perovskite photovoltaic powered indoor electronic devices

The patent landscape for perovskite PVs is rapidly evolving, showcasing emerging key trends, major players and technological advancements. Over the past decade, there has been a significant increase in the number of patents related to perovskite PVs for indoor applications, driven by the growing field of IoT and the need for sustainable, lightweight, flexible and efficient power sources.

To analyse the patent trend over time, the patent data were collected through the Espacenet Patent Search database using the following query string: [Perovskite AND Indoor] for words appearing in the title, abstract or claims of the patents. This procedure yielded an initial sample of 3104 patents in February 2026, which were manually filtered to avoid the inclusion of false positives. According to the time analysis, the annual number of patents in this domain has grown exponentially, particularly since 2015. This trend reflects intensified research and development (R&D) efforts by both academic institutions and commercial enterprises.

Geographically, China, South Korea, Japan and the US are the primary hubs for patent activity in this area, with 56.8% of patents and China leading in the number of patents filed (Fig. 14a). Academic institutions such as the Shanghai Institute of Ceramics, the Wuhan University of Technology, Semiconductor Energy Lab (Japan), Suzhou University and Northwestern Polytechnical University have been at the forefront of fundamental research, resulting in numerous patent filings. Additionally, companies like Ricoh Co. Ltd, Mitsubishi Chemical Corporation and Zeon Corporation have played instrumental roles in translating research into commercially viable technologies (Fig. 14b).

The patent analysis reveals several key technological innovations in the field of perovskite PVs for indoor applications, broadly categorized into material advancement, device

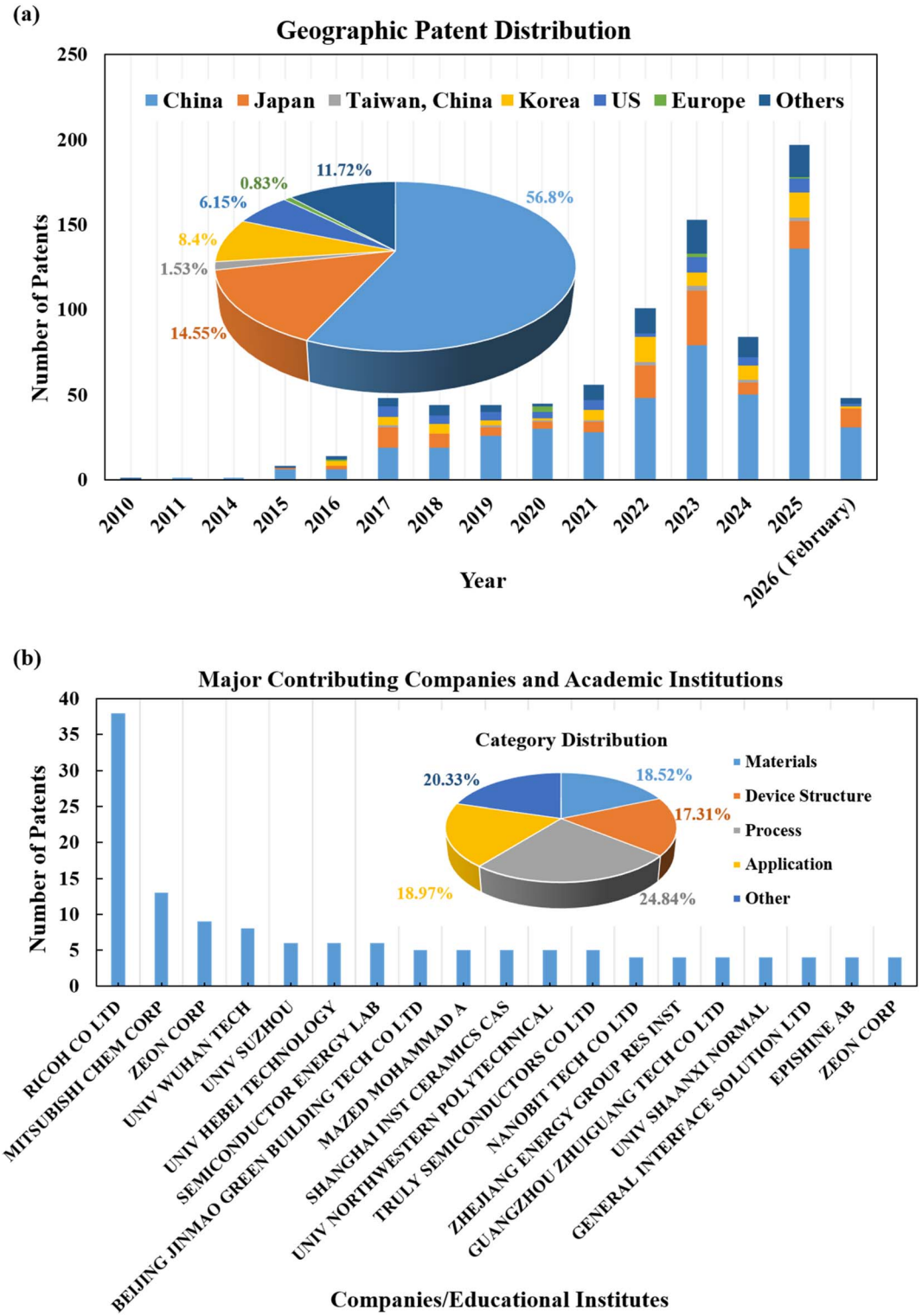

Fig. 14 (a) Geographic distribution of patents over time (data collected in February 2026); (b) key players among companies and academic institutions in the patent landscape (data from July 2025), with insets showing the category distribution of patents (materials, processes, applications, device structures and others). Patent data are sourced from the Espacenet database.

architectures, manufacturing processes and applications (Fig. 14b). Advancing the technology for perovskite photovoltaics for indoor electronic devices is essential for achieving higher efficiencies and versatile applications. The analysis highlights that approximately 20% of the patents detail methods for preparing high-quality materials for stable, low-cost and efficient perovskite thin films and solar cell modules. For instance, the creation of wide bandgap perovskite 2D-3D

heterojunction composite films has facilitated the design of low-light indoor solar cells, enhancing their efficiency in environments where traditional photovoltaic materials are less effective. And the use of sodium dodecyl sulfate (SDS) to treat the interface of all inorganic perovskite ($CsPbI_3$) thin films has improved the short-circuit current density (J_{SC}) (Patent no. CN117156930A, CN103903872A, CN104733617A, CN106463625A, CN106463625B, US2019221692A1, CN109755392A, CN109755392B, CN116487477A and CN111877661A).

The patents filed for the indoor applications of perovskite PVs are relatively few, spanning areas such as low-power communication, sensors, displays and power storage devices. Notable patents include indoor display devices capable of harvesting ambient light energy, featuring integration into electronic shelf labels and digital signage, which have been proposed to enhance energy efficiency in retail environments (Patent no. TWM647441U) (Fig. 15a). Photovoltaic chargers designed to harness low-intensity indoor light have also been developed, providing a sustainable power source for low-power communication devices and sensors. These charges feature a single solar cell unit with a porous light-absorbing layer that includes perovskite along with other materials such as dyed TiO_2, silicon, CdTe, CIGS and GaAs. A boost converter is used to step up the voltage while stepping down the current, ensuring efficient energy transfer (Patent no. TW201947840A and TWI780213B).

Self-sustaining indoor LED displays using perovskite solar cells have also been patented (Patent no. WO2022114776A1, CN115241225A and CN219288074U) (Fig. 15b). Existing LED displays generally rely on external power, have low flexibility and show low light transmission performance. This invention, however, is capable of transmitting various types of information utilizing self-generated power, ensuring flexibility and high light transmittance. The display can be installed on walls or windows of buildings, and when positioned on a window, it can generate its own electricity using sunlight. This makes it economical and allows it to function like a curtain, conveying information without obstructing light. The device not only fulfils the purpose of information transfer but also enhances interior functionality, providing an economical and highly practical display solution.

An RFID electronic tag powered by tin-based perovskite solar cells is another notable application of perovskite PVs, finding

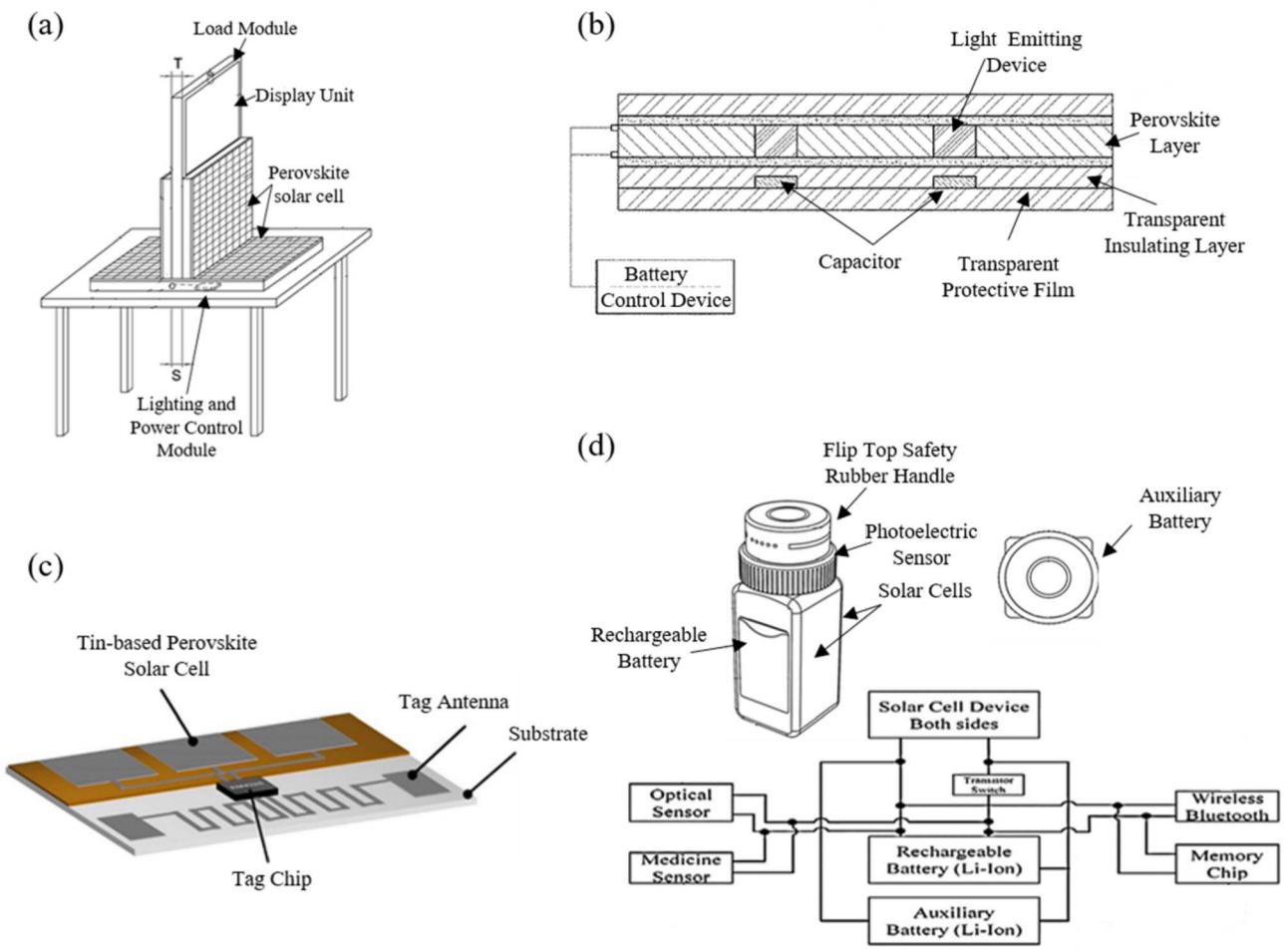

Fig. 15 Illustrations of patented technologies: (a) indoor display device capable of harvesting light energy (Patent no. TWM647441U), (b) self-sustaining LED display (Patent no. WO2022114776A1), (c) RFID electronic tag powered by a tin-based perovskite solar cell (Patent no. CN116245135A) and (d) self-powered intelligent medicine bottle (Patent no. CN215385942U).

usage in various sectors such as logistics, supply chain management, agriculture and environmental monitoring, where long-term and sustainable solutions are crucial (Patent no. CN116245135A) (Fig. 15c). Similarly, a portable notebook computer based on a perovskite luminous energy hull cell efficiently utilizes low light conditions, even in indoor environments, providing a sustainable and environmentally friendly power source. This design reduces reliance on traditional lithium batteries, enhancing portability and energy efficiency (Patent no. CN206649383U).

Perovskite PVs are also envisaged in use for the health sector, offering a sustainable power source for wearable devices that monitor medication adherence, thereby improving healthcare efficiency and outcomes (Patent no. WO2021079358A1). Another patent describes a self-powered intelligent medicine bottle utilizing perovskite solar cells (Patent no. CN215385942U). The solar cells are arranged on the outer side of the bottle body, with the bottom connected to auxiliary batteries for storing solar power. This bottle is provided with the control module, storage module and information prompt module (Fig. 15d).

Patenting has also started to occur in lead-free sustainable technologies in photovoltaics. For instance, a patent introduces a lead-free, wide-band-gap double-perovskite solar cell, specifically tailored for electronic price tag applications (Patent no. CN119907391A). This addresses environmental concerns associated with lead-based materials while extending functionality to low-power commercial displays. Similarly, a patent describes an electronic communication cap embedded with multiple solar cell modules across the crown, side, and visor. Designed to sustain a built-in communication battery, this invention exemplifies the integration of wearable photovoltaics into energy-autonomous communication devices (Patent no. CN119856817A). Lastly, a patent detailing a charging mouse pad for indoor lighting conditions demonstrates the practical deployment of indoor perovskite photovoltaics into workspace accessories, enabling continuous wireless power for peripheral devices (Patent no. CN222462038U).

In addition to consumer and wearable electronics, infrastructure-level applications are also emerging. For instance, a railway track integrated with perovskite solar cells has been proposed to enable distributed energy harvesting along transportation networks, generating electricity even under low-light conditions, such as indoor lighting and train track illumination (Patent no. JP2025114996A). Similarly, in November 2025, a perovskite photovoltaic-powered electronic system designed for stable indoor operation under ambient lighting was disclosed, integrating energy storage and control modules for autonomous low-power devices (Patent no. CN121025546A). These examples further demonstrate the expanding scope of perovskite PV integration beyond conventional device architectures.

These advancements underscore the versatility and potential of perovskite solar cells in revolutionizing indoor energy solutions, promoting sustainability and reducing the dependence on external power sources. As research and development in this field continue to accelerate, further innovations are anticipated, paving the way for more efficient and adaptable energy harvesting technologies tailored for indoor environments.

8 Current challenges and solutions

8.1 Standardized measurement protocols

In recent years, research on indoor photovoltaics has gained significant attention. However, variations in light sources (*e.g.*, LEDs and CFLs), color temperatures (*e.g.*, 3000–6000 K), incident light power at different illuminance levels (*e.g.*, 1000 lx, 500 lx, and 200 lx), and calibration methods used in indoor measurements make it challenging to ensure measurement accuracy. Consequently, direct comparison of results across different laboratories remains difficult. In July 2023, the International Electrotechnical Commission (IEC), the leading global authority on standards for electrical, electronic, and related technologies, published a Technical Specification on nano-enabled photovoltaics—Device Evaluation Method for Indoor Light (IEC TS 62607-7-2:2023), which provides standardized methodologies for measuring device efficiency and represents a key step toward standardization.[229] Although experts have collaborated to refine best practices for standardized indoor PV measurements,[55,56,230–233] the field still needs to continue to develop widely accepted protocols comparable to those meant for outdoor applications. This will help accelerate the industrialization of indoor photovoltaics.

8.2 Scaling up

Indoor solar modules typically range from 1 to 1000 cm^2, depending on the size of the target electronic device, and are much smaller than outdoor panels, which generally span 1.7–1.9 m^2.[19] Unlike outdoor modules, indoor designs differ not only in overall module area but also in individual cell dimensions. The photocurrents generated are in fact low, so geometrical designs should be customized. When scaling from small laboratory cells to modules, defects over larger areas and in cell interconnects can cause performance losses more pronounced than those observed under STC. This necessitates the optimization of deposition and patterning techniques. Furthermore, indoor modules must be seamlessly integrated into consumer products, making geometry, connectivity, aesthetics, and integration strategies (and their associated costs) critical design considerations. Thin, flexible PV devices are often preferred for indoor use, as they enable easier integration and do not require the extended lifetimes demanded by outdoor applications.[19] As a result, indoor perovskite modules require dedicated design and systematic research. Historically, studies on indoor modules have represented only a small fraction of perovskite solar cell research. However, publication trends from 2015 to 2025 indicate that research in this area is gaining increasing attention (Fig. 16a).

8.3 Possible toxicity concerns

Indoo photovoltaic electronics are oriented to products that people come into close contact with and wear in their daily lives. Currently, high-efficiency IPVs based on perovskites usually use

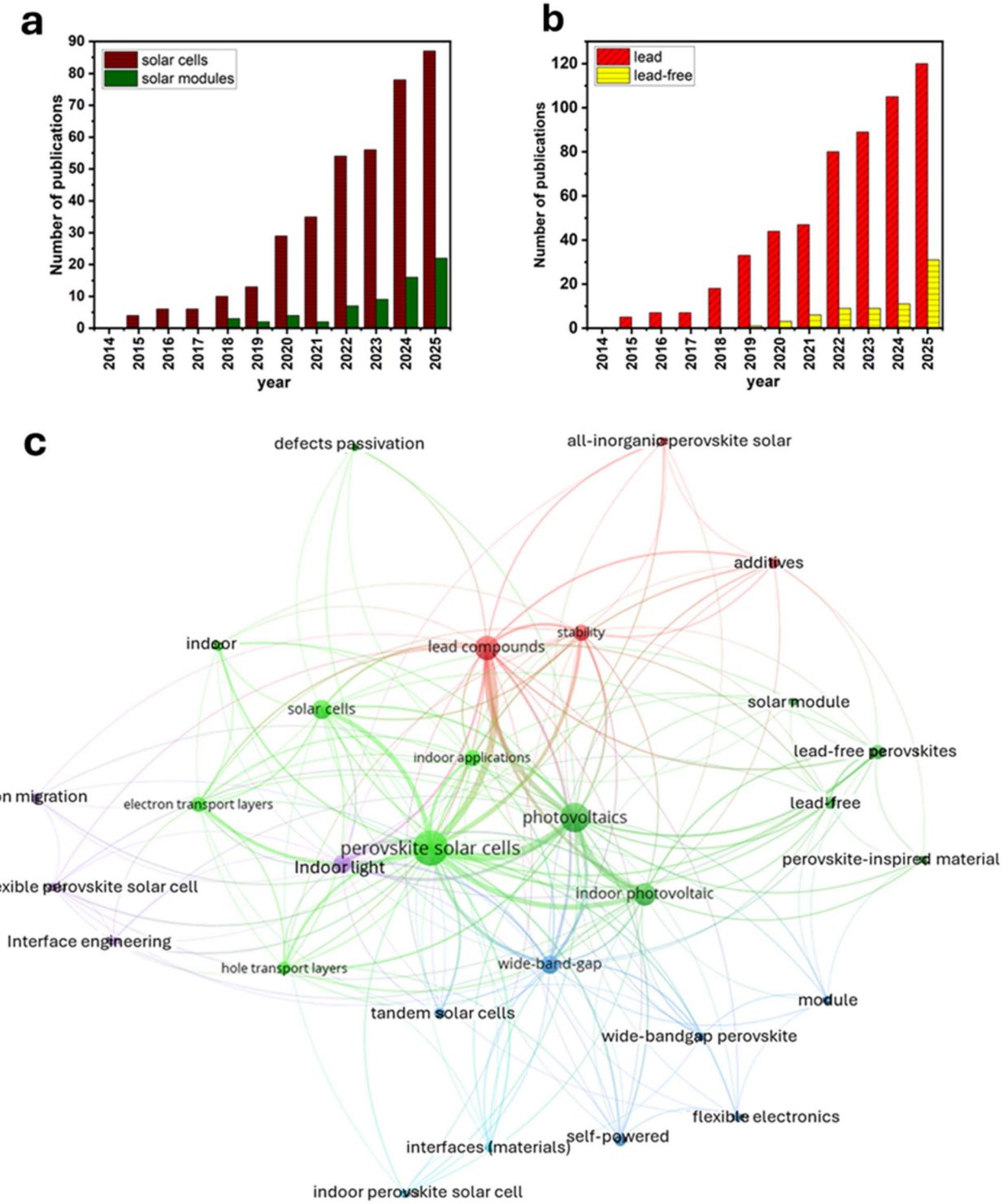

Fig. 16 Analyses of publications in the field of indoor perovskite photovoltaics (data from 30 September 2025). (a) The bar chart compares the annual number of publications on laboratory-scale solar cells and solar modules in the field of indoor perovskite photovoltaics over the past 10 years. (b) The bar chart compares the annual number of publications on lead-halide and lead-free perovskite solar cells in the field of indoor photovoltaics over the 10 years. (c) Visualization of 29 keyword characters in this review from 430 references collected from SCOPUS using VOS viewer software.

absorbers containing the heavy metal lead. The EU Restriction of Hazardous Substances (RoHS) directive stipulates that the lead content in electronic products must be limited to 0.1 wt%.[169,234] While the amounts may not be high and companies industrializing the technology for application indoors affirm that they are below this threshold, there is

interest in eliminating Pb from the materials used. Therefore, focusing on improving the performance of lead-free, low-toxic indoor photovoltaic alternatives and developing highly reliable external and internal encapsulation materials and technologies are also key research goals in the field.[235–238] However, such alternatives have historically lagged behind lead-based counterparts and have only recently begun to attract significant attention from the research community (Fig. 16b). A recent study conducted a LCA comparing lead-containing and lead-free halide perovskite IPV devices to evaluate the environmental sustainability of their absorber layers, precursors, functional layers, and manufacturing processes.[134] The results revealed comparable LCA outcomes among antimony-, tin-, and lead-based IPV absorbers, particularly in terms of toxicity, thereby challenging the widespread assumption that lead-free IPVs are inherently more environmentally benign. Moreover, the study found that the primary environmental impact at the absorber level originates from organic and inorganic halide salts rather than from lead or other metal halides, contradicting the common belief that B-site metal halide toxicity is the main source of environmental pollution. Consequently, future research should prioritize assessing the environmental impacts of frequently used organic and inorganic halide salts (*e.g.*, FAI, FABr, MACl, MABr, RbI, MAI, CsI, and AgI). Overall, while LCAs provide essential insights into the environmental and safety profiles of both lead-containing and lead-free halide perovskites, current research in this area remains limited and warrants greater attention from the research community.[129,134]

8.4 Manufacturing costs

Recently, several startups have developed indoor self-powered electronics integrating perovskite photovoltaics. In the long term, market competitiveness will largely depend on cost, as consumer acceptance is closely tied to product affordability. Therefore, the price of perovskite-based indoor electronic products must be comparable to that of silicon photovoltaic or battery-powered alternatives. Achieving this requires perovskite modules with low manufacturing costs. It has been projected that perovskite modules could be produced using high-throughput, solution-based fabrication methods with an annual production capacity of approximately 10^6 m^2 $year^{-1}$ and a manufacturing cost below \$0.01 cm^{-2}, making them highly competitive for indoor PV applications.[6] Previous studies have shown that improving module efficiency can significantly reduce overall production costs. Therefore, developing high-efficiency modules through precise and scalable fabrication processes represents a promising strategy for further cost reduction. In the future, advancing the industrialization of indoor perovskite photovoltaics will require continued efforts to enhance device efficiency and lifetime while optimizing manufacturing methods to achieve greater cost-effectiveness.[239,240]

8.5 Stability

Compared to photovoltaics for outdoor applications, indoor photovoltaics operate under milder conditions indoors and the lifespan of integrated electronics is usually not required to exceed ten years. Therefore, their stability issues are considered less acute than those of photovoltaics used under outdoor conditions (usually require more than 25 years). However, under low-light indoor conditions, efficiency is more sensitive to defects. Therefore, in future research, it is necessary to systematically study the degradation mechanism of device performance indoors and develop reliable encapsulation technology to meet the life requirements of indoor electronic products. Moreover, the field currently lacks standardized protocols for stability testing, underscoring the need to establish guidelines analogous to ISOS for outdoor photovoltaics to accelerate technological development. The increase in the number of field study of PSCs under realistic indoor conditions and applications will also be important to gauge lifetimes in the variety of different real operational situations.[241]

8.6 Recycling of photovoltaic devices

The end-of-life scenarios for PSCs generally fall into three categories: recycling, landfill disposal, and module failure with subsequent accidental release. Improper disposal of expired devices can pose risks of environmental contamination. Effective recycling of spent PSC modules can mitigate these risks, reduce the energy demand and environmental burden associated with their production, and promote sustainable deployment. In addition to minimizing soil pollution, recycling also enables the recovery of valuable materials such as gold, silver, and other electrode metals.[242–244] Consequently, the development of efficient and scalable recycling technologies represents a critical consideration for the future of IPVs. Recent studies have demonstrated that closed-loop recycling strategies can further diminish the toxicological impacts associated with hazardous constituents in IPVs. Nevertheless, additional research is required to establish industrially viable recycling processes tailored to PSCs with diverse architectures and active layers, particularly those employing robust hydrophobic carbon electrodes and compositionally complex mixed-cation or mixed-halide absorbers. Future efforts should also prioritize the advancement of energy-efficient and economically sustainable recycling methodologies to enable the large-scale industrialization of perovskite photovoltaic technologies.[134,245,246]

8.7 Research trends

Using keyword co-occurrence visualization of 29 terms extracted from 430 references in SCOPUS (Fig. 16c), several key insights into indoor perovskite photovoltaics can be identified. In this network, the size of each label and circle corresponds to the weight of the keyword, indicating its relative importance, while line thickness reflects the strength of connections; keywords positioned closer together exhibit stronger relatedness. The first cluster highlights device physics and performance optimization, with a focus on defect passivation and charge transport engineering as strategies to improve efficiency under low-intensity indoor illumination. The second cluster emphasizes sustainability and integration, where lead-free and perovskite-inspired materials are investigated to address toxicity

concerns, alongside efforts to translate laboratory-scale devices into scalable modules. The third cluster represents advanced architectures and functional devices, including wide-bandgap absorbers, tandem cells, flexible electronics, and self-powered systems designed for IoT, wearables, and consumer electronics. Clusters four and five address long-term performance, focusing on stability and reliability using additives, all-inorganic formulations, and interface engineering to suppress ion migration and degradation, particularly in flexible devices. The sixth cluster highlights interfacial chemistry and material junctions, a unifying theme that connects fundamental device physics with long-term reliability under weak illumination. Collectively, these clusters outline a balanced research landscape where efficiency, sustainability, stability, and integration are being advanced in parallel, reflecting the transition of indoor perovskite photovoltaics from fundamental studies to scalable and practical technologies.

9 Conclusion and outlook

The rapid development of the IoT is significantly advancing IPVs. PSCs have emerged as the most promising candidates for self-powered IoT devices due to their superior IPV performances compared to other technologies. Researchers have achieved over 45% (42%) indoor PCE at 1000 lx (200 lx) on rigid substrates and over 42% (35%) on flexible substrates by employing techniques such as composition and bandgap engineering, device structure optimization, and defect passivation through additives and interface treatment.

Flexible devices, which are light weight and can be easily integrated onto the irregular surfaces of indoor electronic devices, meet the requirements for various indoor applications, including powering wearable electronics. However, the best-reported efficiency for large-area modules on flexible substrates is 31%, significantly lower than the 43% efficiency of rigid modules of the same size. Future research should focus on developing large-area flexible modules.

The integration of IPV electronics into daily-use and wearable products raises concerns about the toxicity of lead in lead-halide perovskites. Among lead-free alternatives, tin-based perovskites have achieved the highest IPV efficiency of 17%, but their poor air stability remains a critical issue. Sb/Bi-based perovskite-inspired solar cells, with their high chemical stability, low toxicity, and suitable bandgap (~2 eV), are ideal for IPV applications. However, due to poor film quality and high trap state density, their indoor efficiency is still below 10%. Future research should prioritize improving the photovoltaic performance of these new lead-free, low-toxicity alternatives for indoor use.

There is an urgent need in the IPV field for a widely recognized standardized measurement protocol, similar to the outdoor AM 1.5 G, 1000 W m^{-2}, standard test conditions. Furthermore, research on recycling methods and technologies for photovoltaic integrated electronic devices may become a key consideration for the future of indoor photovoltaics. This review paper offers a comprehensive introduction and discussion on indoor perovskite photovoltaics, providing constructive suggestions for the development of this field.

Author contributions

Jie Xu: investigation, visualization, formal analysis, writing – original draft, writing – review & editing. Thomas M. Brown, Minggao Ouyang and Xiang Liu: writing – review & editing, supervision, conceptualization. Abhisek Chakraborty, Zeynab Skafi, Vaibhav Singh, Diksha Thakur, Ebin Joseph, Shanyue Hou, Zhoucheng Xu and Xueqing Xu: writing – original draft, writing – review & editing.

Conflicts of interest

There are no conflicts to declare.

Data availability

No data were used for the research described in the article.

Acknowledgements

J. X. gratefully acknowledges financial support from the China Scholarship Council (CSC, No.202004910288) and the China Postdoctoral Science Foundation (2025M780092). This project has received funding from the Italian Ministry of University and Research (MUR) through the PRIN2022 REPLACE (project no. 2022C4YNP8) and PRIN2022 PNRR INPOWER (project no. P2022PXS5S) grants. A. C. acknowledges funding from the European Union's Horizon Europe research and innovation programme under the Marie Skłodowska-Curie grant agreement no. 101111407 (PHOMOTRIPP) and Italian Ministry of University and Research (MUR) "Funding projects presented by young researchers" SOE (Project ID: SOE: 0000101). T.M.B. also acknowledges Lazio Innova for the funding PR FESR LAZIO 2021-2027 "Riposizionamento competitivo RSI di cui alla Det. n. G18823 del 28.12.2022 – Ambito 2 "Economica del mare, Green economy e Agrifood" progetto di riferimento IGEA", and the European Union and MUR for financing the DEPSI project under the framework of the Clean Energy Transition Partnership (CETP Joint Call 2024) (EU Project ID: CETP-FP-2024-00591; MUR code CETP-2024-TRANS-00119).

References

1 M. R. Sarker, A. Riaz, M. S. H. Lipu, M. H. Md Saad, M. N. Ahmad, R. A. Kadir and J. L. Olazagoitia, Micro energy harvesting for IoT platform: Review analysis toward future research opportunities, *Heliyon*, 2024, **10**, e27778, DOI: 10.1016/j.heliyon.2024.e27778.

2 I. Mathews, S. N. Kantareddy, T. Buonassisi and I. M. Peters, Technology and Market Perspective for Indoor Photovoltaic Cells, *Joule*, 2019, **3**, 1415–1426, DOI: 10.1016/j.joule.2019.03.026.

3 State of IoT 2025: Number of connected IoT devices growing 14% to 21.1 billion globally, https://iot-analytics.com/

number-connected-iot-devices/, accessed November 7, 2025.
4 N. Khambunkoed and F.-C. Chen, Perovskite indoor photovoltaic devices for Internet of Things applications, *J. High Energy Phys.*, 2025, **7**, 032003, DOI: 10.1088/2515-7655/ade5c8.
5 G. K. Grandhi, B. Damien, Z. Skafi, K. Sasitharan, H. Kanaan, H. Alkhatib, S. B. Dkhil, M. J. Carnie, M. Freitag, T. M. Brown and P. Vivo, Underexplored Dimensions of Emerging Indoor Photovoltaics, *ACS Energy Lett.*, 2026, **11**, 2474–2490, DOI: 10.1021/acsenergylett.5c03760.
6 V. Pecunia, L. G. Occhipinti and R. L. Z. Hoye, Emerging Indoor Photovoltaic Technologies for Sustainable Internet of Things, *Adv. Energy Mater.*, 2021, **11**, 2100698, DOI: 10.1002/aenm.202100698.
7 J. P. Tiwari, Outlook and Future Directions for Indoor Photovoltaics: Modern Societal Needs and Challenges, *Energy Fuels*, 2025, **39**, 9623–9640, DOI: 10.1021/acs.energyfuels.5c00165.
8 J. Wang, W. Han, B. Yin, W. Li, J. Zhang, J. Cheng, L. Liu, Y. Gao, Y. Wang and Y. Shi, All-carbon-based highly integrated self-powered sensor enabled by flexible perovskite solar cells, *Nano Res.*, 2025, **18**, 94907801, DOI: 10.26599/NR.2025.94907801.
9 J. Xu, S. H. Reddy, L. A. Castriotta, S. K. Podapangi, M. Luce, A. Cricenti, A. Di Carlo and T. M. Brown, 30% efficient triple-cation perovskite solar cells under indoor illumination enabled by rare earth EuCl3 doping, *Sustain. Energy Fuels*, 2023, **7**, 3404–3411, DOI: 10.1039/D2SE01312F.
10 G. K. Grandhi, G. Koutsourakis, J. C. Blakesley, F. De Rossi, F. Brunetti, S. Öz, A. Sinicropi, M. L. Parisi, T. M. Brown, M. J. Carnie, R. L. Z. Hoye and P. Vivo, Promises and challenges of indoor photovoltaics, *Nat. Rev. Clean Technol.*, 2025, **1**, 132–147, DOI: 10.1038/s44359-024-00013-1.
11 A. Sengupta, M. A. Afroz, B. Sharma, S. Choudhary, N. Pant, Y. Gulia, N. P. Kalapparambath Rajendra Pai, D. Angmo and S. Satapathi, Commercialization of perovskite solar cells: opportunities and challenges, *Sustain. Energy Fuels*, 2025, **9**, 3999–4022, DOI: 10.1039/D4SE01813C.
12 G. K. Grandhi, M. Krishnaiah and P. Vivo, in *Lead-free Perovskites and Their Derivatives for Indoor Photovoltaic Applications*, Springer Nature Switzerland, Cham, pp. , pp. 1–18.
13 Z. Wang, C. Zhang, E. Q. Han, H. Xu, D. He, B. Zhang, P. Chen, M. Lyu and L. Wang, Low-toxicity light-absorbing materials for indoor photovoltaic applications, *J. Mater. Chem. A*, 2026, **14**, 6772–6793, DOI: 10.1039/D5TA07584J.
14 V. Pecunia, S. R. P. Silva, J. D. Phillips, E. Artegiani, A. Romeo, H. Shim, J. Park, J. H. Kim, J. S. Yun, G. C. Welch, B. W. Larson, M. Creran, A. Laventure, K. Sasitharan, N. Flores-Diaz, M. Freitag, J. Xu, T. M. Brown, B. Li, Y. Wang, Z. Li, B. Hou, B. H. Hamadani, E. Defay, V. Kovacova, S. Glinsek, S. Kar-Narayan, Y. Bai, D. B. Kim, Y. S. Cho, A. Žukauskaitė, S. Barth, F. R. Fan, W. Wu, P. Costa, J. del Campo, S. Lanceros-Mendez, H. Khanbareh, Z. L. Wang, X. Pu, C. Pan, R. Zhang, J. Xu, X. Zhao, Y. Zhou, G. Chen, T. Tat, I. W. Ock, J. Chen, S. A. Graham, J. S. Yu, L.-Z. Huang, D.-D. Li, M.-G. Ma, J. Luo, F. Jiang, P. S. Lee, B. Dudem, V. Vivekananthan, M. G. Kanatzidis, H. Xie, X.-L. Shi, Z.-G. Chen, A. Riss, M. Parzer, F. Garmroudi, E. Bauer, D. Zavanelli, M. K. Brod, M. A. Malki, G. J. Snyder, K. Kovnir, S. M. Kauzlarich, C. Uher, J. Lan, Y.-H. Lin, L. Fonseca, A. Morata, M. Martin-Gonzalez, G. Pennelli, D. Berthebaud, T. Mori, R. J. Quinn, J.-W. G. Bos, C. Candolfi, P. Gougeon, P. Gall, B. Lenoir, D. Venkateshvaran, B. Kaestner, Y. Zhao, G. Zhang, Y. Nonoguchi, B. C. Schroeder, E. Bilotti, A. K. Menon, J. J. Urban, O. Fenwick, C. Asker, A. A. Talin, T. D. Anthopoulos, T. Losi, F. Viola, M. Caironi, D. G. Georgiadou, L. Ding, L.-M. Peng, Z. Wang, M.-D. Wei, R. Negra, M. C. Lemme, M. Wagih, S. Beeby, T. Ibn-Mohammed, K. B. Mustapha and A. P. Joshi, Roadmap on energy harvesting materials, *Int. J. Mater. Phys.*, 2023, **6**, 042501, DOI: 10.1088/2515-7639/acc550.
15 Z. Guo, A. K. Jena and T. Miyasaka, Halide Perovskites for Indoor Photovoltaics: The Next Possibility, *ACS Energy Lett.*, 2023, **8**, 90–95, DOI: 10.1021/acsenergylett.2c02268.
16 B. T. Muhammad, S. Kar, M. Stephen and W. L. Leong, Halide perovskite-based indoor photovoltaics: recent development and challenges, *Mater. Today Energy*, 2022, **23**, 100907, DOI: 10.1016/j.mtener.2021.100907.
17 F. Di Giacomo, V. Zardetto, G. Lucarelli, L. Cinà, A. Di Carlo, M. Creatore and T. M. Brown, Mesoporous perovskite solar cells and the role of nanoscale compact layers for remarkable all-round high efficiency under both indoor and outdoor illumination, *Nano Energy*, 2016, **30**, 460–469, DOI: 10.1016/j.nanoen.2016.10.030.
18 J. K. W. Ho, H. Yin and S. K. So, From 33% to 57% – an elevated potential of efficiency limit for indoor photovoltaics, *J. Mater. Chem. A*, 2020, **8**, 1717–1723, DOI: 10.1039/C9TA11894B.
19 A. Chakraborty, G. Lucarelli, J. Xu, Z. Skafi, S. Castro-Hermosa, A. B. Kaveramma, R. G. Balakrishna and T. M. Brown, Photovoltaics for indoor energy harvesting, *Nano Energy*, 2024, **128**, 109932, DOI: 10.1016/j.nanoen.2024.109932.
20 M. Freunek, M. Freunek and L. M. Reindl, Maximum efficiencies of indoor photovoltaic devices, *IEEE J. Photovoltaics*, 2013, **3**, 59–64, DOI: 10.1109/JPHOTOV.2012.2225023.
21 P. Kumari, S. Prasanthkumar and L. Giribabu, Recent progress on perovskite based indoor photovoltaics: Challenges and commercialization, *Sol. Energy*, 2024, **284**, 113049, DOI: 10.1016/j.solener.2024.113049.
22 Y. Li, J. Wang, Z. Jiang, Y. Sun, D. Wu, A. Bahtiar, Y. Yang and D. Zhao, Advances in perovskite indoor photovoltaics for intelligent Internet of Things, *Mater. Today*, 2025, **90**, 495–518, DOI: 10.1016/j.mattod.2025.08.028.
23 X. Wu, G. Xiong, Z. Yue, R. Chen, S.-W. Tsang and Y. Cheng, A Perspective on Commercializing Perovskite Solar Cells:

Unlocking Opportunities in Niche Applications, *Small n/a*, 2026, e11874, DOI: 10.1002/smll.202511874.

24 G. Lucarelli, F. Di Giacomo, V. Zardetto, M. Creatore and T. M. Brown, Efficient light harvesting from flexible perovskite solar cells under indoor white light-emitting diode illumination, *Nano Res.*, 2017, **10**, 2130–2145, DOI: 10.1007/s12274-016-1402-5.

25 J. Dagar, S. Castro-Hermosa, G. Lucarelli, F. Cacialli and T. M. Brown, Highly efficient perovskite solar cells for light harvesting under indoor illumination via solution processed SnO2/MgO composite electron transport layers, *Nano Energy*, 2018, **49**, 290–299, DOI: 10.1016/j.nanoen.2018.04.027.

26 Z. Skafi, J. Xu, V. Mottaghitalab, L. Mivehi, B. Taheri, F. Jafarzadeh, S. K. Podapangi, D. Altamura, M. R. Guascito, L. Barba, C. Giannini, A. Rizzo, F. De Rossi, H. Javanbakht Lomeri, L. Sorbello, F. Matteocci, F. Brunetti and T. M. Brown, Highly Efficient Flexible Perovskite Solar Cells on Polyethylene Terephthalate Films via Dual Halide and Low-Dimensional Interface Engineering for Indoor Photovoltaics, *Sol. RRL*, 2023, **7**, 2300324, DOI: 10.1002/solr.202300324.

27 S. Castro-Hermosa, G. Lucarelli, M. Top, M. Fahland, J. Fahlteich and T. M. Brown, Perovskite Photovoltaics on Roll-To-Roll Coated Ultra-thin Glass as Flexible High-Efficiency Indoor Power Generators, *Cell Rep. Phys. Sci.*, 2020, **1**, 100045, DOI: 10.1016/j.xcrp.2020.100045.

28 D. Dou, H. Sun, C. Li, S. Gan and L. Li, Perovskite-Based Indoor Photovoltaics and their Competitors, *Adv. Funct. Mater.*, 2024, **34**, 2314398, DOI: 10.1002/adfm.202314398.

29 Q. Ma, Y. Wang, L. Liu, P. Yang, W. He, X. Zhang, J. Zheng, M. Ma, M. Wan, Y. Yang, C. Zhang, T. Mahmoudi, S. Wu, C. Liu, Y.-B. Hahn and Y. Mai, One-step dual-additive passivated wide-bandgap perovskites to realize 44.72%-efficient indoor photovoltaics, *Energy Environ. Sci.*, 2024, **17**, 1637–1644, DOI: 10.1039/D3EE04022D.

30 Y. Wang, T. Yang, W. Cai, P. Mao, Y. Yang, N. Wu, C. Liu, S. Wang, Y. Du, W. Huang, G. Zhao, Z. Ding, N. Yuan, J. Ding, Y. Zhong, S. Liu and K. Zhao, Defect Passivation Refinement in Perovskite Photovoltaics: Achieving Efficiency over 45% under Low-Light and Low-Temperature Dual Extreme Conditions, *Adv. Mater.*, 2024, **36**, 2312014, DOI: 10.1002/adma.202312014.

31 C. Zhang, C. Liu, Y. Gao, S. Zhu, F. Chen, B. Huang, Y. Xie, Y. Liu, M. Ma, Z. Wang, S. Wu, R. E. I. Schropp and Y. Mai, Br Vacancy Defects Healed Perovskite Indoor Photovoltaic Modules with Certified Power Conversion Efficiency Exceeding 36%, *Advanced Science*, 2022, **9**, 2204138, DOI: 10.1002/advs.202204138.

32 Q. Ma, M. Ma, L. Liu, P. Yang, W. He, X. Zhang, J. Zheng, C. Zhang, C. Liu, S. Wu, Y. Wang and Y. Mai, Wide-band-gap perovskite solar minimodules exceeding 43% efficiency under indoor light illumination, *Device*, 2023, **1**, 100174, DOI: 10.1016/j.device.2023.100174.

33 C.-Y. Chen, J.-H. Chang, K.-M. Chiang, H.-L. Lin, S.-Y. Hsiao and H.-W. Lin, Perovskite Photovoltaics for Dim-Light Applications, *Adv. Funct. Mater.*, 2015, **25**, 7064–7070, DOI: 10.1002/adfm.201503448.

34 M.-J. Wu, C.-C. Kuo, L.-S. Jhuang, P.-H. Chen, Y.-F. Lai and F.-C. Chen, Bandgap Engineering Enhances the Performance of Mixed-Cation Perovskite Materials for Indoor Photovoltaic Applications, *Adv. Energy Mater.*, 2019, **9**, 1901863, DOI: 10.1002/aenm.201901863.

35 J. Xu, S. K. Podapangi, S. H. Reddy, L. A. Castriotta, A. Di Carlo and T. M. Brown, Key Parameters and Thresholds Values for Obtaining High Performance Perovskite Solar Cells Indoors from Full Br Compositional and Bandgap Engineering, *ACS Appl. Energy Mater.*, 2023, **6**, 10215–10224, DOI: 10.1021/acsaem.2c03394.

36 M. Li, C. Zhao, Z.-K. Wang, C.-C. Zhang, H. K. H. Lee, A. Pockett, J. Barbé, W. C. Tsoi, Y.-G. Yang, M. J. Carnie, X.-Y. Gao, W.-X. Yang, J. R. Durrant, L.-S. Liao and S. M. Jain, Interface Modification by Ionic Liquid: A Promising Candidate for Indoor Light Harvesting and Stability Improvement of Planar Perovskite Solar Cells, *Adv. Energy Mater.*, 2018, **8**, 1801509, DOI: 10.1002/aenm.201801509.

37 R. Cheng, C.-C. Chung, H. Zhang, F. Liu, W.-T. Wang, Z. Zhou, S. Wang, A. B. Djurišić and S.-P. Feng, Tailoring Triple-Anion Perovskite Material for Indoor Light Harvesting with Restrained Halide Segregation and Record High Efficiency Beyond 36%, *Adv. Energy Mater.*, 2019, **9**, 1901980, DOI: 10.1002/aenm.201901980.

38 Z. Li, J. Zhang, S. Wu, X. Deng, F. Li, D. Liu, C. C. Lee, F. Lin, D. Lei, C.-C. Chueh, Z. Zhu and A. K. Y. Jen, Minimized surface deficiency on wide-bandgap perovskite for efficient indoor photovoltaics, *Nano Energy*, 2020, **78**, 105377, DOI: 10.1016/j.nanoen.2020.105377.

39 X. He, J. Chen, X. Ren, L. Zhang, Y. Liu, J. Feng, J. Fang, K. Zhao and S. Liu, 40.1% Record Low-Light Solar-Cell Efficiency by Holistic Trap-Passivation using Micrometer-Thick Perovskite Film, *Adv. Mater.*, 2021, **33**, 2100770, DOI: 10.1002/adma.202100770.

40 Y. Du, Q. Tian, X. Chang, J. Fang, X. Gu, X. He, X. Ren, K. Zhao and S. Liu, Ionic Liquid Treatment for Highest-Efficiency Ambient Printed Stable All-Inorganic CsPbI3 Perovskite Solar Cells, *Adv. Mater.*, 2022, **34**, 2106750, DOI: 10.1002/adma.202106750.

41 Y. Li, T. Nie, X. Ren, Y. Wu, J. Zhang, P. Zhao, Y. Yao, Y. Liu, J. Feng, K. Zhao, W. Zhang and S. Liu, In Situ Formation of 2D Perovskite Seeding for Record-Efficiency Indoor Perovskite Photovoltaic Devices, *Adv. Mater.*, 2024, **36**, 2306870, DOI: 10.1002/adma.202306870.

42 K.-L. Wang, H. Lu, M. Li, C.-H. Chen, D. Bo Zhang, J. Chen, J.-J. Wu, Y.-H. Zhou, X.-Q. Wang, Z.-H. Su, Y.-R. Shi, Q.-S. Tian, Y.-X. Ni, X.-Y. Gao, S. M. Zakeeruddin, M. Grätzel, Z.-K. Wang and L.-S. Liao, Ion–Dipole Interaction Enabling Highly Efficient CsPbI3 Perovskite Indoor Photovoltaics, *Adv. Mater.*, 2023, **35**, 2210106, DOI: 10.1002/adma.202210106.

43 Q. Ma, J. Zheng, Z. Chen, L. Wang, T. Du, J. Peng, Y. Peng, D. Xiao, H. Zhu, Y. Wang and Y. Mai, Surface-Reconstructed NiOx via Solvent-Mediated Engineering for Wide-Bandgap

Perovskite Indoor Photovoltaics, *Small Methods*, 2025, **9**, e01887, DOI: 10.1002/smtd.202501887.

44 X.-Y. He, B. Song, K.-L. Wang, N. Li, L. Huang, R.-H. Qin, J. Chen, C.-H. Chen, Y. Xia, I. Yavuz, Y.-H. Lou and Z.-K. Wang, Stopping Phase Separation Enables Durable Wide-Bandgap Photovoltaic Perovskites, *Adv. Mater.*, 2026, **38**, e18492, DOI: 10.1002/adma.202518492.

45 IEC Technical Specification 62607-7-2, https://webstore.iec.ch/en/publication/61819, accessed February 27, 2026.

46 G. Burwell, S. Zeiske, P. Caprioglio, O. J. Sandberg, A. M. Kay, M. D. Farrar, Y. R. Kim, H. J. Snaith, P. Meredith and A. Armin, Wide-Gap Perovskites for Indoor Photovoltaics, *Sol. RRL*, 2024, **8**, 2400180, DOI: 10.1002/solr.202400180.

47 S. S. Dipta, A. H. Howlader, W. B. Tarique and A. Uddin, Comparative Analysis of the Stability and Performance of Double-, Triple-, and Quadruple-Cation Perovskite Solar Cells for Rooftop and Indoor Applications, *Molecules*, 2024, **29**, 2758, DOI: 10.3390/molecules29122758.

48 M. Jošt, Ž. Ajdič and M. Topič, Performance of Triple-Cation Perovskite Solar Cells under Different Indoor Operating Conditions, *ACS Appl. Mater. Interfaces*, 2024, **16**, 62195–62202, DOI: 10.1021/acsami.4c14736.

49 M. M. Agapitova, A. V. Novikov, A. N. Zhivchikova, O. R. Trepalin, I. E. Kuznetsov, O. R. Parfenova, K. D. Zagorovskaia, N. A. Malkin, V. A. Brotsman, E. V. Zhizhin, A. V. Koroleva, S. A. Baryshev, A. E. Goldt, A. G. Boldyreva, A. V. Akkuratov, A. A. Goryunkov, S. Y. Luchkin and M. M. Tepliakova, Boosting the stability of indoor perovskite solar cells by the rational selection of electron transport layers, *Appl. Phys. Lett.*, 2025, **127**, 023906, DOI: 10.1063/5.0270607.

50 S. Huang, S. Hou, G. Sanfo, J. Xu, Y. Wang, H. Muwanwella, L. Pfeifer, X. Liu, S. M. Zakeeruddin, Y. Huang, M. Grätzel, M. T. Sajjad and M. Abdi-Jalebi, Enhancing Indoor Photovoltaic Efficiency to 37.6% Through Triple Passivation Reassembly and n-Type to p-Type Modulation in Wide Bandgap Perovskites, *Adv. Funct. Mater.*, 2025, **35**, 2502152, DOI: 10.1002/adfm.202502152.

51 P. Gnanasekaran, Z.-E. Shi, C.-L. Wang, J.-K. Peng, B.-H. Jiang, C.-P. Chen and Y. J. Chang, Interfacial Engineering Using C-3 Alkyl Linker-Based Carbazole-Derived SAM Layers to Achieve 41.77% Indoor Efficiency in Wide-Bandgap Perovskite Solar Cells, *Small*, 2025, **21**, 2500983, DOI: 10.1002/smll.202500983.

52 R. Wang, J. Wu, Q. Zheng, H. Deng, W. Wang, J. Chen, X. Wang, M. Wei, Z.-K. Wang and S. Cheng, Stable and Efficient Indoor Photovoltaics Through Novel Dual-Phase 2D Perovskite Heterostructures, *Adv. Mater.*, 2025, **37**, 2419573, DOI: 10.1002/adma.202419573.

53 D. Li, T. Nie, G. Zhao, R. Lv, J. Feng, J. Ding, S. Yang, S. Liu and Z. Fang, Dual Optimization via Doping PCBM with Diamine for Efficient Pure-Iodide Wide-Bandgap Perovskite Solar Cells, *Adv. Funct. Mater.*, 2025, **36**, e02847, DOI: 10.1002/adfm.202502847.

54 M. J. Choi, S. W. Lee, H. Shim, S. J. Shin, H. W. Chun, S. E. Yoon, J. A. Prayogo, J. Seidel, J. S. Yun, D. W. Chang and J. H. Kim, Ambipolar Interfacial Molecule for Enhancing Performances of Perovskite Solar Cells with Versatile Architectures Under Various Illumination Environments, *Adv. Energy Mater.*, 2025, **15**, 2501113, DOI: 10.1002/aenm.202501113.

55 J. M. Jailani, A. Luu, E. Salvosa, C. Clegg, V. P. Kamalon, B. Nasrollahi, I. Valitova, S. B. Meier, A. M. Shore, B. H. Hamadani and V. Pecunia, Accurate performance characterization, reporting, and benchmarking for indoor photovoltaics, *Joule*, 2025, **9**, 102126, DOI: 10.1016/j.joule.2025.102126.

56 R. L. Z. Hoye, G. Koutsourakis, M. Freitag, Z. Jehl Li-Kao, T. Österberg, S. Aliwell, M. Bellanger, T. M. Brown, F. Brunetti, M. J. Carnie, A. Chakraborty, G. Grancini, P. Kärhä, M. Kauer, T. Kirchartz, C.-T. Lin, M. Lira-Cantú, Y.-S. Long, S. Öz, S. R. Raga, E. Saucedo, P. Vivo, S. W. Leow, K. Wojciechowski, A. Zampetti, R. Zhou, S. Züfle and G. Burwell, Reaching a consensus on indoor photovoltaics testing, *Joule*, 2025, **9**, 102127, DOI: 10.1016/j.joule.2025.102127.

57 V. Pecunia, Toward reliable characterization of nano-enabled indoor photovoltaics: accounting for device-dependent errors, *Nano Futures*, 2026, **10**, 015001, DOI: 10.1088/2399-1984/ae47a0.

58 W. Khampa, L. Le, W. Passatorntaschakorn, J. Loftus, J. M. Jailani, F. Sandoval Giron, D. Wongratanaphisan, C. Patel and V. Pecunia, A universal design and benchmarking framework for indoor photovoltaics, *Newton*, 2026, 100437, DOI: 10.1016/j.newton.2026.100437.

59 Y. Li, Z. Zhang, Y. Cai, S. Pu, M. Cheng, Z. Xie, Y. Sun, Q. Cao, C. Chen, H. Li, Z. Liu, Z. Wang, S. Liu and Y. Duan, Synergistic Isothiourea–Guanidine Additive for Achieving Stable Perovskite Solar Cells with a High Certified Quasi-Steady-State Output, *Adv. Mater.*, 2026, **38**, e14903, DOI: 10.1002/adma.202514903.

60 Y.-H. Chen, Z.-E. Shi, Y.-C. Liu, B.-S. Peng, C.-K. Wen, C.-L. Wang, S.-C. Chen and C.-P. Chen, Comparative study of DCMS and HiPIMS sputtered NiOx thin films for hole transport in wide bandgap perovskite solar cells, *Electrochim. Acta*, 2026, **557**, 148466, DOI: 10.1016/j.electacta.2026.148466.

61 S. K. Podapangi, L. Mancini, D. Takhellambam, J. Xu, L. A. Castriotta, G. Mattioli, V. Raglione, F. Palmeri, D. Caschera, A. P. Sobolev, A. Cricenti, D. Becerril Rodriguez, M. Luce, A. Di Carlo, G. Zanotti and T. M. Brown, Improved Perovskite Solar Cells with an Environmentally Friendly Phthalocyanine Hole Extracting Interlayer, *ACS Appl. Energy Mater.*, 2026, **9**, 2541–2554, DOI: 10.1021/acsaem.5c03517.

62 S. Shcherbachenko, O. Astakhov, Z. Liu, L.-C. Kin, C. Zahren, U. Rau, T. Kirchartz and T. Merdzhanova, High-Bandgap Perovskites for Efficient Indoor Light Harvesting, *Adv. Energy Sustain. Res.*, 2024, **5**, 2400032, DOI: 10.1002/aesr.202400032.

63 Z.-E. Shi, K. Kollimalaian, J.-K. Peng, C.-W. Lin, W.-T. Peng, B.-H. Jiang, Y. H. Lin, L.-Y. Yang, Y.-C. Lin, P. Venkatakrishnan, Y. J. Chang and C.-P. Chen, Enhanced Indoor Perovskite Solar Cells: Mitigating Interface Defects and Charge Transport Losses with Polyarene-Based Hole-Selective Layers, *Adv. Energy Mater.*, 2025, **15**, 2404234, DOI: 10.1002/aenm.202404234.

64 C.-T. Hsu, C.-W. Lee and F.-C. Chen, Chelating agent-based defect passivation for enhanced indoor performance of wide-bandgap perovskite solar cells, *Appl. Energy*, 2025, **3**, 026111, DOI: 10.1063/5.0260714.

65 U. A. Shah, G. Shankar, C. Malerba, P. P. Bonaccini, F. Zarotti, V. Novelli, A. Di Carlo, A. Mittiga, F. Biccari and E. Calabrò, Comparative Study of Different Passivation Layers for n-i-p Perovskite Solar Cell for Indoor Applications, *Sol. RRL*, 2025, **9**, 2400849, DOI: 10.1002/solr.202400849.

66 T. Wen, Y. Wu, J. Sun, J. Zhou, Q. Tian, Y. Shi, M. Chen, C. Yu, Y. Wang, S. Yang, Y. Hou, Z. Yang and H. Peng, Minimizing Voltage Deficit in Perovskite Indoor Photovoltaics by Interfacial Engineering, *Small*, 2025, **21**, 2408271, DOI: 10.1002/smll.202408271.

67 B. Mondal, R. Tiwari, S. Manna, F. Banerjee, R. Singh and S. K. Samanta, Dual-Strategy from a Single Molecule: Low-Cost, Dopant-Free, Stable D–A–D Type Quinoxaline-Based Hole-Transporting Materials for Perovskite Solar Cells in Both Indoor and Outdoor Applications, *ACS Appl. Energy Mater.*, 2025, **8**, 3459–3469, DOI: 10.1021/acsaem.4c02977.

68 J. Tong, C. Dong, V. M. Arnal, M. Yao, Q. Wang, Y. Song, Y. Deng, Y. Gao, G. Yue, W. Zhang, M. I. Saidaminov and F. Tan, Synergistic potentiation between P3HT and PTAA enables blade-coated carbon-electrode perovskite solar cells with >21% outdoor and >35% indoor efficiencies, *Chem. Eng. J.*, 2024, **501**, 157577, DOI: 10.1016/j.cej.2024.157577.

69 H. Han, J. Xu and -. J. Yao, Defect and stress co-management via bifunctional molecular engineering for high-efficiency and stable $CsPbI_3$ perovskite solar cells, *J. Semiconduct.*, 2026, **47**, 1–6, DOI: 10.1088/1674-4926/25120041.

70 S.-K. Jung, N.-G. Park and J.-W. Lee, Light management in perovskite solar cells, *Mater. Today Energy*, 2023, **37**, 101401, DOI: 10.1016/j.mtener.2023.101401.

71 A. M. Kay, D. B. Riley, G. Burwell and P. Meredith, Thermodynamic principles for optimizing multi-junction photovoltaics—Exemplified for perovskite-based indoor photovoltaics, *Appl. Energy*, 2025, **3**, 036102, DOI: 10.1063/5.0266374.

72 Z. Li, B. Chen, L. Yao, C. Li, W. Wang, J. Zhang, H. Lai, P. Cheng, H. Xu and S. Tang, Asymmetric microcavity to enhance light utilization in colorful semitransparent perovskite solar cells, *Sol. Energy*, 2025, **298**, 113677, DOI: 10.1016/j.solener.2025.113677.

73 A. Venkateswararao, J. K. W. Ho, S. K. So, S.-W. Liu and K.-T. Wong, Device characteristics and material developments of indoor photovoltaic devices, *Mater. Sci. Eng. R Rep.*, 2020, **139**, 100517, DOI: 10.1016/j.mser.2019.100517.

74 E. Karpiola, G. K. Grandhi, C. Doyranli, Y. Han, A. Alexander, L. K. Jagadamma, A. Tewari, D. Manna and P. Vivo, Bulk Passivation of Lead Halide Perovskites: The Key to High-Performance Indoor Photovoltaics at Very Low-Light Intensities, *Sol. RRL*, 2025, **9**, 202500195, DOI: 10.1002/solr.202500195.

75 Z.-E. Shi, K. Kollimalaian, J.-K. Peng, C.-W. Lin, W.-T. Peng, B.-H. Jiang, Y. H. Lin, L.-Y. Yang, Y.-C. Lin, P. Venkatakrishnan, Y. J. Chang and C.-P. Chen, Enhanced Indoor Perovskite Solar Cells: Mitigating Interface Defects and Charge Transport Losses with Polyarene-Based Hole-Selective Layers (Adv. Energy Mater. 6/2025), *Adv. Energy Mater.*, 2025, **15**, 2570029, DOI: 10.1002/aenm.202570029.

76 Y. Han, C. Doyranli, A. Di Vito, M. Auf der Maur, M. Krishnaiah, P. Mäkinen, R. Kumar, B. Al-Anesi, D. Manna and P. Vivo, Pyridine-Based Multifunctional Surface Passivators Enable Efficient and Stable Perovskite Indoor Photovoltaics, *ACS Appl. Mater. Interfaces*, 2025, **17**, 49409–49420, DOI: 10.1021/acsami.5c08539.

77 E. Karpiola, A. Alexander, A. Tewari, S. Toikkonen, P. Mäkinen, H. Chintam, G. K. Grandhi and P. Vivo, Sulfonium-based passivation suppresses trap recombination and hysteresis under bright-to-ultra-dim light in perovskite indoor photovoltaics, *Appl. Phys. Lett.*, 2026, **128**, 073304, DOI: 10.1063/5.0312569.

78 D. Di Girolamo, G. Vidon, J. Barichello, F. Di Giacomo, F. Jafarzadeh, B. Paci, A. Generosi, M. Kim, L. A. Castriotta, M. Frégnaux, J.-F. Guillemoles, F. Brunetti, P. Schulz, D. Ory, S. Cacovich, A. Di Carlo and F. Matteocci, Breaking 1.7 V Open Circuit Voltage in Large Area Transparent Perovskite Solar Cells Using Interfaces Passivation, *Adv. Energy Mater.*, 2024, **14**, 2400663, DOI: 10.1002/aenm.202400663.

79 S. Wang, T. Kodalle, S. Millar, C. M. Sutter-Fella and L. Krishnan Jagadamma, Metal Oxide vs Organic Semiconductor Charge Extraction Layers for Halide Perovskite Indoor Photovoltaics, *Small Science*, 2024, **4**, 2400292, DOI: 10.1002/smsc.202400292.

80 Z. Hu, C. Zhang, J. Wang, W. Dang, X. Zhang, L. Ren, P. Li, Q. Guo, L. Chao, Y. Xia, L. Aigouy, Z. Chen, Z. Hu and Y. Chen, Sandwich polymer structure-based PTAA for 1.78 eV wide-bandgap perovskite solar cells in indoor and all-perovskite tandem photovoltaics, *Sci. China Chem.*, 2025, **68**, 5682–5692, DOI: 10.1007/s11426-025-2836-8.

81 Z.-E. Shi, B.-S. Peng, C.-W. Lin, B.-H. Jiang and C.-P. Chen, Enabling high indoor efficiency in methylammonium-free wide-bandgap perovskite solar cells via in situ passivation, *Sustain. Energy Fuels*, 2025, **9**, 4294–4299, DOI: 10.1039/D5SE00288E.

82 Y. Qi, W. Xu, Y. Lou and L. Feng, Recent progress in indoor photovoltaics based on all-inorganic perovskites, *Appl. Phys. Lett.*, 2025, **127**, 040502, DOI: 10.1063/5.0275628.

83 J. Liu, M. Zhang, X. Sun, L. Xiang, X. Yang, X. Hu, Z. Wang, T. Hou, J. Qin, Y. Huang, M. Abdi-Jalebi and X. Hao,

Scalable Fabrication of Methylammonium-Free Wide-Bandgap Perovskite Solar Cells by Blade Coating in Ambient Air, *Nano-Micro Lett.*, 2025, **17**, 318, DOI: 10.1007/s40820-025-01838-6.

84 D. Xu, J. Nie, Z. Hu and Z. Chen, Synergistic Dual-Halide Anion Engineering for Efficient Interface Passivation in 1.68 eV Wide-Bandgap Perovskite Solar Cells for Indoor Photovoltaics, *ACS Appl. Mater. Interfaces*, 2026, **18**, 3905–3914, DOI: 10.1021/acsami.5c22974.

85 C.-H. Huang, Z.-E. Shi, Y.-H. Zheng, Y.-C. Chen, C.-P. Chen and C.-H. Chen, A Metal-Free Phthalocyanine Additive for Defect Passivation and Processing Tolerance in High-Efficiency Perovskite Solar Cells, *Small*, 2026, e12151, DOI: 10.1002/smll.202512151.

86 S. Huang, S. Hou, Y. Wang, Y. Ren, Y. Wo, J. Xu, J. Qin, G. Sanfo, Z. Albu, K. Qiu, H. Muwanwella, I. Hill, Y. Huang, R. L. Milot, X. Liu, M. T. Sajjad and M. Abdi-Jalebi, Multimodal Strategy for Efficient Semi-Transparent Perovskite Solar Cells and Modules with Record Indoor Performance, *Adv. Energy Mater.*, 2026, e05931, DOI: 10.1002/aenm.202505931.

87 A. Abee Varghese, J. Gong, N. P. Maria Joseph Raj, N. P. Turnbull and J. Lethy Krishnan, Effect of Preheating on Phase Distribution and Orientation of 2D Halide Perovskite for Indoor Photovoltaics, *Energy Technol.*, 2026, **14**, e202501989, DOI: 10.1002/ente.202501989.

88 N. Wu, T. Yang, Z. Wang, Y. Wu, Y. Wang, C. Ma, H. Li, Y. Du, D. Zhao, S. Wang, P. Liu, W. Huang, X. Ren, S. Liu and K. Zhao, Stabilizing Precursor Solution and Controlling Crystallization Kinetics Simultaneously for High-Performance Perovskite Solar Cells, *Adv. Mater.*, 2023, **35**, 2304809, DOI: 10.1002/adma.202304809.

89 W. Chen, K. T. Mularso, B. Jo and H. S. Jung, Indoor light energy harvesting perovskite solar cells: from device physics to AI-driven strategies, *Mater. Horiz.*, 2025, **12**, 3691–3711, DOI: 10.1039/D5MH00133A.

90 T. Xu, N. Li, Z. Wang, T. Nie, J. Zhang, S. Liu and W. Xiang, Synergistic Dual-Defect Passivation via Iodoethoxyethane for High-Efficiency Inverted Inorganic Perovskite Solar Cells, *Adv. Funct. Mater.*, 2026, **36**, e15665, DOI: 10.1002/adfm.202515665.

91 M. Yang, S. J. Kim, T. H. Kim, H. Ahn, M. J. Lee, Y. Kim and J. W. Shim, Bi-synergistic ligand-mediated passivation of surface defects for highly efficient and stable cesium-lead-iodide perovskite quantum dot photovoltaics, *Mater. Horiz.*, 2026, **13**, 1906–1917, DOI: 10.1039/D5MH01763G.

92 L. Liu, Y. Yang, M. Du, Y. Cao, X. Ren, L. Zhang, H. Wang, S. Zhao, K. Wang and S. Liu, Self-Assembled Amphiphilic Monolayer for Efficient and Stable Wide-Bandgap Perovskite Solar Cells, *Adv. Energy Mater.*, 2023, **13**, 2202802, DOI: 10.1002/aenm.202202802.

93 L. Wang, P. Liu, J. Wang, Y. Lu, D. Jin, X. Tian and G. Li, Mixed-SAM interface enables efficient and stable semi-transparent perovskite solar cells for day–night ambient-light energy harvesting, *J. Mater. Chem. A*, 2026, **14**, 3058–3070, DOI: 10.1039/D5TA08178E.

94 B.-H. Jiang, Z.-J. Gao, C.-Y. Lung, Z.-E. Shi, H.-Y. Du, Y.-W. Su, H.-S. Shih, K.-M. Lee, H.-H. Hung, C. K. Chan, C.-P. Chen and K.-T. Wong, Enhancing the Efficiency of Indoor Perovskite Solar Cells through Surface Defect Passivation with Coplanar Heteroacene Cored A–D–A-type Molecules, *Adv. Funct. Mater.*, 2024, **34**, 2312819, DOI: 10.1002/adfm.202312819.

95 Z. Skafi, F. Matteocci, M. Bagheri Khorasgani, P. Amiri, M. A. der Maur, S. Ramamoorthy, E. Nonni, J. Xu, E. Sadeghi, M. Zahedifar, T. M. Brown and A. Di Carlo, All-perovskite Indoor Tandem Solar Cells, *Nano Energy*, 2026, **153**, 111906, DOI: 10.1016/j.nanoen.2026.111906.

96 M. Lee, J. Lim, E. Choi, A. M. Soufiani, S. Lee, F.-J. Ma, S. Lim, J. Seidel, D. H. Seo, J.-S. Park, W. Lee, J. Lim, R. F. Webster, J. Kim, D. Wang, M. A. Green, D. Kim, J. H. Noh, X. Hao and J. S. Yun, Highly Efficient Wide Bandgap Perovskite Solar Cells With Tunneling Junction by Self-Assembled 2D Dielectric Layer, *Adv. Mater.*, 2024, **36**, 2402053, DOI: 10.1002/adma.202402053.

97 F. De Rossi, T. Pontecorvo and T. M. Brown, Characterization of photovoltaic devices for indoor light harvesting and customization of flexible dye solar cells to deliver superior efficiency under artificial lighting, *Appl. Energy*, 2015, **156**, 413–422, DOI: 10.1016/j.apenergy.2015.07.031.

98 I. M. Asuo, A. Mahdavi Varposhti, C. C. F. Kumachang, G. K. Grandhi, V. Pecunia, T. M. Brown, P. Vivo and N. Y. Doumon, Stability of Perovskite Indoor Photovoltaics: A Focused Review and a Call for Standardized Stability Reporting, *Adv. Energy Mater.*, 2026, e06091, DOI: 10.1002/aenm.202506091.

99 M. Pirc, Ž. Ajdič, D. Uršič, M. Jošt and M. Topič, Indoor Energy Harvesting With Perovskite Solar Cells for IoT Applications-A Full Year Monitoring Study, *ACS Appl. Energy Mater.*, 2024, **7**, 565–575, DOI: 10.1021/acsaem.3c02498.

100 Z. Bi, X. Xu, X. Chen, Y. Zhu, C. Liu, H. Yu, Y. Zheng, P. A. Troshin, A. Guerrero and G. Xu, High-performance large-area blade-coated perovskite solar cells with low ohmic loss for low lighting indoor applications, *Chem. Eng. J.*, 2022, **446**, 137164, DOI: 10.1016/j.cej.2022.137164.

101 E. Q. Han, M. Lyu, E. Choi, Y. Zhao, Y. Zhang, J. Lee, S.-M. Lee, Y. Jiao, S. H. A. Ahmad, J. Seidel, J. S. Yun, J.-H. Yun and L. Wang, High-Performance Indoor Perovskite Solar Cells by Self-Suppression of Intrinsic Defects via a Facile Solvent-Engineering Strategy, *Small*, 2024, **20**, 2305192, DOI: 10.1002/smll.202305192.

102 K. Wojciechowski and D. Forgács, Commercial Applications of Indoor Photovoltaics Based on Flexible Perovskite Solar Cells, *ACS Energy Lett.*, 2022, **7**, 3729–3733, DOI: 10.1021/acsenergylett.2c01976.

103 M. Z. Qamar, Z. Khalid, R. Shahid, W. C. Tsoi, Y. K. Mishra, A. K. K. Kyaw and M. A. Saeed, Advancement in indoor energy harvesting through flexible perovskite photovoltaics for self- powered IoT applications, *Nano Energy*, 2024, **129**, 109994, DOI: 10.1016/j.nanoen.2024.109994.

104 R. Datt, J. Guo, R. Lin, L. Li, H. Tan and W. C. Tsoi, Wide bandgap perovskite photovoltaic on rigid and flexible substrates for indoor light harvesting, *Appl. Phys. Lett.*, 2025, **127**, 043903, DOI: 10.1063/5.0284313.

105 G. Tang and F. Yan, Recent progress of flexible perovskite solar cells, *Nano Today*, 2021, **39**, 101155, DOI: 10.1016/j.nantod.2021.101155.

106 F. Jafarzadeh, L. A. Castriotta, M. Legrand, D. Ory, S. Cacovich, Z. Skafi, J. Barichello, F. De Rossi, F. Di Giacomo, A. Di Carlo, T. Brown, F. Brunetti and F. Matteocci, Flexible, Transparent, and Bifacial Perovskite Solar Cells and Modules Using the Wide-Band Gap FAPbBr3 Perovskite Absorber, *ACS Appl. Mater. Interfaces*, 2024, **16**, 17607–17616, DOI: 10.1021/acsami.4c01071.

107 X. Hu, Z. Huang, X. Zhou, P. Li, Y. Wang, Z. Huang, M. Su, W. Ren, F. Li, M. Li, Y. Chen and Y. Song, Wearable Large-Scale Perovskite Solar-Power Source via Nanocellular Scaffold, *Adv. Mater.*, 2017, **29**, 1703236, DOI: 10.1002/adma.201703236.

108 C. Li, S. Cong, Z. Tian, Y. Song, L. Yu, C. Lu, Y. Shao, J. Li, G. Zou, M. H. Rümmeli, S. Dou, J. Sun and Z. Liu, Flexible perovskite solar cell-driven photo-rechargeable lithium-ion capacitor for self-powered wearable strain sensors, *Nano Energy*, 2019, **60**, 247–256, DOI: 10.1016/j.nanoen.2019.03.061.

109 S. Shankar S, G. Gupta, R. Singhal and G. D. Sharma, Exploring the Feasibility of an Annealing-Free ZnO-Based Electron Transport Layer for Flexible Indoor Organic Photovoltaics, Sustainable in Ambient Conditions, *ACS Appl. Electron. Mater.*, 2025, **7**, 10303–10311, DOI: 10.1021/acsaelm.5c01756.

110 J. Min, S. Demchyshyn, J. R. Sempionatto, Y. Song, B. Hailegnaw, C. Xu, Y. Yang, S. Solomon, C. Putz, L. E. Lehner, J. F. Schwarz, C. Schwarzinger, M. C. Scharber, E. Shirzaei Sani, M. Kaltenbrunner and W. Gao, An autonomous wearable biosensor powered by a perovskite solar cell, *Nat. Electron.*, 2023, **6**, 630–641, DOI: 10.1038/s41928-023-00996-y.

111 C. Polyzoidis, K. Rogdakis and E. Kymakis, Indoor Perovskite Photovoltaics for the Internet of Things—Challenges and Opportunities toward Market Uptake, *Adv. Energy Mater.*, 2021, **11**, 2101854, DOI: 10.1002/aenm.202101854.

112 J. Dagar, S. Castro-Hermosa, M. Gasbarri, A. L. Palma, L. Cina, F. Matteocci, E. Calabrò, A. Di Carlo and T. M. Brown, Efficient fully laser-patterned flexible perovskite modules and solar cells based on low-temperature solution-processed SnO2/mesoporous-TiO2 electron transport layers, *Nano Res.*, 2018, **11**, 2669–2681, DOI: 10.1007/s12274-017-1896-5.

113 O. Y. Gong, G. S. Han, S. Lee, M. K. Seo, C. Sohn, G. W. Yoon, J. Jang, J. M. Lee, J. H. Choi, D.-K. Lee, S. B. Kang, M. Choi, N.-G. Park, D. H. Kim and H. S. Jung, Van der Waals Force-Assisted Heat-Transfer Engineering for Overcoming Limited Efficiency of Flexible Perovskite Solar Cells, *ACS Energy Lett.*, 2022, **7**, 2893–2903, DOI: 10.1021/acsenergylett.2c01391.

114 C. Liu, T. Yang, W. Cai, Y. Wang, X. Chen, S. Wang, W. Huang, Y. Du, N. Wu, Z. Wang, Y. Yang, J. Feng, T. Niu, Z. Ding and K. Zhao, Flexible Indoor Perovskite Solar Cells by In Situ Bottom-Up Crystallization Modulation and Interfacial Passivation, *Adv. Mater.*, 2024, **36**, 2311562, DOI: 10.1002/adma.202311562.

115 C. Ma, T. Niu, X. Chen, Y. Yang, S. Wang, Z. Zhang, Y. Tu, C. Tian, X. Ji, F. Sun and K. Zhao, Guanidinium-mediated crystallization modulation for high-performance indoor flexible perovskite solar cells, *Appl. Phys. Lett.*, 2025, **127**, 083905, DOI: 10.1063/5.0278297.

116 S. Kim, H. Oh, G. Kang, I. K. Han, I. Jeong and M. Park, High-Power and Flexible Indoor Solar Cells via Controlled Growth of Perovskite Using a Greener Antisolvent, *ACS Appl. Energy Mater.*, 2020, **3**, 6995–7003, DOI: 10.1021/acsaem.0c00997.

117 C. Dong, J. Chen, C.-H. Chen, Y.-R. Shi, W.-F. Yang, K.-L. Wang, Z.-K. Wang and L.-S. Liao, Annealing-free perovskite films by EDOT-assisted anti-solvent strategy for flexible indoor and outdoor photovoltaics, *Nano Energy*, 2022, **94**, 106866, DOI: 10.1016/j.nanoen.2021.106866.

118 C.-H. Chen, Z.-H. Su, Y.-H. Lou, Y.-J. Yu, K.-L. Wang, G.-L. Liu, Y.-R. Shi, J. Chen, J.-J. Cao, L. Zhang, X.-Y. Gao and Z.-K. Wang, Full-Dimensional Grain Boundary Stress Release for Flexible Perovskite Indoor Photovoltaics, *Adv. Mater.*, 2022, **34**, 2200320, DOI: 10.1002/adma.202200320.

119 Z. Skafi, L. A. Castriotta, B. Taheri, F. Matteocci, M. Fahland, F. Jafarzadeh, E. Joseph, A. Chakraborty, V. Singh, V. Mottaghitalab, L. Mivehi, F. Brunetti, L. Sorbello, A. Di Carlo and T. M. Brown, Flexible Perovskite Solar Cells on Polycarbonate Film Substrates, *Adv. Energy Mater.*, 2024, **14**, 2400912, DOI: 10.1002/aenm.202400912.

120 C. Teixeira, P. Spinelli, L. A. Castriotta, D. Müller, S. Öz, L. Andrade, A. Mendes, A. D. Carlo, U. Würfel, K. Wojciechowski and D. Forgács, Charge Extraction in Flexible Perovskite Solar Cell Architectures for Indoor Applications – with up to 31% Efficiency, *Adv. Funct. Mater.*, 2022, **32**, 2206761, DOI: 10.1002/adfm.202206761.

121 C. Teixeira, R. Fuentes-Pineda, L. Andrade, A. Mendes and D. Forgács, Fabrication of low-cost and flexible perovskite solar cells by slot-die coating for indoor applications, *Mater. Adv.*, 2023, **4**, 3863–3873, DOI: 10.1039/D3MA00285C.

122 C. Zhang, M. He, S. Wu, Y. Gao, M. Ma, C. Liu and Y. Mai, Occlusal Architecture of the Buried Interface Enables Record-Efficiency Flexible Perovskite Photovoltaic Modules with Enhanced In-Plane Bending Mechanical Endurance, *Adv. Funct. Mater.*, 2024, **34**, 2313910, DOI: 10.1002/adfm.202313910.

123 M. He, Y. Gao, H. Tan, H. Zhang, Z. Zhuang, S. Wu, Y. Gao, C. Zhang, L. Liu, Q. Luo, L. Qin, P. Jia, C. Liu, R. E. I. Schropp and Y. Mai, Enhancing Flexible Perovskite Photovoltaic Cells and Modules Through Light-

Trapping and Light-Shifting Strategies, *Small Methods*, 2025, **9**, 2401954, DOI: 10.1002/smtd.202401954.

124 S. Castro-Hermosa, M. Top, J. Dagar, J. Fahlteich and T. M. Brown, Quantifying Performance of Permeation Barrier—Encapsulation Systems for Flexible and Glass-Based Electronics and Their Application to Perovskite Solar Cells, *Adv. Electron. Mater.*, 2019, **5**, 1800978, DOI: 10.1002/aelm.201800978.

125 M. Caputo, N. Cefarin, A. Radivo, N. Demitri, L. Gigli, J. R. Plaisier, M. Panighel, G. Di Santo, S. Moretti, A. Giglia, M. Polentarutti, F. De Angelis, E. Mosconi, P. Umari, M. Tormen and A. Goldoni, Electronic structure of MAPbI3 and MAPbCl3: importance of band alignment, *Sci. Rep.*, 2019, **9**, 15159, DOI: 10.1038/s41598-019-50108-0.

126 L. Chouhan, S. Ghimire, C. Subrahmanyam, T. Miyasaka and V. Biju, Synthesis, optoelectronic properties and applications of halide perovskites, *Chem. Soc. Rev.*, 2020, **49**, 2869–2885, DOI: 10.1039/C9CS00848A.

127 Y. Fu, H. Zhu, J. Chen, M. P. Hautzinger, X. Y. Zhu and S. Jin, Metal halide perovskite nanostructures for optoelectronic applications and the study of physical properties, *Nat. Rev. Mater.*, 2019, **4**, 169–188, DOI: 10.1038/s41578-019-0080-9.

128 M. Krishnaiah, K. Singh, S. Monga, A. Tripathi, S. Karmakar, R. Kumar, C. Tyrpenou, G. Volonakis, D. Manna, P. Mäkinen, K. V. Adarsh, S. Bhattacharya, G. K. Grandhi, K. D. M. Rao and P. Vivo, Perovskite-Inspired $Cs_2AgBi_2I_9$: A Promising Photovoltaic Absorber for Diverse Indoor Environments, *Adv. Energy Mater.*, 2025, **15**, 2404547, DOI: 10.1002/aenm.202404547.

129 R. Vidal, N. Lamminen, V. Holappa, J.-A. Alberola-Borràs, I. P. Franco, G. K. Grandhi and P. Vivo, Assessing the Environmental Impact of Pnictogen-based Perovskite-Inspired Materials for Indoor Photovoltaics, *Adv. Energy Mater.*, 2025, **15**, 2403981, DOI: 10.1002/aenm.202403981.

130 N. Lamminen, J. Lahtinen, M. Krishnaiah, J. Karlsson, M. Saju, G. K. Grandhi and P. Vivo, Surpassing the 10% Efficiency Threshold in Perovskite-Inspired Indoor Photovoltaics, *ACS Energy Lett.*, 2025, **10**, 3415–3418, DOI: 10.1021/acsenergylett.5c01472.

131 M. T. Islam, M. Sk and A. Kumar, Simulation study on the performance of wide band gap quaternary compound Cu2BaSnS4 for indoor solar cells in IoT applications, *Phys. Scr.*, 2025, **100**, 055917, DOI: 10.1088/1402-4896/adc63e.

132 A. Babayigit, A. Ethirajan, M. Muller and B. Conings, Toxicity of organometal halide perovskite solar cells, *Nat. Mater.*, 2016, **15**, 247–251, DOI: 10.1038/nmat4572.

133 M. S. Salem, A. Shaker, T. S. Almurayziq, A. Alanazi, K. A. Al-Dhlan, M. T. Qureshi and M. Okil, Engineering of hole transport layer and back contact for indoor Cs2TiBr6 perovskite solar cells, *Sol. Energy*, 2025, **302**, 114036, DOI: 10.1016/j.solener.2025.114036.

134 C. Clegg, J. Mei, A. U. Fuensanta, T. Ibn-Mohammed and V. Pecunia, Evaluating lead-based vs. lead-free perovskites for environmentally sustainable indoor photovoltaics, *Mater. Sci. Eng. R Rep.*, 2025, **166**, 101037, DOI: 10.1016/j.mser.2025.101037.

135 I. Celik, Z. Song, A. J. Cimaroli, Y. Yan, M. J. Heben and D. Apul, Life Cycle Assessment (LCA) of perovskite PV cells projected from lab to fab, *Sol. Energy Mater. Sol. Cells*, 2016, **156**, 157–169, DOI: 10.1016/j.solmat.2016.04.037.

136 N. Espinosa, L. Serrano-Luján, A. Urbina and F. C. Krebs, Solution and vapour deposited lead perovskite solar cells: Ecotoxicity from a life cycle assessment perspective, *Sol. Energy Mater. Sol. Cells*, 2015, **137**, 303–310, DOI: 10.1016/j.solmat.2015.02.013.

137 G. Schileo and G. Grancini, Lead or no lead? Availability, toxicity, sustainability and environmental impact of lead-free perovskite solar cells, *J. Mater. Chem. C*, 2021, **9**, 67–76, DOI: 10.1039/D0TC04552G.

138 J. Zhang, X. Gao, Y. Deng, B. Li and C. Yuan, Life Cycle Assessment of Titania Perovskite Solar Cell Technology for Sustainable Design and Manufacturing, *ChemSusChem*, 2015, **8**, 3882–3891, DOI: 10.1002/cssc.201500848.

139 P. Nuss and M. J. Eckelman, Life Cycle Assessment of Metals: A Scientific Synthesis, *PLoS One*, 2014, **9**, e101298, DOI: 10.1371/journal.pone.0101298.

140 A. Jain, O. Voznyy and E. H. Sargent, High-Throughput Screening of Lead-Free Perovskite-like Materials for Optoelectronic Applications, *J. Mater. Chem. C*, 2017, **121**, 7183–7187, DOI: 10.1021/acs.jpcc.7b02221.

141 Z. Jin, Z. Zhang, J. Xiu, H. Song, T. Gatti and Z. He, A critical review on bismuth and antimony halide based perovskites and their derivatives for photovoltaic applications: recent advances and challenges, *J. Mater. Chem. A*, 2020, **8**, 16166–16188, DOI: 10.1039/D0TA05433J.

142 M. Abdel-Shakour, J. Wang, H. Wang and X. Meng, Lead-free perovskites for indoor photovoltaics, *Appl. Phys. Lett.*, 2025, **127**, 163312, DOI: 10.1063/5.0291824.

143 V. Pecunia, L. G. Occhipinti, A. Chakraborty, Y. Pan and Y. Peng, Lead-free halide perovskite photovoltaics: Challenges, open questions, and opportunities, *APL Mater.*, 2020, **8**, 100901, DOI: 10.1063/5.0022271.

144 J. Kang and L.-W. Wang, High Defect Tolerance in Lead Halide Perovskite CsPbBr3, *J. Phys. Chem. Lett.*, 2017, **8**, 489–493, DOI: 10.1021/acs.jpclett.6b02800.

145 A. Kamppinen, G. K. Grandhi, M. Hadadian, S. Toikkonen, S. Yli-Paavola, P. Vivo and K. Miettunen, Spectroscopic Ellipsometry Characterization and Radiative Limit Modeling of Bismuth-Based Perovskite-Inspired Absorbers for Indoor Photovoltaics, *Adv. Opt. Mater.*, 2026, **14**, e03237, DOI: 10.1002/adom.202503237.

146 W.-F. Yang, J.-J. Cao, C. Dong, M. Li, Q.-S. Tian, Z.-K. Wang and L.-S. Liao, Suppressed oxidation of tin perovskite by Catechin for eco-friendly indoor photovoltaics, *Appl. Phys. Lett.*, 2021, **118**, 023501, DOI: 10.1063/5.0032951.

147 J.-J. Cao, Y.-H. Lou, W.-F. Yang, K.-L. Wang, Z.-H. Su, J. Chen, C.-H. Chen, C. Dong, X.-Y. Gao and Z.-K. Wang, Multifunctional potassium thiocyanate interlayer for eco-friendly tin perovskite indoor and outdoor photovoltaics,

Chem. Eng. J., 2022, **433**, 133832, DOI: 10.1016/j.cej.2021.133832.

148 Z. Wang, H. Xu, C. Zhang, J. A. Steele, B. Zhang, S. Ding, H. Cheng, D. He, D. Lyu and L. Wang, Intermediate-Phase Engineering of Thermally-Evaporated Lead-Free Halide Perovskites for Indoor Photovoltaics, *ACS Energy Lett.*, 2026, **11**, 3290–3299, DOI: 10.1021/acsenergylett.5c04174.

149 M. Abdel-Shakour, J. Wang, J. Huang, Z. Gao, Y. Pan and X. Meng, 6H-Intermediate Phase Enabled Slow Crystal Growth of Tin Halide Perovskites for Indoor Photovoltaics, *Angew Chem. Int. Ed. Engl.*, 2025, **64**, e202421547, DOI: 10.1002/anie.202421547.

150 D. P. Panda, R. Issaoui, Z. Iqbal, G. K. Grandhi, M. O. Ur Rehman, F. Zu, P. Alippi, M. Rastgoo, S. Zuo, E. Luzzi, M. Simmonds, L. Miele, L. Sanguigno, M. Li, P. Aprea, E. Di Maio, N. Koch, P. Vivo and A. Abate, DMSO-Free Tin Halide Perovskites for Indoor Photovoltaics, *ACS Energy Lett.*, 2025, **10**, 3789–3798, DOI: 10.1021/acsenergylett.5c01581.

151 H. Xiao, E. Cui, J. Wang, T. Liu, X. Wei, J. Huang, M. Abdel-Shakour, J. Li, C. Wang, Z. Zhu and X. Meng, Interfacial engineering via dipolar fullerene derivative for efficient tin halide perovskite indoor photovoltaics, *Nat. Commun.*, 2026, **17**, 1908, DOI: 10.1038/s41467-026-68719-3.

152 N. B. Correa Guerrero, Z. Guo, N. Shibayama, A. K. Jena and T. Miyasaka, A Semitransparent Silver–Bismuth Iodide Solar Cell with Voc above 0.8 V for Indoor Photovoltaics, *ACS Appl. Energy Mater.*, 2023, **6**, 10274–10284, DOI: 10.1021/acsaem.3c00223.

153 B. Al-Anesi, G. K. Grandhi, A. Pecoraro, V. Sugathan, N. S. M. Viswanath, H. Ali-Löytty, M. Liu, T.-P. Ruoko, K. Lahtonen, D. Manna, S. Toikkonen, A. B. Muñoz-García, M. Pavone and P. Vivo, Antimony-Bismuth Alloying: The Key to a Major Boost in the Efficiency of Lead-Free Perovskite-Inspired Photovoltaics, *Small*, 2023, **19**, 2303575, DOI: 10.1002/smll.202303575.

154 A. Singh, P.-T. Lai, A. Mohapatra, C.-Y. Chen, H.-W. Lin, Y.-J. Lu and C. W. Chu, Panchromatic heterojunction solar cells for Pb-free all-inorganic antimony based perovskite, *Chem. Eng. J.*, 2021, **419**, 129424, DOI: 10.1016/j.cej.2021.129424.

155 B. Yan, X. Liu, W. Lu, M. Feng, H.-J. Yan, Z. Li, S. Liu, C. Wang, J.-S. Hu and D.-J. Xue, Indoor photovoltaics awaken the world's first solar cells, *Sci. Adv.*, 2022, **8**, eadc9923, DOI: 10.1126/sciadv.adc9923.

156 W. Lu, M. Feng, Z. Li, B. Yan, S. Wang, X. Wen, X. An, S. Liu, J.-S. Hu and D.-J. Xue, Ordering one-dimensional chains enables efficient selenium photovoltaics, *Joule*, 2024, **8**, 1430–1442, DOI: 10.1016/j.joule.2024.02.024.

157 L. Yang, P. Hou, B. Wang, C. Dall'Agnese, Y. Dall'Agnese, G. Chen, Y. Gogotsi, X. Meng and X.-F. Wang, Performance improvement of dye-sensitized double perovskite solar cells by adding Ti3C2Tx MXene, *Chem. Eng. J.*, 2022, **446**, 136963, DOI: 10.1016/j.cej.2022.136963.

158 I. Turkevych, S. Kazaoui, N. Shirakawa and N. Fukuda, Potential of AgBiI4 rudorffites for indoor photovoltaic energy harvesters in autonomous environmental nanosensors, *Jpn. J. Appl. Phys.*, 2021, **60**, SCCE06, DOI: 10.35848/1347-4065/abf2a5.

159 V. Arivazhagan, F. Gun, R. K. K. Reddy, T. Li, M. Adelt, N. Robertson, Y. Chen and A. Ivaturi, Indoor light harvesting lead-free 2-aminothiazolium bismuth iodide solar cells, *Sustain. Energy Fuels*, 2022, **6**, 3179–3186, DOI: 10.1039/D1SE02017J.

160 A. Chakraborty, N. Pai, J. Zhao, B. R. Tuttle, A. N. Simonov and V. Pecunia, Rudorffites and Beyond: Perovskite-Inspired Silver/Copper Pnictohalides for Next-Generation Environmentally Friendly Photovoltaics and Optoelectronics, *Adv. Funct. Mater.*, 2022, **32**, 2203300, DOI: 10.1002/adfm.202203300.

161 N. Pai, J. Lu, T. R. Gengenbach, A. Seeber, A. S. R. Chesman, L. Jiang, D. C. Senevirathna, P. C. Andrews, U. Bach, Y.-B. Cheng and A. N. Simonov, Silver Bismuth Sulfoiodide Solar Cells: Tuning Optoelectronic Properties by Sulfide Modification for Enhanced Photovoltaic Performance, *Adv. Energy Mater.*, 2019, **9**, 1803396, DOI: 10.1002/aenm.201803396.

162 J. Park, E.-J. Kim, J.-Y. Back, J. Lee, S. Lim, S. An, S.-Y. Kim, K. J. Lee, H. J. Park, J. Kim and T. Moon, Suppressing Metallic Bi0 Defects in Pb-Free Rudorffite Indoor Photovoltaics via Hot-Air-Assisted Modulated Crystallization, *ACS Appl. Energy Mater.*, 2025, **8**, 12398–12404, DOI: 10.1021/acsaem.5c02084.

163 Q. Zhang, L. Tao, S. Ma, X. Jiang, J. Xu, J. Su, J. Kang, H. Yin and S. Chen, Hypophosphorous Acid Additive Engineering for Efficient Cu2AgBiI6 Solar Cells, *Adv. Funct. Mater.*, 2025, **35**, 2504863, DOI: 10.1002/adfm.202504863.

164 G. K. Grandhi, B. Al-Anesi, H. Pasanen, H. Ali-Löytty, K. Lahtonen, S. Granroth, N. Christian, A. Matuhina, M. Liu, A. Berdin, V. Pecunia and P. Vivo, Enhancing the Microstructure of Perovskite-Inspired Cu-Ag-Bi-I Absorber for Efficient Indoor Photovoltaics, *Small*, 2022, **18**, 2203768, DOI: 10.1002/smll.202203768.

165 G. K. Grandhi, S. Toikkonen, B. Al-Anesi, V. Pecunia and P. Vivo, Perovskite-inspired Cu_2AgBiI_6 for mesoscopic indoor photovoltaics under realistic low-light intensity conditions, *Sustain. Energy Fuels*, 2022, **7**, 66–73, DOI: 10.1039/D2SE00995A.

166 J. Xu, L. A. Castriotta, Z. Skafi, A. Chakraborty, A. Di Carlo and T. M. Brown, Lead-free solar cells and modules with antimony-based perovskite inspired materials for indoor photovoltaics, *Mater. Today Energy*, 2025, **49**, 101823, DOI: 10.1016/j.mtener.2025.101823.

167 N. Lamminen, J. Karlsson, R. Kumar, N. S. M. Viswanath, S. Lal, F. Fasulo, M. Righetto, M. Krishnaiah, K. Lahtonen, A. Tewari, A. Katerski, J. Lahtinen, I. Oja Acik, E. M. J. Johansson, A. B. Muñoz-García, M. Pavone, L. M. Herz, G. K. Grandhi and P. Vivo, The promise of operational stability in pnictogen-based perovskite-inspired solar cells, *Polar Res.*, 2025, **1**, 139–156, DOI: 10.1039/D5EL00029G.

168 E. Q. Han, J. H. Yun and M. Lyu, Lead-Free Perovskite and Perovskite-Inspired Materials for Indoor Photovoltaics: A

Perspective, *Mater. Sustain.*, 2026, **2**, 1, DOI: 10.53941/matsus.2026.100001.

169 Y. Peng, T. N. Huq, J. Mei, L. Portilla, R. A. Jagt, L. G. Occhipinti, J. L. MacManus-Driscoll, R. L. Z. Hoye and V. Pecunia, Lead-Free Perovskite-Inspired Absorbers for Indoor Photovoltaics, *Adv. Energy Mater.*, 2021, **11**, 2002761, DOI: 10.1002/aenm.202002761.

170 N. Lamminen, G. K. Grandhi, F. Fasulo, A. Hiltunen, H. Pasanen, M. Liu, B. Al-Anesi, A. Efimov, H. Ali-Löytty, K. Lahtonen, P. Mäkinen, A. Matuhina, A. B. Muñoz-García, M. Pavone and P. Vivo, Triple A-Site Cation Mixing in 2D Perovskite-Inspired Antimony Halide Absorbers for Efficient Indoor Photovoltaics, *Adv. Energy Mater.*, 2023, **13**, 2203175, DOI: 10.1002/aenm.202203175.

171 Y. Guo, F. Zhao, C. Zhang, P. Wu, J. Jiang, J. Tao and J. Chu, Suppressing the Electron–Phonon Coupling in 2D Perovskite Cs3Sb2I9 for Lead-Free Indoor Photovoltaics, *Advanced Science*, 2025, **12**, e09281, DOI: 10.1002/advs.202509281.

172 W. Lu, Z. Li, M. Feng, J. Wei, X. Wen, X. An, Z. Wei, Y. Lin, J.-S. Hu and D.-J. Xue, Lanthanide-Like Contraction Enables the Fabrication of High-Purity Selenium Films for Efficient Indoor Photovoltaics, *Angew. Chem., Int. Ed.*, 2025, **64**, e202413429, DOI: 10.1002/anie.202413429.

173 A. M. Kay, S. N. Ahmed, N. Burridge, D. B. Riley, A. Armin, O. J. Sandberg, Z. Haymoor, M. J. Carnie, P. Meredith and G. Burwell, Optimising photovoltaic modules for indoor energy-harvesting systems, *J. High Energy Phys.*, 2025, **7**, 035019, DOI: 10.1088/2515-7655/ade38b.

174 P. Meredith and A. Armin, Scaling of next generation solution processed organic and perovskite solar cells, *Nat. Commun.*, 2018, **9**, 5261, DOI: 10.1038/s41467-018-05514-9.

175 G. Burwell, O. J. Sandberg, W. Li, P. Meredith, M. Carnie and A. Armin, Scaling Considerations for Organic Photovoltaics for Indoor Applications, *Sol. RRL*, 2022, **6**, 2200315, DOI: 10.1002/solr.202200315.

176 G. G. Jeon, D. S. Lee, M. J. Choi, Y.-H. Seo, S. Huang, J. H. Kim, S. S. Shin and J. Kim, Mitigation of parasitic leakage current in indoor perovskite photovoltaic modules using porous alumina interlayer, *EcoMat*, 2024, **6**, e12455, DOI: 10.1002/eom2.12455.

177 V. Marrugat-Arnal, W. Wang, M. R. Kokaba, S. Dayneko, D. Zhang, S. Qiu, V. Yeddu, Y. Ahmed, A. Amaro, M. Awais and M. I. Saidaminov, Tuning FAPbI3 for scalable perovskite indoor photovoltaics, *Polar Res.*, 2025, **1**, 310–319, DOI: 10.1039/D4EL00030G.

178 F. De Rossi, J. A. Baker, D. Beynon, K. E. A. Hooper, S. M. P. Meroni, D. Williams, Z. Wei, A. Yasin, C. Charbonneau, E. H. Jewell and T. M. Watson, All Printable Perovskite Solar Modules with 198 cm2 Active Area and Over 6% Efficiency, *Adv. Mater. Technol.*, 2018, **3**, 1800156, DOI: 10.1002/admt.201800156.

179 X. Zhu, H. Dong, J. Chen, J. Xu, Z. Li, F. Yuan, J. Dai, B. Jiao, X. Hou, J. Xi and Z. Wu, Photoinduced Cross Linkable Polymerization of Flexible Perovskite Solar Cells and Modules by Incorporating Benzyl Acrylate, *Adv. Funct. Mater.*, 2022, **32**, 2202408, DOI: 10.1002/adfm.202202408.

180 W. Żuraw, F. A. Vinocour Pacheco, J. Sánchez-Diaz, Ł. Przypis, M. A. Mejia Escobar, S. Almosni, G. Vescio, J. P. Martínez-Pastor, B. Garrido, R. Kudrawiec, I. Mora-Seró and S. Öz, Large-Area, Flexible, Lead-Free Sn-Perovskite Solar Modules, *ACS Energy Lett.*, 2023, **8**, 4885–4887, DOI: 10.1021/acsenergylett.3c02066.

181 S. K. Podapangi, F. Jafarzadeh, S. Mattiello, T. B. Korukonda, A. Singh, L. Beverina and T. M. Brown, Green solvents, materials, and lead-free semiconductors for sustainable fabrication of perovskite solar cells, *RSC Adv.*, 2023, **13**, 18165–18206, DOI: 10.1039/D3RA01692G.

182 J. Xu, L. A. Castriotta, A. Di Carlo and T. M. Brown, Air-Stable Lead-Free Antimony-Based Perovskite Inspired Solar Cells and Modules, *ACS Energy Lett.*, 2024, **9**, 671–678, DOI: 10.1021/acsenergylett.3c02409.

183 J. Xu, X. Zhu, J. Dai, M. Zhang, X. Wei, T. Lei, H. Xie, Y. Pan, J. Cao, Z. Wu and H. Dong, Improved humidity resistance and bending stability of flexible perovskite photovoltaic module by Incorporating polymerized networks, *Chem. Eng. J.*, 2025, **510**, 161624, DOI: 10.1016/j.cej.2025.161624.

184 H. C. Weerasinghe, N. Macadam, J.-E. Kim, L. J. Sutherland, D. Angmo, L. W. T. Ng, A. D. Scully, F. Glenn, R. Chantler, N. L. Chang, M. Dehghanimadvar, L. Shi, A. W. Y. Ho-Baillie, R. Egan, A. S. R. Chesman, M. Gao, J. J. Jasieniak, T. Hasan and D. Vak, The first demonstration of entirely roll-to-roll fabricated perovskite solar cell modules under ambient room conditions, *Nat. Commun.*, 2024, **15**, 1656, DOI: 10.1038/s41467-024-46016-1.

185 E. Parvazian and T. Watson, The roll-to-roll revolution to tackle the industrial leap for perovskite solar cells, *Nat. Commun.*, 2024, **15**, 3983, DOI: 10.1038/s41467-024-48518-4.

186 Q. Dong, C. Zhu, M. Chen, C. Jiang, J. Guo, Y. Feng, Z. Dai, S. K. Yadavalli, M. Hu, X. Cao, Y. Li, Y. Huang, Z. Liu, Y. Shi, L. Wang, N. P. Padture and Y. Zhou, Interpenetrating interfaces for efficient perovskite solar cells with high operational stability and mechanical robustness, *Nat. Commun.*, 2021, **12**, 973, DOI: 10.1038/s41467-021-21292-3.

187 K. Fukuda, L. Sun, B. Du, M. Takakuwa, J. Wang, T. Someya, L. F. Marsal, Y. Zhou, Y. Chen, H. Chen, S. R. P. Silva, D. Baran, L. A. Castriotta, T. M. Brown, C. Yang, W. Li, A. W. Y. Ho-Baillie, T. Österberg, N. P. Padture, K. Forberich, C. J. Brabec and O. Almora, A bending test protocol for characterizing the mechanical performance of flexible photovoltaics, *Nat. Energy*, 2024, **9**, 1335–1343, DOI: 10.1038/s41560-024-01651-2.

188 IEC 61215-1:2021 Terrestrial photovoltaic (PV) modules - Design qualification and type approval - Part 1: Test requirements, https://webstore.iec.ch/en/publication/61345, accessed November 7, 2025.

189 M. V. Khenkin, E. A. Katz, A. Abate, G. Bardizza, J. J. Berry, C. Brabec, F. Brunetti, V. Bulović, Q. Burlingame, A. Di Carlo, R. Cheacharoen, Y.-B. Cheng, A. Colsmann, S. Cros, K. Domanski, M. Dusza, C. J. Fell, S. R. Forrest, Y. Galagan, D. Di Girolamo, M. Grätzel, A. Hagfeldt, E. von Hauff, H. Hoppe, J. Kettle, H. Köbler, M. S. Leite, S. Liu, Y.-L. Loo, J. M. Luther, C.-Q. Ma, M. Madsen,

M. Manceau, M. Matheron, M. McGehee, R. Meitzner, M. K. Nazeeruddin, A. F. Nogueira, Ç. Odabaşı, A. Osherov, N.-G. Park, M. O. Reese, F. De Rossi, M. Saliba, U. S. Schubert, H. J. Snaith, S. D. Stranks, W. Tress, P. A. Troshin, V. Turkovic, S. Veenstra, I. Visoly-Fisher, A. Walsh, T. Watson, H. Xie, R. Yıldırım, S. M. Zakeeruddin, K. Zhu and M. Lira-Cantu, Consensus statement for stability assessment and reporting for perovskite photovoltaics based on ISOS procedures, *Nat. Energy*, 2020, **5**, 35–49, DOI: 10.1038/s41560-019-0529-5.

190 S. Zhang, Z. Liu, W. Zhang, Z. Jiang, W. Chen, R. Chen, Y. Huang, Z. Yang, Y. Zhang, L. Han and W. Chen, Barrier Designs in Perovskite Solar Cells for Long-Term Stability, *Adv. Energy Mater.*, 2020, **10**, 2001610, DOI: 10.1002/aenm.202001610.

191 L. J. Sutherland, J. F. Benitez-Rodriguez, D. Angmo, T. A. N. Peiris, G. P. Simon, M. Gao and H. Weerasinghe, Effect of out-gassing from polymeric encapsulant materials on the lifetime of perovskite solar cells, *Sol. Energy Mater. Sol. Cells*, 2022, **246**, 111887, DOI: 10.1016/j.solmat.2022.111887.

192 T. Miyasaka, *Perovskite Photovoltaics and Optoelectronics: from Fundamentals to Advanced Applications*, 2021.

193 S. J. Kim, M. A. Saeed, T. H. Kim, G. Ham, H. Song, H. Ahn, H. Choi, J. W. Jo, Y. Kim, H. Cha and J. W. Shim, Ultrahigh-performance indoor perovskite quantum dot photovoltaics via ligand-passivation engineering, *Chem. Eng. J.*, 2024, **488**, 151154, DOI: 10.1016/j.cej.2024.151154.

194 S. B. Kang, P. Patil, G. W. Yoon, G. S. Han, H. S. Jung and D. H. Kim, Study of interface engineering on perovskite-based indoor photovoltaics for powering Internet-of-Things, *Chem. Eng. J.*, 2024, **502**, 157973, DOI: 10.1016/j.cej.2024.157973.

195 C.-H. Chen, X.-Y. He, R.-H. Qin, K.-L. Wang, L. Huang, R.-J. Jin, X. Chen, Z.-K. Bian, Y.-T. Yang, K. Jin, J. Chen, Y. Xia, I. Yavuz and Z.-K. Wang, Reliable perovskite indoor photovoltaics for self-powered devices, *Natl. Sci. Rev.*, 2025, **12**, nwaf242, DOI: 10.1093/nsr/nwaf242.

196 K. Seunarine, Z. Haymoor, M. Spence, G. Burwell, A. Kay, P. Meredith, A. Armin and M. Carnie, Light power resource availability for energy harvesting photovoltaics for self-powered IoT, *J. High Energy Phys.*, 2024, **6**, 015018, DOI: 10.1088/2515-7655/ad1764.

197 M. A. Hannan, M. Faisal, P. J. Ker, L. H. Mun, K. Parvin, T. M. I. Mahlia and F. Blaabjerg, A Review of Internet of Energy Based Building Energy Management Systems: Issues and Recommendations, *IEEE Access*, 2018, **6**, 38997–39014, DOI: 10.1109/ACCESS.2018.2852811.

198 Y. Olzhabay, A. Ng and I. A. Ukaegbu, Perovskite PV Energy Harvesting System for Uninterrupted IoT Device Applications, *Energies*, 2021, **14**, 7946, DOI: 10.3390/en14237946.

199 J. Panidi, D. G. Georgiadou, T. Schoetz and T. Prodromakis, Advances in Organic and Perovskite Photovoltaics Enabling a Greener Internet of Things, *Adv. Funct. Mater.*, 2022, **32**, 2200694, DOI: 10.1002/adfm.202200694.

200 W. Zhu, R. Xuan, Y. Xu, X. Gan, Q. Wang, J. Xiong, X. Liu, L. Huang, J. Zhang, Q. Tai, Y. Yang, J. Cuan, W. Li, Y. Zhu and L. Han, Front-Edge Research Progress of Photo-Rechargeable Perovskite Solar Cell-Zinc-Ion Batteries, *Adv. Funct. Mater.*, 2025, e15939, DOI: 10.1002/adfm.202515939.

201 X. Long, H. Xia, L. Qian, G. Shi, X. Wang, Y. Wang and Y. Xia, An Efficient Photovoltaic Energy Harvesting System Using MPPT Control Based on Partial Open-Circuit Voltage Sampling, *Int. J. Circ. Theor. Appl.*, 2025, DOI: 10.1002/cta.70182.

202 I. Mathews, S. N. R. Kantareddy, S. Sun, M. Layurova, J. Thapa, J.-P. Correa-Baena, R. Bhattacharyya, T. Buonassisi, S. Sarma and I. M. Peters, Self-Powered Sensors Enabled by Wide-Bandgap Perovskite Indoor Photovoltaic Cells, *Adv. Funct. Mater.*, 2019, **29**, 1904072, DOI: 10.1002/adfm.201904072.

203 V. Talla, M. Hessar, B. Kellogg, A. Najafi, J. R. Smith and S. Gollakota, LoRa Backscatter: Enabling The Vision of Ubiquitous Connectivity, *Proc. ACM Interact. Mob. Wearable Ubiquitous Technol.*, 2017, **1**, 105, DOI: 10.1145/3130970.

204 W. Han, R. Nie, B. Yin, J. Zhang, S. Qiu, J. Wei, M. Pei, Y. Qin, W. Wang, X. Zhang, J. Cheng, L. Liu and Y. Shi, All Irradiance-Applicable, Perovskite Solar Cells-Powered Flexible Self-Sustaining Sensor Nodes for Wireless Internet-of-Things, *Adv. Funct. Mater.*, 2025, **35**, 2425697, DOI: 10.1002/adfm.202425697.

205 D. P. Milyutin, O. R. Parfenova, V. A. Parfenov and A. G. Boldyreva, Temperature–humidity wireless sensor powered by a wide-bandgap perovskite solar cell, *Appl. Phys. Lett.*, 2025, **127**, 073902, DOI: 10.1063/5.0281143.

206 D. Uršič, M. Pirc, M. Jošt, M. Topič and M. Jankovec, Ultra-Low-Power Indoor Light Harvesting and Solar Cell Characterization System, *IEEE Access*, 2024, **12**, 169442–169451, DOI: 10.1109/ACCESS.2024.3492319.

207 H. J. Lomeri, A. Patra, G. Polino, J. Ali, F. Jafarzadeh, C. S. Rout, F. Matteocci, F. De Rossi and F. Brunetti, Integration of a Paper-Based Supercapacitor and Flexible Perovskite Mini-Module: Toward Self-Powered Portable and Wearable Electronics, *Adv. Funct. Mater.*, 2024, **34**, 2313267, DOI: 10.1002/adfm.202313267.

208 H. Sun, K. Deng, Y. Jiang, J. Ni, J. Xiong and L. Li, Realizing Stable Artificial Photon Energy Harvesting Based on Perovskite Solar Cells for Diverse Applications, *Small*, 2020, **16**, 1906681, DOI: 10.1002/smll.201906681.

209 S. Valastro, S. Ferranti, R. Previti, M. Dellutri, S. Galliano and A. Alberti, Design and Performance of Two-Sided Self-Protecting Perovskite Solar Cells for Indoor Vertical Applications, *Small Science*, 2026, **6**, e202500603, DOI: 10.1002/smsc.202500603.

210 A. A. Smith, R. Li and Z. T. H. Tse, Reshaping healthcare with wearable biosensors, *Sci. Rep.*, 2023, **13**, 4998, DOI: 10.1038/s41598-022-26951-z.

211 Z. Gao, J. Wang, H. Xiao, M. Abdel-Shakour, T. Liu, S. Zhang, J. Huang, D.-J. Xue, S. Yang and X. Meng, Adhesion-Controlled Heterogeneous Nucleation of Tin Halide Perovskites for Eco-Friendly Indoor Photovoltaics,

Adv. Mater., 2024, **36**, 2403413, DOI: 10.1002/adma.202403413.

212 C. Li, Y. Liang, Y. Zhang, L. Du, J. Min and Z. Li, Enhanced Efficiency and Stability of Wide-Bandgap Perovskites via Br-Rich Bulk and Surface 2D Passivation for Indoor Photovoltaics, *Sol. RRL*, 2024, **8**, 2400231, DOI: 10.1002/solr.202400231.

213 H. Jinno, S. B. Shivarudraiah, R. Asbjörn, G. Vagli, T. Marcato, F. T. Eickemeyer, L. Pfeifer, T. Yokota, T. Someya and C.-J. Shih, Indoor Self-Powered Perovskite Optoelectronics with Ultraflexible Monochromatic Light Source, *Adv. Mater.*, 2024, **36**, 2304604, DOI: 10.1002/adma.202304604.

214 S. K. Thomas, A. Pockett, K. Seunarine, M. Spence, D. Raptis, S. Meroni, T. Watson, M. Jones and M. J. Carnie, Will the Internet of Things Be Perovskite Powered? Energy Yield Measurement and Real-World Performance of Perovskite Solar Cells in Ambient Light Conditions, *IoT*, 2022, **3**, 109–121, DOI: 10.3390/iot3010006.

215 G. Landi, G. Avallone, C. Barone and S. Pagano, Design of Environmental Sensor Board for Energy Harvesting: Integration of Conventional and Eco-Friendly Sensors with Power Generation Sources, *Electronics*, 2024, **13**, 3801, DOI: 10.3390/electronics13193801.

216 J. Bi, S. Li, D. Liu, B. Li, K. Yang, M. Xu, C. Fu, Y. Zhao and W. Zhang, Highly Integrated Perovskite Solar Cells-Based Photorechargeable System with Excellent Photoelectric Conversion and Energy Storage Ability, *ENERGY & ENVIRONMENTAL MATERIALS*, 2024, **7**, e12728, DOI: 10.1002/eem2.12728.

217 https://www.pv-magazine.com/2025/08/25/solaires-entreprises-ships-indoor-perovskite-pv-modules-to-first-customer/, accessed November 7, 2025.

218 https://sauletech.com/wp-content/uploads/2025/01/Product-Catalog-Saule.pdf, accessed November 7, 2025.

219 https://perovskia.solar/products/, accessed November 7, 2025.

220 https://enecoat.com/technology/index_en.html, accessed November 7, 2025.

221 https://shop.halocell.energy/products/halocell-ambient-module-60x41_4, accessed November 7, 2025.

222 https://sauletech.com/press/, accessed November 7, 2025.

223 https://www.halocell.energy/perovskite-solar-modules-halocell, accessed November 7, 2025.

224 https://www.solaires.net/products/, accessed November 7, 2025.

225 https://www.venturekick.ch/perovskia-solar, accessed February 27, 2026.

226 https://www.wnp.pl/energia/to-miala-byc-polska-rewolucja-w-fotowoltaice-konieczne-moga-byc-jednak-potezne-naklady,955478.html, accessed February 27, 2026.

227 https://xyz.pl/poland-unpacked/perovskite-promise-management-turmoil-saule-technologies-in-crisis-3697/, accessed February 27, 2026.

228 https://singfilmsolar.com/product.html, accessed November 7, 2025.

229 IEC TS 62607-7-2:2023 Nanomanufacturing - Key control characteristics - Part 7-2: Nano-enabled photovoltaics - Device evaluation method for indoor light. https://webstore.iec.ch/en/publication/61819, accessed November 7, 2025.

230 Y. Cui, L. Hong, T. Zhang, H. Meng, H. Yan, F. Gao and J. Hou, Accurate photovoltaic measurement of organic cells for indoor applications, *Joule*, 2021, **5**, 1016–1023, DOI: 10.1016/j.joule.2021.03.029.

231 B. Minnaert and P. Veelaert, A Proposal for Typical Artificial Light Sources for the Characterization of Indoor Photovoltaic Applications, *Energies*, 2014, **7**, 1500–1516, DOI: 10.3390/en7031500.

232 B. H. Hamadani and M. B. Campanelli, Photovoltaic Characterization Under Artificial Low Irradiance Conditions Using Reference Solar Cells, *IEEE J. Photovoltaics*, 2020, **10**, 1119–1125, DOI: 10.1109/JPHOTOV.2020.2996241.

233 S. Zeiske, P. Meredith, A. Armin and G. Burwell, Importance of spectrally invariant broadband attenuation of light in indoor photovoltaic characterization, *Appl. Energy*, 2023, **1**, 026103, DOI: 10.1063/5.0159289.

234 N. Moody, S. Sesena, D. W. deQuilettes, B. D. Dou, R. Swartwout, J. T. Buchman, A. Johnson, U. Eze, R. Brenes, M. Johnston, C. L. Haynes, V. Bulović and M. G. Bawendi, Assessing the Regulatory Requirements of Lead-Based Perovskite Photovoltaics, *Joule*, 2020, **4**, 970–974, DOI: 10.1016/j.joule.2020.03.018.

235 M. H. Miah, M. U. Khandaker, M. J. Hossen, E. A. Noor, I. Jahan, M. Shahinuzzaman, M. Nur-E-Alam, M. Y. Hanfi, M. H. Ullah and M. A. Islam, Lead-free alternatives and toxicity mitigation strategies for sustainable perovskite solar cells: a critical review, *Mater. Adv.*, 2025, **6**, 2718–2752, DOI: 10.1039/D5MA00010F.

236 J. Suo, H. Pettersson and B. Yang, Sustainable Approaches to Address Lead Toxicity in Halide Perovskite Solar Cells: A Review of Lead Encapsulation and Recycling Solutions, *EcoMat*, 2025, **7**, e12511, DOI: 10.1002/eom2.12511.

237 S. Gao, J.-J. Bae, D. S. Lee, T.-Y. Yang and S. S. Shin, Toward Sustainable Perovskite Solar Cells: From Lead-Free Materials to Environmental Concerns and Mitigation Strategies, *EcoMat*, 2025, **7**, e70001, DOI: 10.1002/eom2.70001.

238 S. S. Dipta, A. J. Christofferson, P. V. Kumar, V. Kundi, M. Hanif, J. Tang, N. Flores, K. Kalantar-Zadeh, A. Uddin and M. A. Rahim, Stable and Lead-Safe Polyphenol-Encapsulated Perovskite Solar Cells, *Advanced Science*, 2024, **11**, 2403057, DOI: 10.1002/advs.202403057.

239 M. Cai, Y. Wu, H. Chen, X. Yang, Y. Qiang and L. Han, Cost-Performance Analysis of Perovskite Solar Modules, *Advanced Science*, 2017, **4**, 1600269, DOI: 10.1002/advs.201600269.

240 Y. Yang, S. Senanayake, M. T. Hoang, J. Ye, N. D. Pham and H. Wang, Non-Metallic Back Contacts for Indoor Perovskite Solar Cells: Material Criteria, Recent Progress, and Future Outlook, *Adv. Mater.*, 2025, **38**, e12402, DOI: 10.1002/adma.202512402.

241 D. Uršič, M. Pirc, M. Jošt, M. Topič and M. Jankovec, Long-term performance of perovskite solar cells in low-power indoor energy harvesting applications, *Sol. Energy Mater. Sol. Cells*, 2026, **300**, 114254, DOI: 10.1016/j.solmat.2026.114254.

242 R. Sun, X. Yuan, X. Yang, Y. Wu, Y. Shao, X. Wu, C. J. Brabec and J. Min, Cost-efficient recycling of organic photovoltaic devices, *Joule*, 2024, **8**, 2523–2538, DOI: 10.1016/j.joule.2024.06.006.

243 Z. Ngagoum Ndalloka, H. Vijayakumar Nair, S. Alpert and C. Schmid, Solar photovoltaic recycling strategies, *Sol. Energy*, 2024, **270**, 112379, DOI: 10.1016/j.solener.2024.112379.

244 M. Akhter, A. Al Mansur, M. I. Islam, M. S. H. Lipu, T. F. Karim, M. G. M. Abdolrasol and T. A. H. Alghamdi, Sustainable Strategies for Crystalline Solar Cell Recycling: A Review on Recycling Techniques, Companies, and Environmental Impact Analysis, *Sustainability*, 2024, **16**, 5785, DOI: 10.3390/su16135785.

245 X. Tian, S. D. Stranks and F. You, Life cycle assessment of recycling strategies for perovskite photovoltaic modules, *Nat Sustainability*, 2021, **4**, 821–829, DOI: 10.1038/s41893-021-00737-z.

246 S. Y. Park, J.-S. Park, B. J. Kim, H. Lee, A. Walsh, K. Zhu, D. H. Kim and H. S. Jung, Sustainable lead management in halide perovskite solar cells, *Nat Sustainability*, 2020, **3**, 1044–1051, DOI: 10.1038/s41893-020-0586-6.